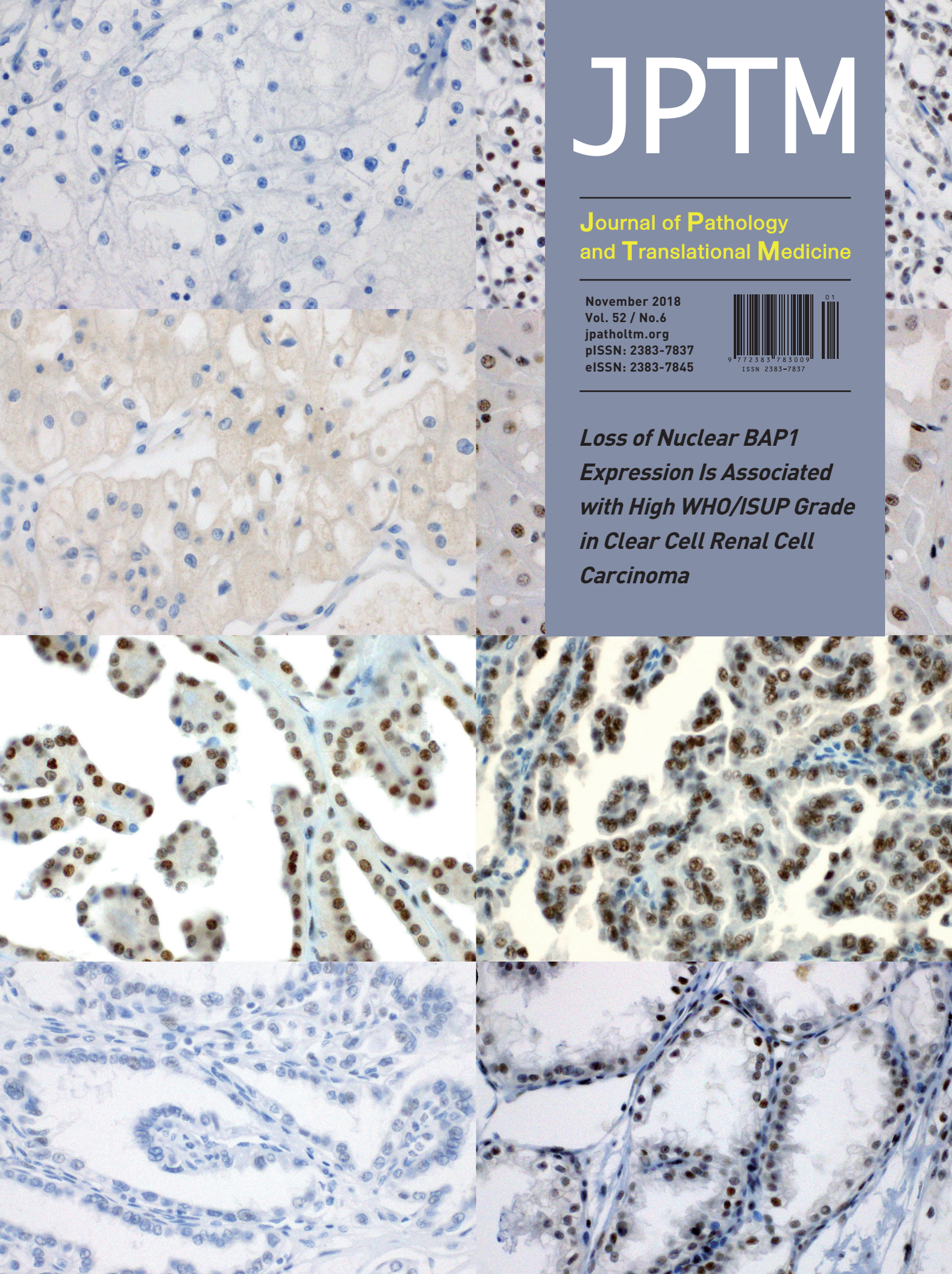

JPTM

Journal of Pathology and Translational Medicine

November 2018
Vol. 52 / No.6
jpatholtm.org
pISSN: 2383-7837
eISSN: 2383-7845

Loss of Nuclear BAP1 Expression Is Associated with High WHO/ISUP Grade in Clear Cell Renal Cell Carcinoma

Journal of Pathology and Translational Medicine

Volume 52 • Number 6 • November 2018 (bimonthly)
Published since 1967
Printed on 11 November 2018 Published on 15 November 2018

J Pathol Transl Med
pISSN: 2383-7837
eISSN: 2383-7845

Aims & Scope

The Journal of Pathology and Translational Medicine is an open venue for the rapid publication of major achievements in various fields of pathology, cytopathology, and biomedical and translational research. The Journal aims to share new insights into the molecular and cellular mechanisms of human diseases and to report major advances in both experimental and clinical medicine, with a particular emphasis on translational research. The investigations of human cells and tissues using high-dimensional biology techniques such as genomics and proteomics will be given a high priority. Articles on stem cell biology are also welcome. The categories of manuscript include original articles, review and perspective articles, case studies, brief case reports, and letters to the editor.

Subscription Information

To subscribe to this journal, please contact the Korean Society of Pathologists/the Korean Society for Cytopathology. Full text PDF files are also available at the official website (http://jpatholtm.org). *Journal of Pathology and Translational Medicine* is indexed by Emerging Sources Citation Index (ESCI), PubMed, PubMed Central, Scopus, KoreaMed, KoMCI, WPRIM, Directory of Open Access Journals (DOAJ), and CrossRef. Circulation number per issue is 700.

Contact the Korean Society of Pathologists/the Korean Society for Cytopathology

Publishers: Jae Bok Park, MD, Hye Kyoung Yoon, MD
Editors-in-Chief: Soon Won Hong, MD, Chong Jai Kim, MD
Published by the Korean Society of Pathologists/the Korean Society for Cytopathology

Editorial Office
Room 1209 Gwanghwamun Officia, 92 Saemunan-ro, Jongno-gu, Seoul 03186, Korea
Tel: +82-2-795-3094 Fax: +82-2-790-6635 E-mail: office@jpatholtm.org

#1508 Renaissancetower, 14 Mallijae-ro, Mapo-gu, Seoul 04195, Korea
Tel: +82-2-593-6943 Fax: +82-2-593-6944 E-mail: office@jpatholtm.org

Printed by iMiS Company Co., Ltd. (JMC)
Jungang Bldg. 18-8 Wonhyo-ro 89-gil, Yongsan-gu, Seoul 04314, Korea
Tel: +82-2-717-5511 Fax: +82-2-717-5515 E-mail: ml@smileml.com

Manuscript Editing by InfoLumi Co.
210-202, 421 Pangyo-ro, Bundang-gu, Seongnam 13522, Korea
Tel: +82-70-8839-8800 E-mail: infolumi.chang@gmail.com

Front cover image: Immunohistochemical staining of BRCA1-associated protein 1 in clear cell RCC (1st row), chromophobe RCC (2nd row), papillaryRCC type 1 (3rd row, left), papillary RCC type 2 (3rd row, right), and clear cell papillary RCC (4th row) (Fig. 1). p380.

This journal was supported by the Korean Federation of Science and Technology Societies Grant funded by the Korean Government.

Journal of Pathology and Translational Medicine

J Pathol Transl Med
pISSN: 2383-7837
eISSN: 2383-7845

Volume 52, Number 6, November 2018

CONTENTS

LETTER TO THE EDITOR

ORIGINAL ARTICLES

CONTENTS CONTINUED

CASE REPORTS

Instructions for Authors for *Journal of Pathology and Translational Medicine* are available at http://jpatholtm.org/authors/authors.php

Journal of Pathology and Translational Medicine 2018; 52: 355-356
https://doi.org/10.4132/jptm.2018.09.07

Alveolar Squamous Cell Metaplasia: Preneoplastic Lesion?

Adriana Handra-Luca[1,2]

[1]Service d'Anatomie Pathologique, APHP GHU Avicenne, Bobigny; [2]Universite Paris Nord Sorbonne Cite, Bobigny, France

To the Editor,

We have read with great interest the report of Song *et al*.[1] on lung squamous cell carcinomas (SCC) developing in the context of usual interstitial pneumonia. Squamous dysplastic foci were detected at the tumor periphery. However, such lesions are rarely mentioned in the medical literature, possibly because most tumors are already at an advanced stage when resected.

We would like to draw attention on microscopic lesions of the same morphological spectrum, those of squamous cell metaplasia (SCM) of the alveolar lining that we have recently identified in a zone of mild alveolar fibrosis on a lung resection specimen for a 2.3-cm large adenocarcinoma. The lesions consisted of several foci of nonkeratinizing SCM developing/in continuity with the unilayered alveolar lining (Fig. 1). When multicellular and pluristratified, the SCM lesions protruded in the underlying fibrous tissue of the alveolar wall. The zone of mild interstitial fibrosis with approximatively 10 SCM foci measured 2.5–3 mm and was detected in normal lung parencyma, at distance from the tumor. There were no well-defined honeycomb-type lesions in the resected lung. In the SCM foci, p63 was positive in basal and suprabasal cells and negative in superficial cells. There were no major cellular atypia, dyskeratosis, or keratin foci. Rare alveolar cells also showed nuclear p63 expression as well as several rounded buds (cystic or not), some reminiscent of thyroid solid cell nests. Thyroid transcription factor 1 and cytokeratin 5/6 (CK5/6) were positive throughout the whole thickness of SCM foci (Fig. 1). Pneumocyte bi-/multinucleation was also seen as well as lymphocytic foci, one of them at contact to a SCM focus.

Here, we report SCM of the alveolar unilayered epithelium. Multicellular, stratified SCM foci were detected on the hematoxilin and eosin stained slide while only paucicellular foci were detected on the immunohistochemistry slides for p63 or CK5/6. The precise origin of these lesions is difficult to identify, $p63^{+}CK5^{+}$ cells being reported in alveolar regeneration of chronic pulmonary fibrosis, diffuse alveolar damage, acute/usual interstitial pneumonia or influenza infection.[2-6] In the present case, the presence of lymphocytic foci may suggest a viral origin. However, given the fact that SCCs may also develop in the peripheral lung tissue, a putative preneoplastic potential can be proposed for alveolar SCM.[7]

In conclusion, SCM may develop from the unilayered alveolar lining. The presence of several SCM foci may constitute a preneoplastic background for peripheral squamous cell carcinomas or squamous-type component in adenocarcinomas.

Corresponding Author
Adriana Handra-Luca, MD, PhD
Service d'Anatomie Pathologique, APHP GHU Avicenne, Universite Paris Nord Sorbonne Cite, 125 rue Stalingrad, 93009 Bobigny, France
Tel: +33-148955555 (deck 52047), Fax: +33-14895555602/5480
E-mail: adriana.handra-luca@aphp.fr, adriana.handra-luca@hotmail.com

Received: August 27, 2018 **Accepted:** September 7, 2018

ORCID

Adriana Handra-Luca: https://orcid.org/0000-0003-3816-058X

Conflicts of Interest

No potential conflict of interest relevant to this article was reported.

Acknowledgments

The author thanks the administrative and technical teams APHP/Hôpitaux Universitaires Paris Seine-Saint-Denis, the NCA/APHP Avicenne, the CMDP/APHP and BIUM teams.

REFERENCES

1. Song DH, Choi IH, Ha SY, *et al*. Usual interstitial pneumonia with

pISSN 2383-7837
eISSN 2383-7845

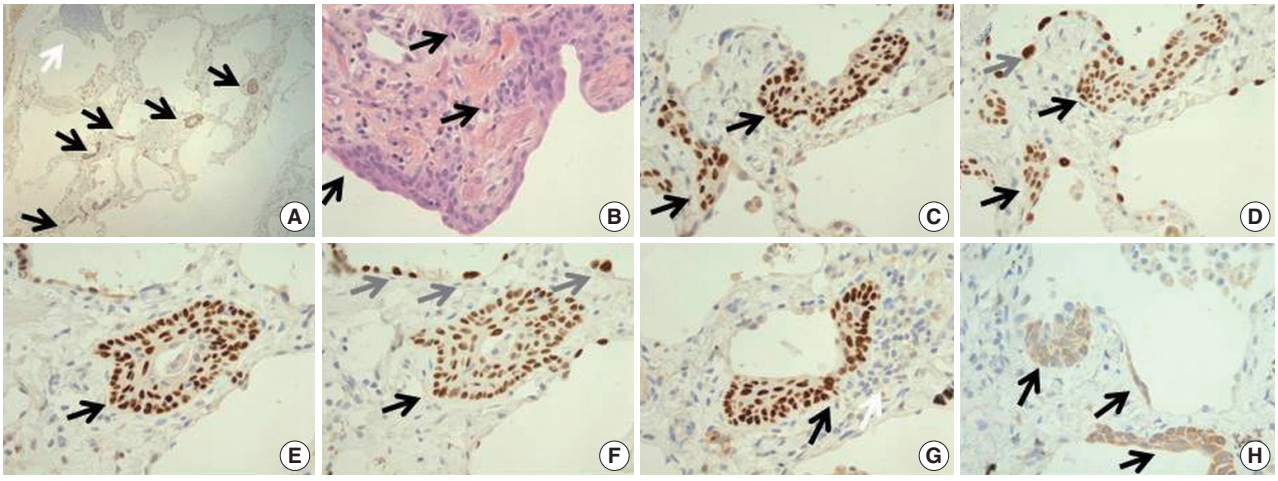

Fig. 1. (A) The lung parenchyma shows a zone of multiple (approximatively 10) p63-positive squamous cell metaplasia (SCM) foci (black arrows for SCM foci, white arrow for lymphocytic focus). (B) On the hematoxylin and eosin stained slide, the lesions consist in a multilayered epithelium composed of basal cuboidal cells, suprabasal cells and superficial spindle-appearing cells (black arrows). (C) The basal and suprabasal cells are immunoreactive for p63 while superficial cells are negative (black arrows for $p63^+$ cells). (D) Thyroid transcription factor 1 is expressed by the cells throughout the entire thickness of the lesion, in both $p63^+$ and $p63^-$ cells (black arrows for SCM foci, gray arrow for atypical pneumocyte nuclei). (E, F) A cystic cellular bud (reminiscent of thyroid solid cell nests) is detected in an alveolar septum (black arrows for the SCM bud, gray arrows for binucleated pneumocytes). (G) One of the SCM foci develop at close contact to the lymphocytic infiltrate (p63 immunohistochemistry, black arrow for the SCM focus, white arrow for the lymphcytic infiltrate). To note would be the presence of a binucleation with immunoreactivity to p63 in the SCM focus. (H) Cytokeratin 5/6 is expressed in spindle-appearing cells lining the alveoli and in the SCM foci (black arrows for cytokeratin $5/6^+$ cells).

lung cancer: clinicopathological analysis of 43 cases. Korean J Pathol 2014; 48: 10-6.
2. Meyer EC, Liebow AA. Relationship of interstitial pneumonia honeycombing and atypical epithelial proliferation to cancer of the lung. Cancer 1965; 18: 322-51.
3. Rosai J. Rosai and Ackerman's surgical pathology. 10th ed. Philadelphia: Elsevier Mosby, 2011.
4. Chilosi M, Poletti V, Murer B, *et al*. Abnormal re-epithelialization and lung remodeling in idiopathic pulmonary fibrosis: the role of deltaN-p63. Lab Invest 2002; 82: 1335-45.
5. Zuo W, Zhang T, Wu DZ, *et al*. p63(+)Krt5(+) distal airway stem cells are essential for lung regeneration. Nature 2015; 517: 616-20.
6. Kato E, Takayanagi N, Takaku Y, *et al*. Incidence and predictive factors of lung cancer in patients with idiopathic pulmonary fibrosis. ERJ Open Res 2018; 4: 00111-2016.
7. Krimsky W, Muganlinskaya N, Sarkar S, *et al*. The changing anatomic position of squamous cell carcinoma of the lung: a new conundrum. J Community Hosp Intern Med Perspect 2016; 6: 33299.

 https://doi.org/10.4132/jptm.2018.09.07

Journal of Pathology and Translational Medicine 2018; 52: 357-362
https://doi.org/10.4132/jptm.2018.09.13

■ ORIGINAL ARTICLE ■

The Expression of Adipophilin Is Frequently Found in Solid Subtype Adenocarcinoma and Is Associated with Adverse Outcomes in Lung Adenocarcinoma

Sun Ah Shin · Hee Young Na[1]
Ji Young Choe[2] · Doohyun Chung
Mira Park[3] · Sohee Oh[4] · Ji Eun Kim[3]

Department of Pathology, Seoul National University Hospital, Seoul; [1]Department of Pathology, Seoul National University Bundang Hospital, Seongnam; [2]Department of Pathology, Hallym University Sacred Heart Hospital, Anyang; Departments of [3]Pathology and [4]Biostatics, Seoul National University Boramae Hospital, Seoul, Korea

Received: August 7, 2018
Revised: September 5, 2018
Accepted: September 13, 2018

Corresponding Author
Ji Eun Kim, MD, PhD
Department of Pathology, Seoul National University Boramae Hospital, 20 Boramae-ro 5-gil, Dongjak-gu, Seoul 07061, Korea
Tel: +82-2-870-2642
Fax: +82-2-831-0261
E-mail: npol181@snu.ac.kr

Background: The up-regulation of the lipogenic pathway has been reported in many types of malignant tumors. However, its pathogenic role or clinical significance is not fully understood. The objective of this study was to examine the expression levels of adipophilin and related hypoxic signaling proteins and to determine their prognostic impacts and associations with the pathologic characteristics of lung adenocarcinoma. **Methods:** Expression levels of adipophilin, heat shock protein 27 (HSP27), carbonic anhydrase IX, and hypoxia-inducible factor 1α were examined by immunohistochemical staining using tissue microarray blocks. Correlations between protein expression levels and various clinicopathologic features were analyzed. **Results:** A total of 230 cases of primary adenocarcinoma of the lung were enrolled in this study. Adipophilin expression was more frequent in males and with the solid histologic type. It was correlated with HSP27 expression. Patients with adipophilin-positive adenocarcinoma showed a shorter progression-free survival (PFS) (median PFS, 17.2 months vs 18.4 months) in a univariable survival analysis, whereas HSP27 positivity correlated with favorable overall survival (OS) and PFS. In a multivariable analysis, adipophilin and HSP27 were independent prognostic markers of both OS and PFS. **Conclusions:** Activated lipid metabolism and the hypoxic signaling pathway might play a major role in the progression of lung adenocarcinoma, especially in the solid histologic type.

Key Words: Adipophilin; Lung adenocarcinoma; Hypoxia; Prognosis

Metabolic shifts, as well as mutations, are a distinguishing feature of cancer biology.[1] Cancer cells can modify their metabolic pathways to obtain more energy required for proliferation or dissemination, initially affect glucose metabolism but largely in lipid-cholesterol. Therefore, a high lipid content in cancer cells is an indicator of an aggressive potential.[2] The up-regulation of the lipid metabolism associated pathway has been reported in many malignancies, including breast cancer, retinoblastoma, lung cancer, and colon cancer.[3-6]

Although lipid droplets (LDs) are almost ubiquitously present in eukaryotic cells, lipid storage is markedly increased in diseases associated with tissue damage or ischemia, as seen in atherosclerosis or organ infarct.[7] Visualization of LDs best be facilitated by the immunohistochemical expression of adipophilin, a vehicle of small LDs in non-adipogenic cells.[8] The role of adipophilin in cancer was recently investigated, and it was found to be not only a diagnostic marker, but also an independent poor prognostic marker for certain cancers, including clear cell renal cell carcinoma and brain glioma.[9,10] However, studies about the prognostic value of adipophilin in lung cancer were limited, and the association between the adipophilin and hypoxic ischemic pathways remains unclear. The objective of this study was to investigate the clinicopathologic correlation between adipophilin and hypoxic signaling molecules in primary adenocarcinoma of the lung.

MATERIALS AND METHODS

Patients and tumor samples

Cases were selected from the archives of biopsied or resected lung adenocarcinoma samples from the Seoul National University Boramae Hostpital, between June 2005 and December 2012, and from the Seoul National University Hospital between Feb-

pISSN 2383-7837
eISSN 2383-7845

ruary 1996 and April 2009. Patients with primary lung adenocarcioma without a prior history of other malignancies or preoperative treatment were included in this study. A histological subtype of primary lung adenocarcinoma was reviewed and classified according to the 2015 World Health Organization classification. Tissue microarray blocks (TMAs) were constructed from the most representative tumor areas and consisted of two cores of tumor samples with diameters of 0.2 cm. Most samples were from resected lung specimens; however, seven were from biopsy samples, which were larger than 1 cm in diameter. Clinical information was retrieved from electric medical records. Clinical staging was estimated according to the American Joint Committee on Cancer, eighth grading system.[11] Overall survival (OS) was measured from the date of biopsy or surgery until the time of death or the last follow-up. Progression-free survival (PFS) was measured from the date of biopsy or surgery until disease progression (i.e., recurrence or metastasis) or death. This study was approved by the Institutional Review Board of Seoul National University Boramae Hospital (20180706/10-2018-69/081) and patient consent was waived.

Immunohistochemical staining

Protein expression levels of the adipophilin and hypoxic signaling markers were assessed by immunohistochemistry (IHC) from TMA blocks using an automated immunostainer (Benchmark Ventana, Tucson, AZ, USA) following the manufacturer's recommended procedure. The primary antibodies used in this study were as follows: adipophilin (1:2; Progen Biotechnik, Heidelberg, Germany), heat shock protein 27 (HSP27, 1:1,000; Novusbio, Littleton, CO, USA), carbonic anhydrase IX (CAIX, 1:1,000; Novusbio), and hypoxia-inducible factor 1α (HIF1α, 1:200, Abcam, Cambridge, UK). Expression of adipophilin was classified as positive if at least 5% of tumor cells showed cytoplasmic staining as described in a previous study.[12] Other protein markers were evaluated by the H-score: intensity multiplied by percentage of positive cells. Cases were regarded as positive when the H-score was greater than 10. All cases were independently reviewed by two pathologists (S.A.S and J.E.K), and agreement was reached for discordant cases.

Statistical analysis

All statistical analyses were performed using SPSS ver. 21.0 (IBM Co., Armonk, NY, USA). Correlations between the IHC results and clinicopathologic parameters were assessed with the chi-square test or Fisher exact test for nominal variables, and the Spearman's rank test for numeric variables. A univariable survival analysis was performed using Kaplan-Meier analysis with the log-rank test. The Cox multiple regression model was generated to confirm independent prognostic markers in the multivariable survival analysis. Statistical significance was considered when the

Table 1. Summary of the clinicopathologic characteristics of patients

Parameter	No. (%) (n=230)
Sex	
Male	108 (47.0)
Female	122 (53.0)
Age (yr)	
≤60	92 (40.0)
>60	138 (60.0)
Smoking status	
Never	136 (59.1)
Former/current	88 (38.3)
TNM category (8th)	
I	61 (26.5)
II	97 (42.2)
I+II	158 (68.7)
III	25 (10.9)
IV	15 (6.5)
III+IV	40 (17.4)
Tumor size (cm)	
<3	103 (44.8)
≥3	92 (40.0)
LN metastasis	
Negative	125 (54.3)
Positive	76 (33.0)
Distant metastasis	
Negative	186 (80.9)
Positive	28 (12.2)
EGFR	
Wild type	77 (33.5)
Mutated	83 (36.1)
Not tested	70 (30.4)
KRAS	
Wild type	119 (51.7)
Mutated	12 (5.2)
Not tested	99 (43.0)
ALK	
Wild type	225 (97.8)
Translocation	5 (2.2)
Histologic subtype	
Lepidic	9 (3.9)
Acinar	147 (63.9)
Papillary	22 (9.6)
Solid	28 (12.2)
Micropapillary	7 (3.0)
Others	17 (7.4)
Progression	
No	82 (35.7)
Yes	148 (64.3)
Death	
No	122 (53.0)
Yes	108 (47.0)

LN, lymph node; *EGFR*, epidermal growth factor receptor; *ALK*, anaplastic lymphoma kinase.

https://doi.org/10.4132/jptm.2018.09.13

two-tailed p-value was less than .05.

RESULTS

Patients and samples

The clinicopathologic characteristics for all of the cases are summarized in Table 1. A total of 230 cases (107 males and 123 females) with a median age of 63.4 years (range, 22.8 to 89.1 years) were enrolled in this study. The histologic type was lepidic in nine patients (4%), acinar in 147 (64%), papillary in 22 (10%), solid in 28 (12%), and micropapillary in seven cases (3%). The epidermal growth factor receptor (*EGFR*) mutation was found in 83 of the 160 tested samples (52%). The *KRAS* mutation was present in 12 of the 131 tested samples (9%), and the anaplastic lymphoma kinase (*ALK*) translocation was identified in five of the 230 samples. At the time of initial diagnosis, 61 patients were stage I, 97 patients were stage II, 25 patients were stage III, and 15 patients were stage IV, all according to the eighth edition of TNM classification.

Immunohistochemical results

Adipophilin expression in the cytoplasm had a spotty granular pattern, as described in the manufacturer's guidelines. Normal lung parenchymal cells were adipophilin-negative, except for alveolar macrophages, which served as the positive control.[12] Overall, 30 of the 230 cases (13%) were adipophilin-positive. Most cases (19 of 30, 63%) showed pan-cytopalsmic patterns, while 11 (37%) showed subnuclear basal staining patterns (Fig. 1). Positive expression of HSP27 was found in 146 cases (63%), while CAIX showed positive staining in the cytoplasm in 129 cases (56%). However, HIF1α was only positive in two cases (1%) (Fig. 2).

Association of protein expression with clinicopathologic features

Adipophilin positivity was significantly higher in males and in the solid histologic subtype (Fig. 3), and correlated with HSP27 expression (all $p < .05$). Expression of HSP27 was associated with smaller tumor sizes, low TNM stages, frequent *EGFR* mutation, and negative or low HIF1α (all $p < .01$).

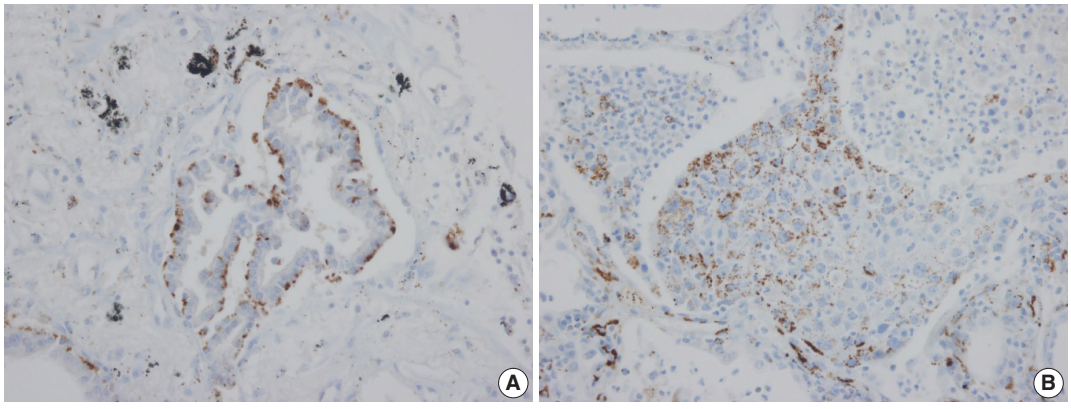

Fig. 1. Immunohistochemical staining pattern of Adipophilin in adenocarcinoma. (A) Subnuclear basal staining pattern in acinar type adenocarcinoma. (B) Pancytoplasmic pattern in solid type adenocarcinoma.

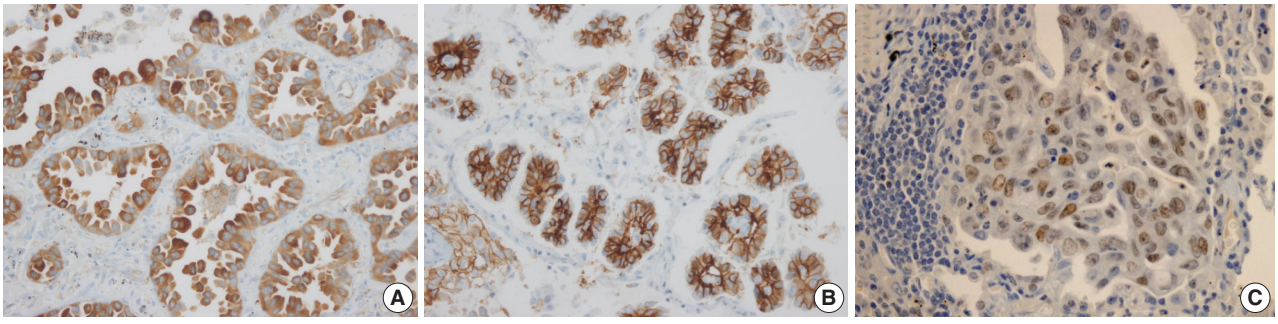

Fig. 2. Expression of hypoxic signaling proteins in lung adenocarcinoma. Strong cytoplasmic positivity of heat shock protein 27 (A) and carbonic anhydrase IX (B) is found. Nuclear expression of hypoxia-inducible factor 1α is only focally present (C).

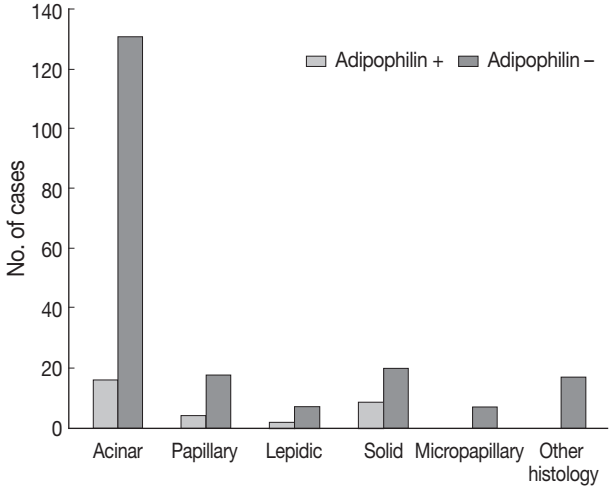

Fig. 3. Adipophilin expression according to predominant subtype of adenocarcinoma.

Clinical significance of expression of adipophilin or HSP27

The median follow-up of patients was 49.55 months (range, 1.2 to 162.7 months). Recurrence or progression was found in 148 patients, and 108 patients were deceased during the follow-up period. In the univariable survival analysis, patients with adipophilin positive tumors showed significantly shorter PFS (median, 17.2 months vs 18.4 months; p = .041) compared to those with adipophilin negative tumors, although there was no significant difference in OS. However, the expression of HSP27 was associated with better OS and PFS (p = .032 and p = .002, respectively) (Fig. 4). Other poor prognostic markers included younger patients, vascular invasion, larger tumor sizes, solid histology, and advanced TNM stages. The multivariable Cox regression analysis was performed after integrating parameters were found to have prognostic significances in the univariable analysis. As a result, adipophilin expression was an independent marker of disease progression only, whereas HSP27 expression indicated better survival in both OS and PFS (Table 2).

DISCUSSION

The goal of this study was to investigate the association of lipid metabolism with hypoxic signaling and to determine clinicopathologic significances of these molecules in primary lung adenocarcinoma. Our results showed that adipophilin was more frequently expressed in male patients with solid variant adenocarcinoma. Its expression was associated with HSP27. Moreover, the expression of adipophilin or HSP27 was an independent prognostic factor, although they behaved in a reciprocal manner.

Very few studies have focused on lipid metabolism or adipophilin in lung cancer, and its pathologic role and clinical significance remain unclear. One previous study reported that the adipophilin expression level was significantly higher in lung adenocarcinoma than in squamous cell carcinoma. However, that study failed to find any clinicopathologic significance, primarily due to insufficient numbers of cohorts.[13] In contrast, the positive rate of adipophilin expression in squamous cell carcinoma in our study was higher than that in adenocarcinoma (25% vs 13%, unpublished data). Another recent study by Fujimoto *et al*.[12] found that adipophilin positivity was associated with apocrine-like features and worse outcomes in lung adenocarcinoma. Our results partially coincided with that study with regard to prognostication. However, we could not find apocrine-like histologic patterns represented by the eosinophilic granular cytoplasm. The only relative predominance of a solid histologic pattern in adipophilin positive tumors was found in our study. Among various malignancies, one of the best-known examples of adipophilin positive tumors are renal cell carcinomas and ductal carcinomas of the breast, characterized by frequent solid architectures and plump cytoplasms.[9,14] Taken together, these results suggested that the lipidogenic pathway is activated in adenocarcinoma with solid phenotypes in various organs.

The accumulation of LDs is a common finding in the tissues after ischemic injury, as seen in atherosclerosis or organ infarct.[7] Ischemia followed by activation of hypoxic signaling is a typical finding of malignant tumors, and is strongly associated with aggressive behavior.[9,10] Recent studies demonstrated that the fractional contribution of glutamine to fatty acid synthesis increased during hypoxia.[15] We hypothesized that the coordination of metabolic deregulation and hypoxic signaling contributed to the biologic aggressiveness of lung adenocarcinomas. The strong correlation between adipophilin expression and HSP27 in our study supported this hypothesis. To further verify our hypothesis, we examined several well-known biomarkers in hypoxic signaling, including HIF1α, a master regulator of hypoxia and related proteins. Although the expression of HSP27 and CAIX was frequently found regardless of histologic type, the expression of HIF1α was particularly low. One possible cause of such low positivity of HIF1α might be the extremely short half-life of that protein. The ubiquitin-proteasome pathway is responsible for the stability of HIF1α, which is rapidly degraded in normoxia, resulting in undetectable levels in immunohistochemistries.[16] Previous studies found inconsistent results of HIF1α expression in various cancers, and many studies suggested that HIF1α stability was regulated in a cell-type specific manner.[16] Although we cannot completely explain the low HIF1α incidence in our subjects, many of the

https://doi.org/10.4132/jptm.2018.09.13

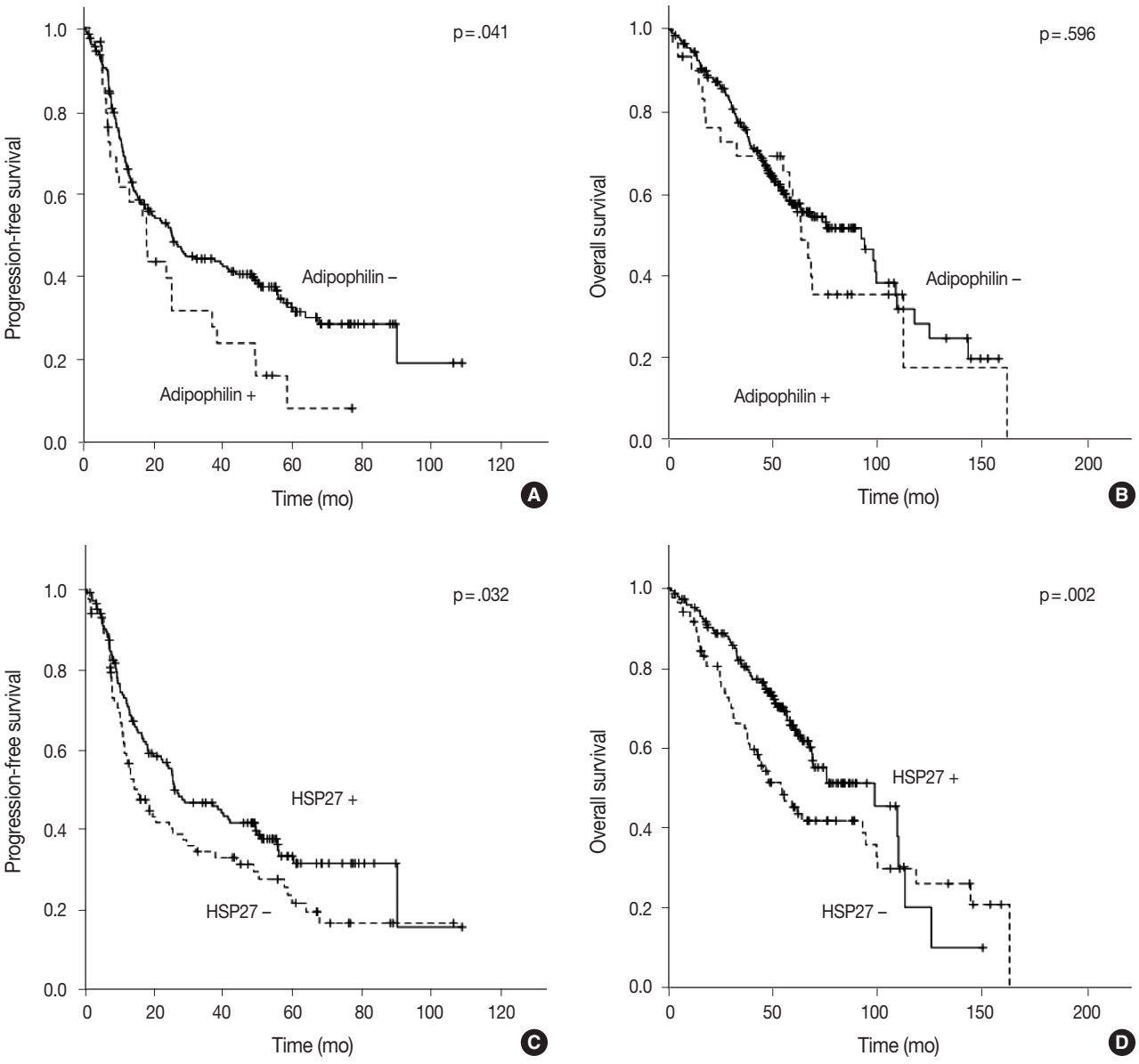

Fig. 4. Results of univariable survival analysis represented by Kaplan-Meier plots according to protein expression. Expression of adipophilin is significantly associated with worse progression-free survival (PFS) (A) but is not related to overall survival (OS) (B). Heat shock protein 27 shows poor prognostic impacts in both PFS (C) and OS (D).

Table 2. Results of multivariate Cox regression analysis

Variable	Overall survival			Progression free survival		
	HR	95% CI	p-value	HR	95% CI	p-value
Age (>60 yr)	0.542	0.250–1.173	.120	0.561	0.260–1.208	.140
Tumor size (≥3 cm)	1.168	0.511–2.668	.713	1.627	0.686–3.858	.269
TNM (III, IV vs I, II)	8.355	3.486–20.029	<.001***	8.318	3.322–20.832	<.001***
EGFR mutation	0.637	0.270–1.501	.302	1.209	0.531–2.751	.651
Vascular invasion	1.132	0.456–2.808	.789	1.024	0.415–2.524	.959
Adipophilin (≥5%)	4.467	1.783–11.190	.001**	4.476	1.792–11.183	.001**
HSP27 (≥0 by H score)	0.280	0.123–0.641	.003**	0.391	0.170–0.897	.027*

HR, hazard ratio; CI, confidence interval; *EGFR*, epidermal growth factor receptor; HSP27, heat shock protein 27.
Statistically significant *p<.05, **p<.01, ***p<.001.

factors listed above might have contributed to its low immunoreactivity.

An interesting observation of this study was the reciprocal action of adipophilin and HSP27 in terms of prognostication. As expected, adipophilin was an independent negative prognostic factor of lung adenocarcinoma. However, its prediction was inversed in HSP27, even with the strong correlation between two proteins. It is believed that HSP27 has either a protective or a counter-protective role in various malignancies.[17] Typically, HSP27 responds to hypoxic conditions to lower reactive oxygen species in a protective way. This protection also provides a shelter for both normal and cancer cells. In this study, the frequent expression of HSP27 or CAIX indicated activation of hypoxic signaling and possible link of metabolic deregulation. However, further research, including functional studies, are needed to better understand the precise interaction between these proteins.

In conclusion, adipophilin positivity was common in solid histologic types of lung adenocarcinoma, and was associated with adverse outcomes. The deregulation of lipid metabolism with hypoxic signaling might play a role in the pathogenesis of lung adenocarcinoma.

ORCID

Ji Eun Kim: https://orcid.org/0000-0002-2156-9875

Conflicts of Interest

No potential conflict of interest relevant to this article was reported.

Acknowledgments

This study was supported by the Grant of National Research Foundation of Korea (2017R1A2B4005052).

REFERENCES

1. Hsu PP, Sabatini DM. Cancer cell metabolism: Warburg and beyond. Cell 2008; 134: 703-7.
2. Beloribi-Djefaflia S, Vasseur S, Guillaumond F. Lipid metabolic reprogramming in cancer cells. Oncogenesis 2016; 5: e189.
3. Alo PL, Visca P, Marci A, Mangoni A, Botti C, Di Tondo U. Expression of fatty acid synthase (FAS) as a predictor of recurrence in stage I breast carcinoma patients. Cancer 1996; 77: 474-82.
4. Camassei FD, Cozza R, Acquaviva A, *et al*. Expression of the lipogenic enzyme fatty acid synthase (FAS) in retinoblastoma and its correlation with tumor aggressiveness. Invest Ophthalmol Vis Sci 2003; 44: 2399-403.
5. Migita T, Narita T, Nomura K, *et al*. ATP citrate lyase: activation and therapeutic implications in non-small cell lung cancer. Cancer Res 2008; 68: 8547-54.
6. Luque-García JL, Martínez-Torrecuadrada JL, Epifano C, Cañamero M, Babel I, Casal JI. Differential protein expression on the cell surface of colorectal cancer cells associated to tumor metastasis. Proteomics 2010; 10: 940-52.
7. Straub BK, Gyoengyoesi B, Koenig M, *et al*. Adipophilin/perilipin-2 as a lipid droplet-specific marker for metabolically active cells and diseases associated with metabolic dysregulation. Histopathology 2013; 62: 617-31.
8. Heid HW, Moll R, Schwetlick I, Rackwitz HR, Keenan TW. Adipophilin is a specific marker of lipid accumulation in diverse cell types and diseases. Cell Tissue Res 1998; 294: 309-21.
9. Tolkach Y, Luders C, Meller S, Jung K, Stephan C, Kristiansen G. Adipophilin as prognostic biomarker in clear cell renal cell carcinoma. Oncotarget 2017; 8: 28672-82.
10. Kohe S, Colmenero I, McConville C, Peet A. Immunohistochemical staining of lipid droplets with adipophilin in paraffin-embedded glioma tissue identifies an association between lipid droplets and tumour grade. J Histol Histopathol 2017; 4: 4.
11. Brierley JD, Gospodarowicz MK, Wittekind C. TNM classfication of malignant tumours. 8th ed. Oxford: Wiley-Blackwell, 2017.
12. Fujimoto M, Yoshizawa A, Sumiyoshi S, *et al*. Adipophilin expression in lung adenocarcinoma is associated with apocrine-like features and poor clinical prognosis: an immunohistochemical study of 328 cases. Histopathology 2017; 70: 232-41.
13. Zhang XD, Li W, Zhang N, *et al*. Identification of adipophilin as a potential diagnostic tumor marker for lung adenocarcinoma. Int J Clin Exp Med 2014; 7: 1190-6.
14. Moritani S, Ichihara S, Hasegawa M, *et al*. Intracytoplasmic lipid accumulation in apocrine carcinoma of the breast evaluated with adipophilin immunoreactivity: a possible link between apocrine carcinoma and lipid-rich carcinoma. Am J Surg Pathol 2011; 35: 861-7.
15. Kamphorst JJ, Cross JR, Fan J, *et al*. Hypoxic and Ras-transformed cells support growth by scavenging unsaturated fatty acids from lysophospholipids. Proc Natl Acad Sci U S A 2013; 110: 8882-7.
16. Zheng X, Ruas JL, Cao R, *et al*. Cell-type-specific regulation of degradation of hypoxia-inducible factor 1 alpha: role of subcellular compartmentalization. Mol Cell Biol 2006; 26: 4628-41.
17. Kaigorodova EV, Bogatyuk MV. Heat shock proteins as prognostic markers of cancer. Curr Cancer Drug Targets 2014; 14: 713-26.

Journal of Pathology and Translational Medicine 2018; 52: 363-368
https://doi.org/10.4132/jptm.2018.09.18

■ ORIGINAL ARTICLE ■

Immunohistochemistry of Janus Kinase 1 (JAK1) Expression in Vitiligo

Asmaa Gaber Abdou · Alaa Maraee[1]
Hossam Yassien[1] · Mona Sarhan[1]

Departments of Pathology and [1]Dermatology, Faculty of Medicine, Menoufia University, Shebein Elkom, Egypt

Received: August 5, 2018
Revised: September 16, 2018
Accepted: September 18, 2018

Corresponding Author
Asmaa Gaber Abdou, MD
Department of Pathology, Faculty of Medicine, Menoufia University, Shebein Elkom 32511, Egypt
Tel: +20-048-2281714
Fax: +20-048-2233521
E-mail: Asmaa_elsaidy@yahoo.com

Background: Vitiligo is a chronic autoimmune disease in which the destruction of melanocytes causes white spots on the affected skin. Janus kinase (JAK) is a family of intracellular, non-receptor tyrosine kinases that transduce cytokine-mediated signals via the JAK–signal transducer and activator of transcription pathway. The aim of the present study is to explore the possible role of JAK1 in the pathogenesis of vitiligo using immunohistochemical methods. **Methods:** The current study was conducted in a sample of 39 patients who presented with vitiligo and 22 healthy individuals who were age and sex matched as a control group. We used immunohistochemistry to evaluate JAK1 status (intensity and distribution) and assess the percentage of residual melanocytes using human melanoma black 45 (HMB45). **Results:** Intense and diffuse JAK1 expression was significantly more likely to indicate vitiliginous skin compared to normal skin ($p < .001$). Strong and diffuse JAK1 expression was associated with short disease duration, female sex, and lower percentage of melanocytes (detected by HMB45) ($p < .05$). **Conclusions:** JAK1 may be involved in the pathogenesis of vitiligo, as indicated by intense and diffuse expression compared to control and association with lower percentage of melanocytes detected by HMB45 immunostaining.

Key Words: Vitiligo; Janus kinase 1; HMB45; Immunohistochemistry

Vitiligo is a chronic autoimmune disease that results from destruction of melanocytes, causing white spots on the affected skin. Vitiligo affects approximately 1% of people worldwide and can affect both adults and children, causing diminished quality of life and marked psychological distress.[1]

Janus kinase (JAK) is a family of intracellular, non-receptor tyrosine kinases that transduce cytokine-mediated signals via the JAK–signal transducer and activator of transcription (STAT) pathway. Approximately 2,000 kinases are known, and more than 90 protein tyrosine kinases (PTKs) have been found in the human genome.[2]

The JAK family differs markedly from other classes of PTKs due to the presence of an additional kinase domain. To denote this unique structural feature, these kinases were renamed "Janus kinases" in reference to the ancient two-faced Roman god of gates and doorways. The members of this tyrosine kinase family include JAK1, JAK2, JAK3, and tyrosine kinase 2.[3]

Studies have shown that various cytokines including interferon γ (IFN-γ),[4,5] tumor necrosis factor α,[6] and chemokine (C-C motif) ligand 22[7] are differentially expressed in the lesional skin and serum of vitiligo patients compared to controls, indicating roles in vitiligo. IFN-γ bound receptor complex recruits JAK1 and JAK2 kinases, leading to phosphorylation and nuclear translocation of STAT, which in turn transcriptionally activates downstream IFN-γ–inducible genes. The use of JAK1/3 inhibitors such as tofacitinib may effectively lead to blockade of IFN-γ signaling and downstream CXCL10 expression, thus giving rise to repigmentation in vitiligo.[8]

The current study aimed to explore the role of JAK1 in the pathogenesis of vitiligo using immunohistochemical methods.

MATERIALS AND METHODS

This prospective case-control study was carried out in a sample of 61 cases, comprising 39 patients who presented with vitiligo and 22 individuals without vitiligo who were age- and sex-matched as a control group. Cases were selected from the Dermatology Outpatient Clinic, Menoufia University Hospital, from February 2017 to July 2017.

Biopsies were performed in 22 apparently healthy age-, sex-, and site-matched normal subjects who were selected as a control group from the Department of Plastic Surgery, Faculty of Medicine, Menoufia University, between February 2017 and July 2017.

A written consent form was approved by the Committee of Human Rights in Research at Menoufia University (443/2018) and obtained from every participant before study initiation.

Exclusion criteria were as follows: (1) patients who received local or systemic treatment before the start of the study; (2) patients

pISSN 2383-7837
eISSN 2383-7845

who had other autoimmune diseases; and (3) patients less than 18 years of age.

All patients were subjected to the following: complete history including age, sex, onset of disease (younger than 20 years or at and older than 20 years), and disease course assessed by vitiligo disease activity (VIDA) score.[9] Duration of lesion(s) expressed in years, sites, and extension of the lesions and family history of similar conditions were also assessed.

Examination

Detailed dermatological examinations were performed to classify types (segmental and nonsegmental) and distribution (acral, acrofacial, focal, vulgaris, segmental, and generalized) of vitiligo.

Skin biopsy

The patients did not receive any treatment (local or systemic) for at least one month before biopsy. A 3-mm punch biopsy was performed in involved skin of each patient under local anesthesia and in control subjects. Biopsy samples were fixed in neutral formalin 10% and submitted for routine tissue processing in paraffin embedded blocks to the Pathology Department, Faculty of Medicine, Menoufia University. Several 4-μm-thick paraffin embedded sections were cut from each block. One section from each block was stained with hematoxylin and eosin to evaluate pathological changes, while the remaining sections were cut on positive charged slides for immunostaining detection of JAK1 and human melanoma black 45 (HMB45).

Histopathological evaluation

Hematoxylin and eosin–stained slides were examined microscopically to evaluate and verify epidermal and dermal pathological changes: (1) evaluation of dermal perivascular inflammatory infiltrate density, divided into mild, moderate and severe; (2) signs of pigmentation in the form of residual melanin in epidermis or dermal melanophages and defined as present or absent.

Immunohistochemical staining

The method used for immunostaining was a streptavidin-biotin–amplified system. The primary antibodies were rabbit polyclonal antibody against JAK (diluted to 1/100 in antibody diluent; cat. No. Gtx55099, -P1, or –P; 1.0 mL at 100 μg/mL; Genetex, Irvine, CA, USA) and mouse monoclonal antibody directed against HMB45 (ready to use, clone HMB-45, Dako, Copenhagen, Denmark). Slides were subjected to deparaffinization and rehydration. Antigen retrieval was performed by boiling in citrate buffer saline (pH 6), followed by cooling at room temperature. Endogenous perioxidase was blocked by incubation with H_2O_2, 3%. The primary antibodies were incubated overnight at room temperature, and then the secondary antibody (ready-to-use, Ultravision detection system anti-polyvalent HRP/DAB, Neomarker, Labvision Corp., Fremont, CA, USA) was applied with DAB as a chromogenic substrate and Mayer's hematoxylin as a counter stain. Human breast cancer was used as a positive control for JAK. Replacement of the primary antibody in the staining procedure with a blocking buffer was included as a negative control.

Table 1. Clinicopathological data of vitiligo patients

Characteristic	No. (%)
Age (yr)	
Mean ± SD	34.95 ± 15.05
Median (range)	27.00 (18–64)
Disease duration (yr)	
Mean ± SD	5.13 ± 3.62
Median (range)	4.00 (2–15)
Sex	
Male	16 (41)
Female	23 (59)
Onset (yr)	
< 20	10 (25.6)
≥ 20	29 (74.4)
Family history	
Negative	26 (66.7)
Positive	13 (33.3)
Type	
Acral	10 (25.6)
Acrofacial	6 (15.4)
Focal	3 (7.7)
Generalized	3 (7.7)
Segmental	4 (10.3)
Vulgaris	13 (33.3)
Distribution	
NSV	13 (33.3)
SV	26 (66.7)
Melanin	
Absent	22 (56.4)
Present	17 (43.6)
Dermal inflammation	
Mild	26 (66.7)
Moderate	13 (33.3)
HMB45 status	
Negative	16 (41.0)
Positive	23 (59.0)
HMB-45 (%)	
Mean ± SD	18.17 ± 27.99
Median (range)	1.00 (0–90)

SD, standard deviation; NSV, non-segmental vitiligo; SV, segmental vitiligo; HMB45, human melanoma black 45.

https://doi.org/10.4132/jptm.2018.09.18

Interpretation of JAK1immunohistochemical staining

Positive expression was identified when cytoplasmic expression was seen in any cells. The intensity of expression was evaluated subjectively according to depth of immunostaining as mild (+), moderate (++), and strong (+++). The distribution of staining was diffuse when staining was seen in all epidermal layers and focal otherwise.

Interpretation of HMB45 immunohistochemical staining

Membranous expression in any number of cells was considered positive for HMB45. The percentage of positive cells (melanocytes) in relation to the number of basal keratinocytes was evaluated and expressed as mean, median, and range.

Statistical analysis

Data were collected, tabulated, and statistically analyzed using a personal computer with SPSS ver. 23 (IBM Corp., Armonk, NY, USA). The chi-square and Fisher exact tests were used for comparisons between qualitative variables. The Mann-Whitney U test and Kruskal-Wallis tests were used for comparisons between quantitative variables. $p < .05$ was considered significant.

RESULTS

The clinical data for vitiligo patients are presented in Table 1.

Immunohistochemical results of JAK1expression in vitiligo patients and controls

JAK1 was expressed in all involved vitiliginous skin (100%), with mild intensity in 18 cases (46.2%) (Fig. 1A), moderate intensity in nine cases (23.1%) (Fig. 1B), and strong intensity in 12 cases (30.8%) (Fig. 1C). There was focal distribution of JAK1 in 21 cases (53.8%) (Fig. 1A) and diffuse expression (Fig. 1A, C) in 18 cases (46.3%). JAK1 expression was mild and exhibited focal distribution in all control samples (Fig. 1D). Only one case of vitiliginous skin showed nuclear and cytoplasmic expression of JAK 1 (Fig. 1B). There was a significant difference in JAK1 expression between vitiliginous and normal skin ($p < .001$) since intense and diffuse expression was significantly more frequent in vitiliginous skin (Table 2).

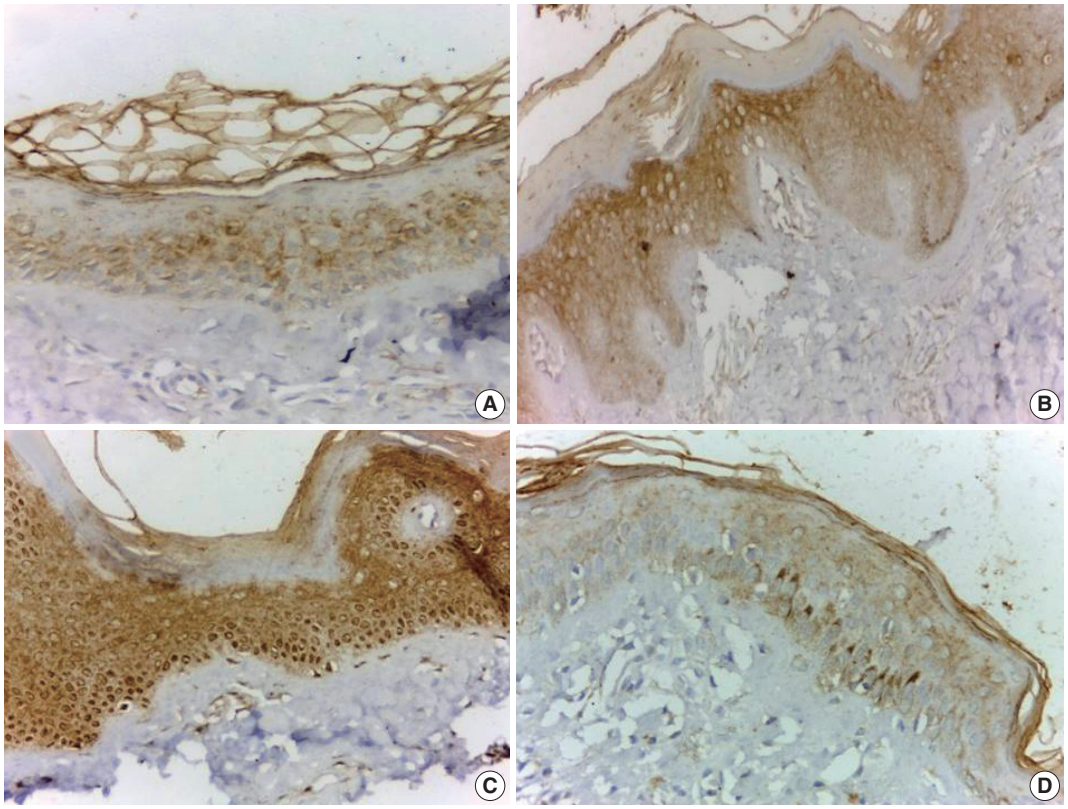

Fig. 1. Vitiliginous skin shows mild and focal cytoplasmic staining (A), moderate and diffuse cytoplasmic staining (B), and strong diffuse cytoplasmic and nuclear staining (C). Normal skin shows mild and focal cytoplasmic staining (D).

Relationships between intensity of JAK1 expression in vitiliginous lesions and clinicopathological variables

JAK1 intensity of expression was associated with disease duration (p = .030), sex (p = .003), presence of melanin pigment (p = .007), and percentage of HMB45 (p = .002). Strong JAK1 expression was associated with short disease duration, female sex, presence of lesional melanin pigment, and lower percentage of HMB45 compared to moderate and mild cases (Table 3). When mild and moderate cases were lumped together versus strong cases by intensity of JAK1, the same correlations were found except for the association with sex (data not shown).

Table 2. JAK1 immunohistochemical expression in the skin of vitiligo patients and controls

JAK	Case (n = 39)	Control (n = 22)	Chi-square test	p-value
Distribution			14.40	< .001
Focal	21 (53.8)	22 (100)		
Diffuse	18 (46.2)	0		
Intensity			18.06	< .001
Mild	18 (46.2)	22 (100)		
Moderate	9 (23.1)	0		
Strong	12 (30.8)	0		

JAK, Janus kinase.

Relationships between distribution of JAK1 expression in vitiliginous lesions and clinicopathological variables

JAK1 distribution (diffuse vs focal) was associated with disease duration (p = .030), sex (p = .020), and percentage of HMB45 (p = .001). Since diffuse expression was associated with short disease duration, female sex, and lower percentage of HMB45 compared to cases with long disease duration, male sex and high percentage HMB45 showed focal expression (Table 4).

Table 3. The relationships between intensity of JAK1expression and clinicopathological parameters in vitiligo patients

Clinicopathological parameter	Mild (n = 18)	Moderate (n = 9)	Strong (n = 12)	Statistical test	p-value
Age (yr)					
Mean ± SD	37.00 ± 17.60	38.33 ± 12.76	29.33 ± 11.57	3.48[a]	.170
Median (range)	35.00 (18–64)	33.00 (27–55)	22.00 (21–45)		
Disease duration (yr)					
Mean ± SD	5.67 ± 4.35	6.00 ± 3.00	3.67 ± 2.46	6.53[a]	.030*
Median (range)	4.00 (3–15)	4.00 (4–10)			
Sex				11.44[b]	.003*
Male	12 (66.7)	0	4 (33.3)		
Female	6 (33.3)	9 (100)	8 (66.7)		
Onset (yr)				4.03[b]	.130
< 20	6 (33.3)	0	4 (33.3)		
≥ 20	12 (66.7)	9 (100)	8 (66.7)		
Family history				0.000[b]	> .999
Negative	12 (66.7)	6 (66.7)	8 (66.7)		
Positive	6 (33.3)	3 (33.3)	4 (33.3)		
Distribution				0.000[b]	> .999
NSV	6 (33.3)	3 (33.3)	4 (33.3)		
SV	12 (66.7)	6 (66.7)	8 (66.7)		
Melanin				9.85[b]	.007*
Absent	9 (50.0)	9 (100)	4 (33.3)		
Present	9 (50.0)	0	8 (66.7)		
Dermal inflammation				0.000[b]	> .999
Mild	12 (66.7)	6 (66.7)	8 (66.7)		
Moderate	6 (33.3)	3 (33.3)	4 (33.3)		
HMB45 status				1.11[b]	.570
Negative	9 (50)	3 (33.3)	4 (33.3)		
Positive	9 (50)	6 (66.7)	8 (66.7)		
HMB45 (%)				12.20[a]	.002*
Mean ± SD	34.38 ± 34.59	6.66 ± 6.61	2.5 ± 4.52		
Median (range)	30.00 (0–90)	10.00 (0–15)	4.52 (0–10)		

JAK, Janus kinase 1; SD, standard deviation; NSV, non-segmental vitiligo; SV, segmental vitiligo; HMB45, human melanoma black 45.
*Significant.
[a]Kruskal-Wallis test; [b]Fisher exact test.

https://doi.org/10.4132/jptm.2018.09.18

Table 4. The distribution of JAK1 expression and clinicopathological variables in vitiligo patients

Clinicopathological parameter	Focal (n=21)	Diffuse (n=18)	Statistical test	p-value
Age (yr)				
Mean±SD	36.43±16.29	33.22±13.71	0.17[a]	.860
Median (range)	33.00 (18–64)	27.00 (21–55)		
Disease duration (yr)			2.16[a]	.030*
Mean±SD	6.29±4.30	3.78±1.98		
Median (range)	4.00 (3–15)	4.00 (2–7)		
Sex			4.88[b]	.020*
Male	12 (57.1)	4 (22.2)		
Female	9 (42.9)	14 (77.8)		
Onset (yr)			0.21[c]	.650
<20	6 (28.6)	4 (22.2)		
≥20	15 (71.4)	14 (77.8)		
Family history				
Negative	12 (57.1)	14 (77.8)	1.85[b]	.170
Positive	9 (42.9)	4 (22.2)		
Distribution				
NSV	6 (28.6)	7 (38.9)	0.46[b]	.490
SV	15 (71.4)	11 (61.1)		
Melanin			0.01[b]	.920
Absent	12 (57.1)	10 (55.6)		
Present	9 (42.9)	8 (44.4)		
Dermal inflammation				
Mild	15 (71.4)	11 (61.1)	0.46[b]	.490
Moderate	6 (28.6)	7 (38.9)		
HMB45 status			0.06[b]	.800
Negative	9 (42.9)	7 (38.9)		
Positive	12 (57.1)	11 (61.1)		
HMB45 (%)			3.42[a]	.001*
Mean±SD	30.90±33.18	3.33±4.85		
Median (range)	15.00 (0–90)	0 (0–10)		

JAK1, Janus kinase 1; SD, standard deviation; NSV, non-segmental vitiligo; SV, segmental vitiligo; HMB45, human melanoma black 45.
*Significant.
[a]Mann-Whitney test; [b]Chi-square test; [c]Fisher exact test.

DISCUSSION

The current study demonstrated intense and diffuse JAK1 expression in lesional skin of vitiligo patients compared to controls, where the latter showed mild and focal JAK 1 expression. Our findings agree with those of Nada *et al*.,[10] who found that the level of JAK1 was significantly higher in vitiligo patients than controls. Furthermore, they found that the level of JAK1 in the skin of vitiligo patients after exposure to ultraviolet rays was significantly decreased in comparison to the level before treatment.[10] These findings suggest that JAK1 plays a role in the pathogenesis of vitiligo, and that JAK1 inhibitors may be useful for treatment of vitiligo.[10] JAK inhibitors are reported to delay the onset and reduce the severity of atopic dermatitis-like lesions, resulting in reductions of Th1 and Th2 responses.[11]

JAK1 level (intensity and distribution) was associated with sex in vitiligo patients in the present study, as it showed significantly more intense and diffuse expression in females compared to males. No prior studies support or contradict this finding. However, JAKs play important roles in adipose tissue development,[12] and females usually have more fatty tissue compared to males, which could explain the high level of JAK in females.

In the current study, we demonstrated that vitiligo cases of short duration were associated with diffuse and intense JAK1 expression compared to cases with prolonged duration. Ineterleukin 17 (IL-17) in patients with vitiligo was previously correlated positively with early age of vitiligo onset and may contribute to immune response in early onset disease through activation by a different pathway.[13] IL-17 activates nuclear factor-kB (NF-κB) and mitogen-activated protein kinase pathways. The adaptor protein NF-κB activator 1 plays an essential role in IL-17–dependent signaling, as well as in activation of JAK1-associated phosphoionositide 3-kinase.[14] On the other hand, positive correlation between JAK1 and long disease duration has been reported in psoriasis, according to Nada *et al*. (2018),[10] a relationship that highlights the major role of JAK1 in the pathogenesis of psoriasis.

According to the present study, lower percentages of HMB45 were associated with strong and diffuse JAK1 expression in vitiligo lesions. This suggests a role of JAK1 in promoting melanocyte destruction and disappearance. The activation of JAK1 was primarily responsible for transmission of promigration signals that antagonized proliferation and melanogenesis.[15] The association of intense JAK1 expression with the presence of melanin may indicate a role in melanocyte destruction, since melanin was usually present in the dermis due to pigment incontinence descending from the epidermis.

Contradicting our findings, a previous study found that increasing STAT activation was accompanied by up-regulation of JAK, where STATs display significant level of activity in melanocytes and play roles in the survival and growth of melanoma cells.[16] However, Nada *et al*. (2018)[10] were unable to detect correlations between JAK1 level and clinical and pathological parameters in vitiligo.

Although moderate and strong JAK1 indicated moderate inflammation (Table 3), and diffuse JAK1 expression was more likely in cases of moderate inflammation than focal JAK1 (Table 4), these differences were not significant. This may be due to the limited number of cases in the sample and the absence of cases with intense inflammation

In summary, JAK1 may be involved in the pathogenesis of vitiligo, indicated by its intense and diffuse expression in the skin of vitiligo patients compared to controls and its association with lower percentages of melanocytes detected by HMB45 immunostaining. The association between vitiligo cases of short duration with intense and diffuse JAK1 expression may reflect its immunomodulatory role. Further studies including several clinical types of vitiligo with different VIDA scores are recommended to verify and elucidate the possible role of JAK1 in the etiopathogenesis of vitiligo.

ORCID

Asmaa Gaber Abdou: https://orcid.org/0000-0002-5095-2937

Conflicts of Interest

No potential conflict of interest relevant to this article was reported.

REFERENCES

1. Bonotis K, Pantelis K, Karaoulanis S, *et al*. Investigation of factors associated with health-related quality of life and psychological distress in vitiligo. J Dtsch Dermatol Ges 2016; 14: 45-9.
2. Bhise SB, Nalawade AD, Wadhawa H. Role of protein tyrosine kinase inhibitors in cancer therapeutics. Indian J Biochem Biophys 2004; 41: 273-80.
3. Rane SG, Reddy EP. Janus kinases: components of multiple signaling pathways. Oncogene 2000; 19: 5662-79.
4. Basak PY, Adiloglu AK, Koc IG, Tas T, Akkaya VB. Evaluation of activatory and inhibitory natural killer cell receptors in non-segmental vitiligo: a flow cytometric study. J Eur Acad Dermatol Venereol 2008; 22: 970-6.
5. van den Boorn JG, Konijnenberg D, Dellemijn TA, *et al*. Autoimmune destruction of skin melanocytes by perilesional T cells from vitiligo patients. J Invest Dermatol 2009; 129: 2220-32.
6. Attwa E, Gamil H, Assaf M, Ghonemy S. Over-expression of tumor necrosis factor-alpha in vitiligo lesions after narrow-band UVB therapy: an immunohistochemical study. Arch Dermatol Res 2012; 304: 823-30.
7. Klarquist J, Denman CJ, Hernandez C, *et al*. Reduced skin homing by functional Treg in vitiligo. Pigment Cell Melanoma Res 2010; 23: 276-86.
8. Craiglow BG, King BA. Tofacitinib citrate for the treatment of vitiligo: a pathogenesis-directed therapy. JAMA Dermatol 2015; 151: 1110-2.
9. Bhor U, Pande S. Scoring systems in dermatology. Indian J Dermatol Venereol Leprol 2006; 72: 315-21.
10. Nada HR, El Sharkawy DA, Elmasry MF, Rashed LA, Mamdouh S. Expression of Janus kinase 1 in vitiligo & psoriasis before and after narrow band UVB: a case-control study. Arch Dermatol Res 2018; 310: 39-46.
11. Landry DA, Sormany F, Haché J, Roumaud P, Martin LJ. Steroidogenic genes expressions are repressed by high levels of leptin and the JAK/STAT signaling pathway in MA-10 Leydig cells. Mol Cell Biochem 2017; 433: 79-95.
12. Bassiouny DA, Shaker O. Role of interleukin-17 in the pathogenesis of vitiligo. Clin Exp Dermatol 2011; 36: 292-7.
13. Qian Y, Liu C, Hartupee J, *et al*. The adaptor Act1 is required for interleukin 17-dependent signaling associated with autoimmune and inflammatory disease. Nat Immunol 2007; 8: 247-56.
14. Alexeev V, Yoon K. Distinctive role of the cKit receptor tyrosine kinase signaling in mammalian melanocytes. J Invest Dermatol 2006; 126: 1102-10.
15. Kortylewski M, Jove R, Yu H. Targeting STAT3 affects melanoma on multiple fronts. Cancer Metastasis Rev 2005; 24: 315-27.
16. Nakagawa R, Yoshida H, Asakawa M, *et al*. Pyridone 6, a pan-JAK inhibitor, ameliorates allergic skin inflammation of NC/Nga mice via suppression of Th2 and enhancement of Th17. J Immunol 2011; 187: 4611-20.

Journal of Pathology and Translational Medicine 2018; 52: 369-377
https://doi.org/10.4132/jptm.2018.09.19

ORIGINAL ARTICLE

High Cytoplasmic CXCR4 Expression Predicts Prolonged Survival in Triple-Negative Breast Cancer Patients Treated with Adjuvant Chemotherapy

Bobae Shim · Min-Sun Jin[1]
Ji Hye Moon · In Ae Park
Han Suk Ryu

Department of Pathology, Seoul National University Hospital, Seoul National University College of Medicine, Seoul; [1]Department of Pathology, Bucheon St. Mary's Hospital, College of Medicine, The Catholic University of Korea, Bucheon, Korea

Received: August 7, 2018
Revised: September 12, 2018
Accepted: September 18, 2018

Corresponding Author
Han Suk Ryu, MD, PhD
Department of Pathology, Seoul National University Hospital, Seoul National University College of Medicine, 101 Daehak-ro, Jongno-gu, Seoul 03080, Korea
Tel: +82-2-2072-3361
Fax: +82-2-743-5530
E-mail: karlnash@naver.com

Background: Chemokine receptor CXC chemokine receptor type 4 (CXCR4) and its ligand CXC motif chemokine 12 (CXCL12; stromal cell-derived factor-1) are implicated in tumor growth, metastasis, and tumor cell-microenvironment interaction. A number of studies have reported that increased CXCR4 expression is associated with worse prognosis in triple-negative breast cancer (TNBC), but its prognostic significance has not been studied in TNBC patients treated with adjuvant chemotherapy. **Methods:** Two hundred eighty-three TNBC patients who received adjuvant chemotherapy were retrospectively analyzed. Tissue microarray was constructed from formalin-fixed, paraffin-embedded tumor tissue and immunohistochemistry for CXCR4 and CXCL12 was performed. Expression of each marker was compared with clinicopathologic characteristics and outcome. **Results:** High cytoplasmic CXCR4 expression was associated with younger age ($p = .008$), higher histologic grade ($p = .007$) and lower pathologic stage ($p = .045$), while high CXCL12 expression was related to larger tumor size ($p = .045$), positive lymph node metastasis ($p = .005$), and higher pathologic stage ($p = .017$). The patients with high cytoplasmic CXCR4 experienced lower distant recurrence ($p = .006$) and better recurrence-free survival (RFS) (log-rank $p = .020$) after adjuvant chemotherapy. Cytoplasmic CXCR4 expression remained an independent factor of distant recurrence ($p = .019$) and RFS ($p = .038$) after multivariate analysis. **Conclusions:** High cytoplasmic CXCR4 expression was associated with lower distant recurrence and better RFS in TNBC patients treated with adjuvant chemotherapy. This is the first study to correlate high CXCR4 expression to better TNBC prognosis, and the underlying mechanism needs to be elucidated in further studies.

Key Words: CXCR4; CXCL12; Triple negative breast neoplasms; Prognostic marker

Triple-negative breast cancer (TNBC) refers to the breast cancer subtype which does not express estrogen receptor (ER), progesterone receptor (PR), and lacks overexpression of human epidermal growth factor receptor 2 (HER2). It comprises 10%–20% of all breast cancer cases and is associated with aggressive behavior and poor prognosis.[1] TNBC is generally considered an individual subtype of breast cancer, but it is also a highly heterogeneous disease which consists of various subgroups of tumors with different molecular, histologic, and clinical characteristics.[2] Advances in endocrine therapy and HER2-targeted therapy have greatly improved the survival of the patients with hormone receptor–positive and HER2-positive tumors, but TNBC patients still suffer from absence of specific treatment target. Systemic chemotherapy continues to be the mainstay of TNBC treatment, and there is an urgent need for novel biomarkers which can be used to predict prognosis, identify patients who will benefit from therapy, and provide potential treatment target.[2]

CXC chemokine receptor type 4 (CXCR4) is a member of G protein-coupled receptors which is bound by its only ligand CXC motif chemokine 12 (CXCL12), also known as stromal cell-derived factor-1.[3] It is physiologically involved in embryonic development, leukocyte trafficking and homing of hematopoietic cells to bone marrow.[4-6] In tumor biology, the CXCR4/CXCL12 axis is known to promote proliferation of tumor cells, direct metastasis by attracting CXCR4-positive tumor cells to CXCL12-rich organs, and mediate the interaction between the tumor cell and their microenvironment.[7-9] CXCR4 is expressed in different cancer types, and its overexpression and association with distant metastasis and unfavorable prognosis have been reported in breast cancer.[3,9-11] In addition, targeting of CXCR4 significantly reduced both primary and metastatic breast cancer in the mouse model, suggesting that CXCR4/CXCL12 axis may be a promising therapeutic target in breast cancer treatment.[12,13]

A number of studies have reported the negative prognostic sig-

pISSN 2383-7837
eISSN 2383-7845

nificance of CXCR4 expression in TNBC, but adjuvant treatment information is not clearly documented in most of these reports, leaving the possibility of confounding.[14-16] Moreover, although systemic chemotherapy is an essential element of TNBC treatment, the prognostic significance of CXCR4 has not been studied in TNBC patients treated with adjuvant chemotherapy. Therefore, we aimed to evaluate the expression of CXCR4 in TNBC tumor tissue, compare it with clinicopathologic parameters, and investigate its relationship with the outcome of the patients who received adjuvant chemotherapy. Since the expression of CXCL12 has not been well-addressed in TNBC, we planned to evaluate its expression as well.

MATERIALS AND METHODS

Patients and tissue samples

The study group consisted of primary unilateral TNBC patients who underwent surgical resection in Seoul National University Hospital between December 2000 and December 2006 and received adjuvant chemotherapy. The cases with available formalin-fixed, paraffin-embedded (FFPE) tissue for tissue microarray (TMA) were retrospectively collected. The patients who had distant metastasis at initial diagnosis, received neoadjuvant chemotherapy, underwent surgical resection for bilateral breast cancer, or had a history of ipsilateral or contralateral breast cancer were excluded from the study. Immunohistochemistry (IHC) for ER, PR, and HER2 was routinely performed on resection specimen at the time of diagnosis, and the IHC slides were reviewed. According to the American Society of Clinical Oncology/College of American Pathologists (ASCO/CAP) guidelines, ER and PR negativity was defined as nuclear staining in < 1% of tumor cells in IHC, and HER2 was considered negative if a tumor was scored 0 or 1+ in HER2 IHC or 2+ with a negative HER2 fluorescence *in situ* hybridization result.[17,18] Among the 313 primary TNBC patients identified, 283 patients (90.4%) received adjuvant chemotherapy. The patients were treated with standard chemotherapy and the regimens were classified into three categories: anthracycline-based regimen, taxane-anthracycline-based regimen and CMF (cyclophosphamide, methotrexate, and 5-fluorouracil). Use of taxane-anthracycline-based regimen was limited to node-positive tumors due to insurance constraints. More detailed information on chemotherapy regimen is shown in Table 1.

Clinicopathologic characteristics, treatment details, and follow-up data were retrieved from medical records and the original pathology report. Histologic grade was scored according to the Nottingham grading system and the pathologic stage was determined based on the American Joint Committee on Cancer staging system, seventh edition.[19] Follow-up and survival data were collected until the end of 2014. The date of recurrence, death, and last follow-up were obtained from medical records, and recurrence-free survival (RFS) and overall survival (OS) were assessed according to STEEP criteria.[20] Recurrence was diagnosed either pathologically or radiologically and was classified as locoregional or distant. This study was approved by the Institutional Review Board of Seoul National University Hospital with a waiver of informed consent (IRB No. 1512-076-728).

Table 1. Chemotherapy regimen in patients treated with adjuvant chemotherapy

Adjuvant chemotherapy regimen	No. of patients
Anthracycline-based	164
FAC	132
AC	10
FEC	21
EC	1
Taxane-anthracycline-based	51
AC → paclitaxel and/or docetaxel	50
FEC → paclitaxel	1
CMF	65
Change of regimen	1[a]
Unknown	2
Total	283

FAC, 5-fluorouracil (5-FU), doxorubicin, and cyclophosphamide; AC, doxorubicin and cyclophosphamide; FEC, 5-FU, epirubicin, and cyclophosphamide; EC, epirubicin and cyclophosphamide; CMF, cyclophosphamide, methotrexate, and 5-FU.
[a]AC to CMF.

TMA construction and IHC

Hematoxylin and eosin–stained slides of each tumor were reviewed and the representative area was marked. Cylindrical tissue core with a diameter of 2 mm was extracted from the corresponding area of the FFPE tumor block and transferred into recipient paraffin block (SuperBioChips Laboratories, Seoul, Korea). Each TMA block included a maximum of 59 cores. TMA blocks were sectioned at the 3-μm thickness and IHC for CXCR4 and CXCL12 was performed with automated staining system (BenchMark XT, Ventana Medical Systems, Tucson, AZ, USA) following the manufacturer's protocols. TMA sections were first deparaffinized, and antigen retrieval was done using cell conditioning solution (CC1, Ventana Medical Systems). Then sections were incubated with primary rabbit polyclonal anti-CXCR4 (1:50, ab2074, Abcam, Cambridge, UK) and mouse monoclonal anti-CXCL12 (1:10, MAB350, R&D Systems, Minneapolis, MN, USA) antibodies. The positive antigen-antibody reaction was visualized using diaminobenzidine detection kit (OptiView DAB,

https://doi.org/10.4132/jptm.2018.09.19

Ventana Medical Systems), and counterstaining was performed with hematoxylin and bluing reagent.

The IHC slides were examined blindly without knowledge of clinicopathologic information, and the expression of CXCR4 and CXCL12 was assessed by IHC using a semiquantitative scoring system. The staining intensity was scored as 0 (negative), 1 (weak), 2 (moderate), and 3 (strong), and percentage of positively stained cells were scored as 0 (0%), 1 (1%–25%), 2 (26%–50%), 3 (51%–75%), and 4 (>75%). The final score was calculated by multiplying the intensity and percentage scores, ranging from 0 to 12. The patients were divided into high or low expression groups using the median score of each marker as a cutoff point.

Statistical analysis

Differences in clinicopathologic variables and outcomes between high and low expression groups were compared using the chi-square test, or Fischer exact test when applicable. Survival curves were generated using the Kaplan-Meier method and compared using the log-rank test. Cox proportional hazards model and logistic regression analysis were used to evaluate the prognostic significance of each variable in the univariate and multivariate analysis. Variables with a p-value of < .20 in univariate analysis were included in multivariate analysis, and forward conditional method was used to select the significant variables. All statistical analyses were performed using SPSS Statistics software ver. 22.0 (IBM Corp., Armonk, NY, USA), and a p-value of < .05 was considered statistically significant.

RESULTS

Expression of CXCR4 and CXCL12 in TNBC tissues

IHC for CXCR4 and CXCL12 was performed on TMA section, and due to core loss and noninformative cores with no invasive carcinoma, expression of CXCR4 and CXCL12 were evaluable in 259 (91.5%) and 238 (84.1%) cases, respectively. Immunostaining for CXCR4 was observed in tumor cells, stromal cells,

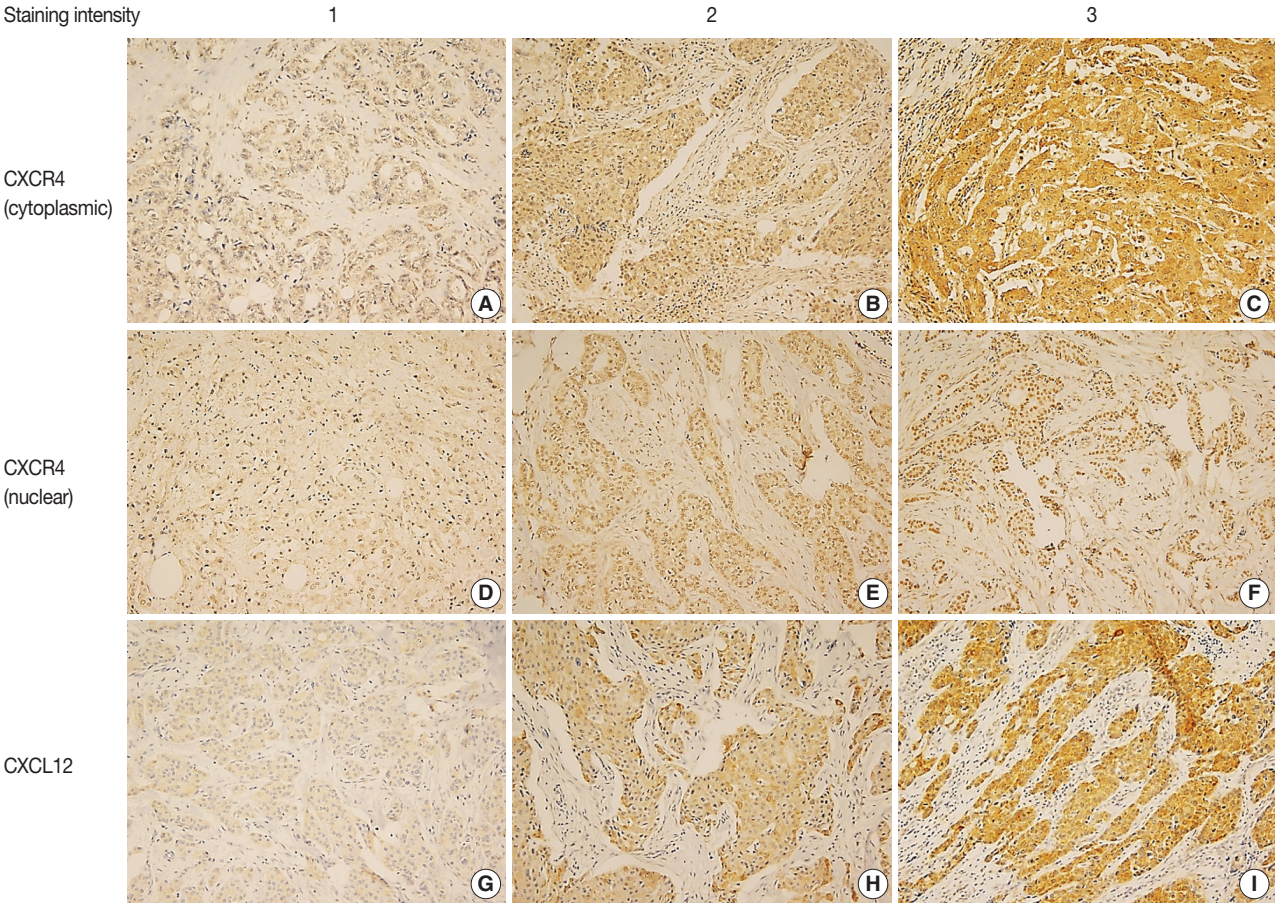

Fig. 1. Immunohistochemistry for CXC chemokine receptor type 4 (CXCR4) and CXC motif chemokine 12 (CXCL12). Representative immunohistochemistry images of cytoplasmic CXCR4 (A–C), nuclear CXCR4 (D–F), and CXCL12 (G–I) in order of staining intensity. CXCR4 and CXCL12 expression are mainly observed in tumor cells. CXCR4 shows cytoplasmic and nuclear staining, and CXCL12 shows cytoplasmic staining.

and inflammatory cells, but staining was most prominent in the cytoplasm and nucleus of tumor cells (Fig. 1A–F). Staining for CXCL12 was mainly observed in tumor cell cytoplasm (Fig. 1G–I). Expression of each marker was scored in tumor cells, and cytoplasmic and nuclear expression were separately assessed for CXCR4. Based on the median IHC score, high cytoplasmic CXCR4, high nuclear CXCR4, and high CXCL12 expression were defined as IHC score of > 7, > 6 and > 2, and the tumors were classified into high cytoplasmic CXCR4, high nuclear CXCR4, and high CXCL12 groups in 194 (74.9%), 115 (44.4%), and 115 (48.3%) cases, respectively.

Clinicopathologic characteristics and expression of CXCR4 and CXCL12

Correlations between clinicopathologic characteristics and expression of each marker are shown in Tables 2 and 3. All patients were female and the median age at surgery was 48 years (range, 21 to 71 years). High cytoplasmic CXCR4 expression was significantly associated with younger age (p = .008), higher histologic grade (p = .007), and lower pathologic stage (p = .045), but it was not related to tumor size or lymph node metastasis. On the other hand, high CXCL12 expression showed a significant correlation with larger tumor size (p = .045), positive lymph node metastasis (p = .005), and higher pathologic stage (p = .017). Nuclear CXCR4 expression was not associated with any of the clinicopathologic parameters studied. There was a significant difference in adjuvant chemotherapy regimen between high and low cytoplasmic CXCR4 groups (p = .009), but otherwise, no significant difference in adjuvant chemotherapy regimen or radiation therapy was observed between groups in other markers.

Clinical outcome and pattern of recurrence after adjuvant chemotherapy

The median follow-up time was 100 months (range, 1 to 141 months). During the follow-up period, the tumor recurred in 53 patients (18.7%), and 17 patients (6.0%) died. Locoregional and

Table 2. Clinicopathologic characteristics in relation to CXCR4 expression

Variable	Total (n = 259)	CXCR4 (cytoplasmic)			CXCR4 (nuclear)		
		Low (n = 65)	High (n = 194)	p-value	Low (n=144)	High (n = 115)	p-value
Age (yr)				.008			.524
≤50	152	29 (19.1)	123 (80.9)		82 (53.9)	70 (46.1)	
>50	107	36 (33.6)	71 (66.4)		62 (57.9)	45 (42.1)	
Histologic grade				.007			.310
I, II	47	19 (40.4)	28 (59.6)		23 (48.9)	24 (51.1)	
III	212	46 (21.7)	166 (78.3)		121 (57.1)	91 (42.9)	
Size (cm)				.131[a]			.957
≤5	243	58 (23.9)	185 (76.1)		135 (55.6)	108 (44.4)	
>5	16	7 (43.8)	9 (56.3)		9 (56.3)	7 (43.8)	
Lymph node metastasis				.473			.476
Negative	165	39 (23.6)	126 (76.4)		89 (53.9)	76 (46.1)	
Positive	94	26 (27.7)	68 (72.3)		55 (58.5)	39 (41.5)	
Stage				.045			.087
I, II	216	49 (22.7)	167 (77.3)		115 (53.2)	101 (46.8)	
III	43	16 (37.2)	27 (62.8)		29 (67.4)	14 (32.6)	
Histologic type				.992			.144
IDC	239	60 (25.1)	179 (74.9)		136 (56.9)	103 (43.1)	
Other[b]	20	5 (25.0)	15 (75.0)		8 (40.0)	12 (60.0)	
Adjuvant chemotherapy regimen[c]				.009			.538
Anthracycline-based	149	27 (18.1)	122 (81.9)		79 (53.0)	70 (47.0)	
Taxane-anthracycline-based	49	14 (28.6)	35 (71.4)		30 (61.2)	19 (38.8)	
CMF	58	22 (37.9)	36 (62.1)		34 (58.6)	24 (41.4)	
Radiation therapy[d]				.506			.975
No	84	23 (27.4)	61 (72.6)		47 (56.0)	37 (44.0)	
Yes	174	41 (23.6)	133 (76.4)		97 (55.7)	77 (44.3)	

Values are presented as number (%).
CXCR4, CXC chemokine receptor type 4; IDC, Invasive ductal carcinoma; CMF, cyclophosphamide, methotrexate, and 5-fluorouracil.
[a]Fisher exact test; [b]Invasive lobular carcinoma (2), mixed invasive ductal and lobular carcinoma (3), invasive papillary carcinoma (2), metaplastic carcinoma (8), medullary carcinoma (1), apocrine carcinoma (3), signet ring cell carcinoma (1); [c]3 missing values, unknown (2), change of regimen (1); [d]1 missing value, unknown (1).

 https://doi.org/10.4132/jptm.2018.09.19

Table 3. Clinicopathologic characteristics in relation to CXCL12 expression

Variable	Total (n = 238)	CXCL12		p-value
		Low (n = 123)	High (n = 115)	
Age (yr)				.721
≤ 50	140	71 (50.7)	69 (49.3)	
> 50	98	52 (53.1)	46 (46.9)	
Histologic grade				.155
I, II	43	18 (41.9)	25 (58.1)	
III	195	105 (53.8)	90 (46.2)	
Size (cm)				.045
≤ 5	223	119 (53.4)	104 (46.6)	
> 5	15	4 (26.7)	11 (73.3)	
Lymph node metastasis				.005
Negative	158	92 (58.2)	66 (41.8)	
Positive	80	31 (38.8)	49 (61.3)	
Stage				.017
I, II	202	111 (55.0)	91 (45.0)	
III	36	12 (33.3)	24 (66.7)	
Histologic type				.931
IDC	219	113 (51.6)	106 (48.4)	
Other[a]	19	10 (52.6)	9 (47.4)	
Adjuvant chemotherapy regimen[b]				.117
Anthracycline-based	144	82 (56.9)	62 (43.1)	
Taxane-anthracycline-based	38	15 (39.5)	23 (60.5)	
CMF	53	25 (47.2)	28 (52.8)	
Radiation therapy[c]				.408
No	79	38 (48.1)	41 (51.9)	
Yes	158	85 (53.8)	73 (46.2)	

Values are presented as number (%).
CXCL12, CXC motif chemokine 12; IDC, Invasive ductal carcinoma; CMF, cyclophosphamide, methotrexate, and 5-fluorouracil.
[a]Invasive lobular carcinoma (2), mixed invasive ductal and lobular carcinoma (2), invasive papillary carcinoma (2), metaplastic carcinoma (6), apocrine carcinoma (4), medullary carcinoma (1), signet ring cell carcinoma (1), clear cell carcinoma (1); [b]3 missing values, unknown (2), change of regimen (1); [c]1 missing value, unknown (1).

distant recurrence occurred in 18 (6.4%) and 37 (13.1%) patients, respectively. Distant recurrence was less frequent in the high cytoplasmic CXCR4 group (p = .006), whereas nuclear CXCR4 and CXCL12 showed no significant association with any pattern of recurrence (Fig. 2A, B). Univariate logistic regression analysis revealed that high cytoplasmic CXCR4 expression was associated with lower distant recurrence (p = .007). After multivariate analysis, high cytoplasmic CXCR4 expression remained an independent variable for lower distant recurrence (p = .019) along with smaller tumor size (p = .042) and negative lymph node metastasis (p = .001) (Table 4).

RFS and OS after adjuvant chemotherapy

Kaplan-Meier curves for RFS and OS was plotted according to the expression of each marker. A significant difference in RFS was observed between high and low cytoplasmic CXCR4 groups (log-rank p = .020), but the difference was not significant in OS (log-rank p = .076) (Fig. 3A, B). The 5-year RFS in high and low cytoplasmic CXCR4 groups were 86.0% and 75.1%, respectively. The 5-year OS in high and low cytoplasmic CXCR4 groups were 96.0% and 90.7%, respectively. No significant difference in survival was observed between groups in nuclear CXCR4 (log-rank p = .637 for RFS, p = .121 for OS) and CXCL12 (log-rank p = .521 for RFS, p = .538 for OS). In univariate Cox regression analysis, high cytoplasmic CXCR4 expression was associated with better RFS (p = .022). Multivariate analysis revealed that cytoplasmic CXCR4 expression (p = .038) and lymph node metastasis (p < .001) were independent factors of RFS (Table 5).

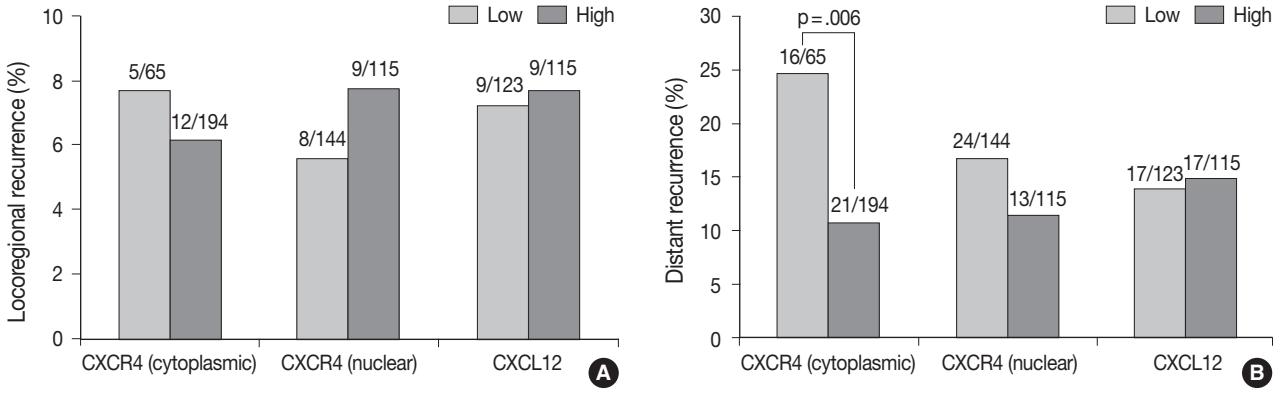

Fig. 2. The pattern of recurrence after adjuvant chemotherapy according to CXC chemokine receptor type 4 (CXCR4) and CXC motif chemokine 12 (CXCL12) expression. CXCR4 and CXCL12 expression do not show a significant association with locoregional recurrence (A), while high cytoplasmic CXCR4 expression is significantly associated with lower distant recurrence (B). Figures above each bar refer to the number of recurrences/the number of patients in each group.

DISCUSSION

Expression of CXCR4 is reported in various types of tumors, and its ligand CXCL12 is expressed widely in tumor and normal tissues by cancer cells, stromal cells, endothelial cells, and immune cells.[3,21] Binding of CXCL12 to CXCR4 activates multiple signaling pathways promoting tumor growth and metastasis, and CXCR4/CXCL12 axis has a role in tumor cell-microenvironment interac-

Table 4. Logistic regression analysis for distant recurrence after adjuvant chemotherapy

	Univariate analysis			Multivariate analysis		
	OR	95% CI	p-value	OR	95% CI	p-value
Age > 50 yr	1.431	0.715–2.862	.311	-	-	-
Histologic grade III	0.790	0.338–1.844	.585	-	-	-
Tumor size > 5 cm	4.985	1.796–13.837	.002	3.231	1.046–9.985	.042
Lymph node metastasis	4.462	2.153–9.246	< .001	3.491	1.630–7.478	.001
Radiation therapy	1.029	0.492–2.152	.940	-	-	-
High CXCR4 (cytoplasmic)	0.372	0.180–0.766	.007	0.400	0.186–0.860	.019
High CXCR4 (nuclear)	0.637	0.309–1.315	.223	-	-	-
High CXCL12	1.082	0.523–2.236	.832	-	-	-

OR, odds ratio; CI, confidence interval; CXCR4, CXC chemokine receptor type 4; CXCL12, CXC motif chemokine 12.

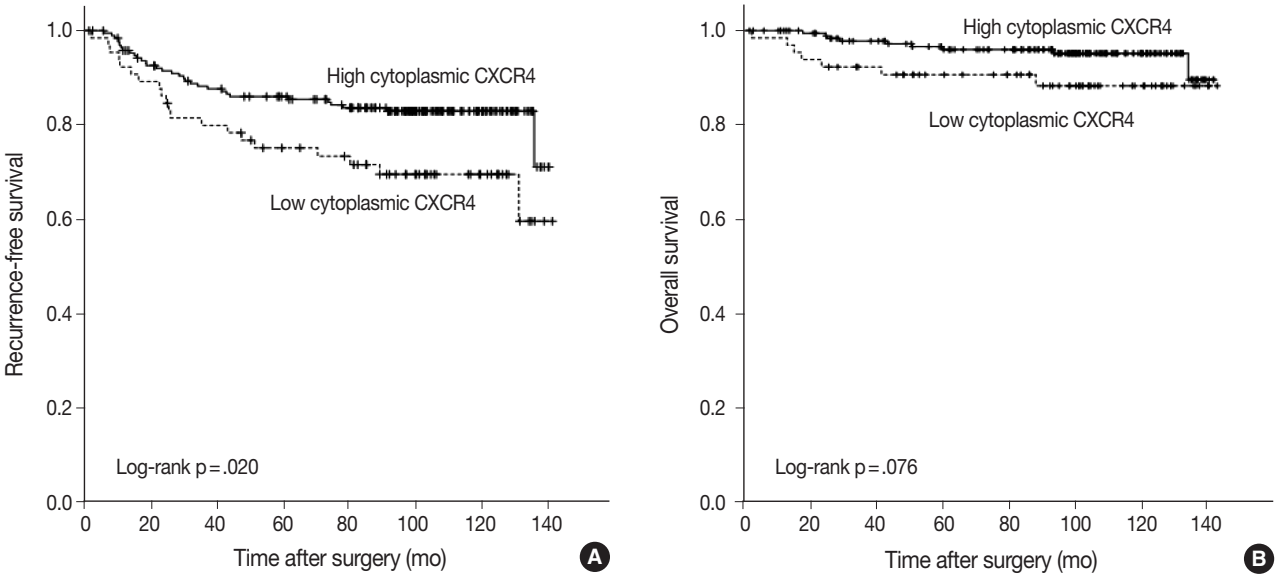

Fig. 3. Recurrence-free and overall survival after adjuvant chemotherapy according to cytoplasmic CXC chemokine receptor type 4 (CXCR4) expression. Recurrence-free survival is significantly better in the high cytoplasmic CXCR4 group (A), but the difference in overall survival is not significant between high and low cytoplasmic CXCR4 groups (B).

Table 5. Cox regression analysis for recurrence-free survival after adjuvant chemotherapy

	Univariate analysis			Multivariate analysis		
	HR	95% CI	p-value	HR	95% CI	p-value
Age > 50 yr	0.959	0.554–1.660	.881	-	-	-
Histologic grade III	0.909	0.468–1.766	.779	-	-	-
Tumor size > 5 cm	3.116	1.467–6.617	.003	-	-	-
Lymph node metastasis	3.298	1.908–5.702	< .001	3.005	1.724–5.237	< .001
Radiation therapy	0.912	0.516–1.612	.751	-	-	-
High CXCR4 (cytoplasmic)	0.521	0.298–0.912	.022	0.552	0.316–0.967	.038
High CXCR4 (nuclear)	0.875	0.503–1.524	.637	-	-	-
High CXCL12	1.199	0.688–2.089	.522	-	-	-

HR, hazard ratio; CI, confidence interval; CXCR4, CXC chemokine receptor type 4; CXCL12, CXC motif chemokine 12.

https://doi.org/10.4132/jptm.2018.09.19

tion.[21] In the present study, we evaluated the expression of CXCR4 and CXCL12 on TMA constructed from TNBC tissue using the immunohistochemical method. Immunoreactivity for CXCR4 was observed primarily in the cytoplasm and nucleus of tumor cells, and CXCL12 was stained mostly in tumor cell cytoplasm. While CXCR4 is a membrane-bound G protein–coupled receptor, it is rapidly internalized by binding of its ligand CXCL12, and cytoplasmic and nuclear expression of CXCR4 was previously demonstrated in breast cancer by IHC.[22-24] Our study also revealed that high cytoplasmic CXCR4 expression was associated with higher histologic grade, and this finding was consistent with previous studies regarding breast cancer and TNBC.[15,16,23-25] With respect to CXCL12 expression, Kobayashi *et al*.[26] previously demonstrated that cytoplasmic-dominant CXCL12 immunoreactivity is associated with higher CXCL12 mRNA level in resected breast cancer.

Currently, there are a number of studies which evaluated the expression of CXCL12 in breast cancer. High CXCL12 expression correlated with better survival in most of these studies, but discrepant report exists.[26-29] Ours is the first study to evaluate the expression of CXCL12 in TNBC subtype and showed that high CXCL12 expression was associated with known negative prognostic markers such as large tumor size, positive lymph node metastasis and higher stage in TNBC, although no significant difference in survival was observed between high and low CXCL12 groups. Loss of CXCL12 has been reported to have a role in distant metastasis of tumor cells, but overexpression of CXCL12 correlates with increased invasiveness, higher tumor grade and stage in several human cancers.[30] The discordant result between the present and previous studies seems to suggest the different role of CXCL12 in TNBC subtype, and the different proportion of breast cancer subtypes in study population might have resulted in the discrepant results between previous studies.

In the evaluation of outcome and survival, the present study showed better survival compared with previous reports which studied the expression of CXCR4 in TNBC.[14-16] TNBC is known to be more sensitive to chemotherapy than other breast cancer subtypes, and since the study group was restricted to the patients who received adjuvant chemotherapy, it is likely that the effect of chemotherapy has contributed to the better survival observed in our study.[2] The patient group with lower pathologic stage might have affected the survival as well. Our study also revealed that increased cytoplasmic expression of CXCR4 was associated with a better prognosis in TNBC patients treated with adjuvant chemotherapy in terms of lower distant recurrence and better RFS. However, previous studies have reported high CXCR4 expression as a poor prognostic marker of TNBC, and antitumor effect of CXCR4 inhibitors has been studied on breast cancer and shown efficacies in preclinical studies.[12-16] On the other hand, Lefort *et al*.[31] recently reported that CXCR4 inhibitors may not benefit TNBC patients and could even be detrimental in the study using patient-derived xenograft (PDX) model. In previous studies which evaluated the expression of CXCR4 in TNBC, Chu *et al*.[14] used western blot analysis on 151 frozen tissue, and Yu *et al*.[15] and Chen *et al*.[16] performed IHC on 148 and 75 FFPE samples, respectively. The difference in patient demographics, tissue preservation method, protein detection method, and scoring system may have caused the discordant results. However, this is the largest series of TNBC cases studied for the expression of CXCR4 and CXCL12 to date, with 259 and 238 cases studied for CXCR4 and CXCL12, respectively. Therefore, despite the limitation of retrospective study, we assumed that our data might have implications regarding the prognosis of TNBC.

The expression level of CXCR4 and CXCL12 has been correlated with different hormone receptor and HER2 status in breast cancer. For example, high CXCL12 expression was associated with ER positivity in resected breast cancer, and CXCL12 expression was induced by estradiol treatment in ER-positive breast cancer cell lines.[26,27] Salvucci *et al*.[23] demonstrated that cytoplasmic CXCR4 expression was correlated with ER negativity, PR negativity, and HER2 expression, and Hassan *et al*.[24] and Chen *et al*.[16] reported that CXCR4 expression level correlates with triple-negative status in breast cancer. Additionally, in the PDX model which recapitulated the stromal components of human breast cancer, CXCR4 inhibition did not reduce tumor growth and even increased the distant metastasis of TNBC.[31] Taken together, the difference in expression level and response to CXCR4 inhibition suggests that CXCR4/CXCL12 axis may exert a different effect on metastasis and prognosis of TNBC compared with other breast cancer subtypes. Other components of tumor microenvironment may have a role in this phenomenon, but the exact mechanism needs to be investigated in future studies.

The study population in our study was restricted to the TNBC patients treated with adjuvant chemotherapy, and the result revealed that high cytoplasmic CXCR4 expression is associated with lower distant recurrence and better RFS. Since adjuvant chemotherapy is indicated or recommended in most TNBC cases under current practice guideline, our result is clinically relevant and CXCR4 expression might be useful in predicting outcome in TNBC patients after adjuvant chemotherapy.[32] More importantly, we demonstrate for the first time that high CXCR4 expression may be associated with better prognosis in TNBC patients,

and suggest the possibility of the different mechanism underlying the metastasis and prognosis of TNBC.

This study has limitations. As previously noted, this was a retrospective study with known disadvantages. In addition, the patient population was heterogeneous in terms of chemotherapy regimen, and there was a significant difference in chemotherapy regimen between high and low cytoplasmic CXCR4 expression groups. Use of taxane-anthracycline-based regimen was limited to node-positive cases, and since the patients received different chemotherapy based on nodal status, we could not compare the outcomes according to the chemotherapy regimen. Therefore, our results should be validated in prospective controlled cohort studies, and it would be beneficial to re-evaluate the prognostic significance of CXCR4 in patients treated with the same chemotherapy regimen.

In conclusion, the present study indicates that high cytoplasmic expression of CXCR4 may have a prognostic value in TNBC patients and predict lower distant recurrence and better RFS after adjuvant chemotherapy. To our knowledge, this is the first study to correlate high CXCR4 expression with better prognosis in TNBC, and the underlying mechanism needs to be explored in further studies.

Conflicts of Interest

No potential conflict of interest relevant to this article was reported.

REFERENCES

1. Boyle P. Triple-negative breast cancer: epidemiological considerations and recommendations. Ann Oncol 2012; 23 Suppl 6: vi7-12.
2. Bianchini G, Balko JM, Mayer IA, Sanders ME, Gianni L. Triple-negative breast cancer: challenges and opportunities of a heterogeneous disease. Nat Rev Clin Oncol 2016; 13: 674-90.
3. Balkwill F. Cancer and the chemokine network. Nat Rev Cancer 2004; 4: 540-50.
4. Nagasawa T, Hirota S, Tachibana K, *et al*. Defects of B-cell lymphopoiesis and bone-marrow myelopoiesis in mice lacking the CXC chemokine PBSF/SDF-1. Nature 1996; 382: 635-8.
5. Baggiolini M. Chemokines and leukocyte traffic. Nature 1998; 392: 565-8.
6. Zou YR, Kottmann AH, Kuroda M, Taniuchi I, Littman DR. Function of the chemokine receptor CXCR4 in haematopoiesis and in cerebellar development. Nature 1998; 393: 595-9.
7. Domanska UM, Kruizinga RC, Nagengast WB, *et al*. A review on CXCR4/CXCL12 axis in oncology: no place to hide. Eur J Cancer 2013; 49: 219-30.
8. Orimo A, Gupta PB, Sgroi DC, *et al*. Stromal fibroblasts present in invasive human breast carcinomas promote tumor growth and angiogenesis through elevated SDF-1/CXCL12 secretion. Cell 2005; 121: 335-48.
9. Muller A, Homey B, Soto H, *et al*. Involvement of chemokine receptors in breast cancer metastasis. Nature 2001; 410: 50-6.
10. Liu Y, Ji R, Li J, *et al*. Correlation effect of EGFR and CXCR4 and CCR7 chemokine receptors in predicting breast cancer metastasis and prognosis. J Exp Clin Cancer Res 2010; 29: 16.
11. Zhang Z, Ni C, Chen W, *et al*. Expression of CXCR4 and breast cancer prognosis: a systematic review and meta-analysis. BMC Cancer 2014; 14: 49.
12. Smith MC, Luker KE, Garbow JR, *et al*. CXCR4 regulates growth of both primary and metastatic breast cancer. Cancer Res 2004; 64: 8604-12.
13. Huang EH, Singh B, Cristofanilli M, *et al*. A CXCR4 antagonist CTCE-9908 inhibits primary tumor growth and metastasis of breast cancer. J Surg Res 2009; 155: 231-6.
14. Chu QD, Panu L, Holm NT, Li BD, Johnson LW, Zhang S. High chemokine receptor CXCR4 level in triple negative breast cancer specimens predicts poor clinical outcome. J Surg Res 2010; 159: 689-95.
15. Yu S, Wang X, Liu G, Zhu X, Chen Y. High level of CXCR4 in triple-negative breast cancer specimens associated with a poor clinical outcome. Acta Med Okayama 2013; 67: 369-75.
16. Chen HW, Du CW, Wei XL, Khoo US, Zhang GJ. Cytoplasmic CXCR4 high-expression exhibits distinct poor clinicopathological characteristics and predicts poor prognosis in triple-negative breast cancer. Curr Mol Med 2013; 13: 410-6.
17. Hammond ME, Hayes DF, Dowsett M, *et al*. American Society of Clinical Oncology/College of American Pathologists guideline recommendations for immunohistochemical testing of estrogen and progesterone receptors in breast cancer. J Clin Oncol 2010; 28: 2784-95.
18. Wolff AC, Hammond ME, Hicks DG, *et al*. Recommendations for human epidermal growth factor receptor 2 testing in breast cancer: American Society of Clinical Oncology/College of American Pathologists clinical practice guideline update. J Clin Oncol 2013; 31: 3997-4013.
19. Elston CW, Ellis IO. Pathological prognostic factors in breast cancer. I. The value of histological grade in breast cancer: experience from a large study with long-term follow-up. Histopathology 1991; 19: 403-10.
20. Hudis CA, Barlow WE, Costantino JP, *et al*. Proposal for standardized definitions for efficacy end points in adjuvant breast cancer trials:

the STEEP system. J Clin Oncol 2007; 25: 2127-32.
21. Guo F, Wang Y, Liu J, Mok SC, Xue F, Zhang W. CXCL12/CXCR4: a symbiotic bridge linking cancer cells and their stromal neighbors in oncogenic communication networks. Oncogene 2016; 35: 816-26.
22. Haribabu B, Richardson RM, Fisher I, *et al*. Regulation of human chemokine receptors CXCR4. Role of phosphorylation in desensitization and internalization. J Biol Chem 1997; 272: 28726-31.
23. Salvucci O, Bouchard A, Baccarelli A, *et al*. The role of CXCR4 receptor expression in breast cancer: a large tissue microarray study. Breast Cancer Res Treat 2006; 97: 275-83.
24. Hassan S, Ferrario C, Saragovi U, *et al*. The influence of tumor-host interactions in the stromal cell-derived factor-1/CXCR4 ligand/receptor axis in determining metastatic risk in breast cancer. Am J Pathol 2009; 175: 66-73.
25. Guembarovski AL, Guembarovski RL, Hirata BK, *et al*. CXCL12 chemokine and CXCR4 receptor: association with susceptibility and prognostic markers in triple negative breast cancer. Mol Biol Rep 2018 Jun 20 [Epub]. https://doi.org/10.1007/s11033-018-4215-7.
26. Kobayashi T, Tsuda H, Moriya T, *et al*. Expression pattern of stromal cell-derived factor-1 chemokine in invasive breast cancer is correlated with estrogen receptor status and patient prognosis. Breast Cancer Res Treat 2010; 123: 733-45.
27. Mirisola V, Zuccarino A, Bachmeier BE, *et al*. CXCL12/SDF1 expression by breast cancers is an independent prognostic marker of disease-free and overall survival. Eur J Cancer 2009; 45: 2579-87.
28. Yan M, Jene N, Byrne D, *et al*. Recruitment of regulatory T cells is correlated with hypoxia-induced CXCR4 expression, and is associated with poor prognosis in basal-like breast cancers. Breast Cancer Res 2011; 13: R47.
29. Kang H, Watkins G, Parr C, Douglas-Jones A, Mansel RE, Jiang WG. Stromal cell derived factor-1: its influence on invasiveness and migration of breast cancer cells in vitro, and its association with prognosis and survival in human breast cancer. Breast Cancer Res 2005; 7: R402-10.
30. Samarendra H, Jones K, Petrinic T, *et al*. A meta-analysis of CXCL12 expression for cancer prognosis. Br J Cancer 2017; 117: 124-35.
31. Lefort S, Thuleau A, Kieffer Y, *et al*. CXCR4 inhibitors could benefit to HER2 but not to triple-negative breast cancer patients. Oncogene 2017; 36: 1211-22.
32. Lebert JM, Lester R, Powell E, Seal M, McCarthy J. Advances in the systemic treatment of triple-negative breast cancer. Curr Oncol 2018; 25(Suppl 1): S142-S50.

Journal of Pathology and Translational Medicine 2018; 52: 378-385
https://doi.org/10.4132/jptm.2018.09.21

■ ORIGINAL ARTICLE ■

Loss of Nuclear BAP1 Expression Is Associated with High WHO/ISUP Grade in Clear Cell Renal Cell Carcinoma

Young Chan Wi · Ahrim Moon[1]
Min Jung Jung[1] · Yeseul Kim
Seong Sik Bang · Kiseok Jang
Seung Sam Paik · Su-Jin Shin

Department of Pathology, Hanyang University College of Medicine, Seoul; [1]Department of Pathology, Soonchunhyang University Bucheon Hospital, Soonchunhyang University College of Medicine, Bucheon, Korea

Received: July 13, 2018
Revised: August 24, 2018
Accepted: September 21, 2018

Corresponding Author
Su-Jin Shin, MD, PhD
Department of Pathology, Hanyang University College of Medicine, 222-1 Wangsimni-ro, Seongdong-gu, Seoul 04763, Korea
Tel: +82-2-2220-8250
Fax: +82-2-2296-7502
E-mail: charm@hanyang.ac.kr

Background: BRCA1-associated protein 1 (*BAP1*) mutations are frequently reported in clear cell renal cell carcinoma (ccRCC); however, very few studies have evaluated the role of these mutations in other renal cell carcinoma (RCC) subtypes. Therefore, we analyzed BAP1 protein expression using immunohistochemistry in several RCC subtypes and assessed its relationship with clinicopathological characteristics of patients. **Methods:** BAP1 expression was immunohistochemically evaluated in tissue microarray blocks constructed from 371 samples of RCC collected from two medical institutions. BAP1 expression was evaluated based on the extent of nuclear staining in tumor cells, and no expression or expression in <10% of tumor cells was defined as negative. **Results:** Loss of BAP1 expression was observed in ccRCC (56/300, 18.7%), chromophobe RCC (6/26, 23.1%), and clear cell papillary RCC (1/4, 25%), while we failed to detect BAP1 expression loss in papillary RCC, acquired cystic disease-associated RCC, or collecting duct carcinoma. In ccRCC, loss of BAP1 expression was significantly associated with high World Health Organization (WHO)/International Society of Urological Pathology (ISUP) grade (p=.002); however, no significant correlation was observed between loss of BAP1 expression and survival in ccRCC. Loss of BAP1 expression showed no association with prognostic factors in chromophobe RCC. **Conclusions:** Loss of BAP1 nuclear expression was observed in both ccRCC and chromophobe RCC. In addition, BAP1 expression loss was associated with poor prognostic factors such as high WHO/ISUP grade in ccRCC.

Key Words: Carcinoma, renal cell; Clear cell; BAP1; Immunostaining

Renal cell carcinoma (RCC) accounts for 2%–3% of all malignant diseases in adults.[1] Clear cell renal cell carcinoma (ccRCC) is the most common renal tumor subtype and is closely associated with von Hippel Lindau (*VHL*) tumor suppressor gene mutations that lead to the stabilization of hypoxia-inducible factors in both sporadic and familial forms. Recently, three tumor suppressor gene mutations, namely, *PBRM1*, *SETD2*, and *BAP1*, located close to *VHL* on chromosome 3p were reported.[2-4]

Studies have reported *BAP1* mutation in about 10%–15% of ccRCC cases.[5,6] BRCA1-associated protein 1 (BAP1) is a nuclear-localized deubiquitinating enzyme that was initially discovered as a BRCA1-associated protein and known to interact with multiple proteins. BAP1 was shown to exhibit a tumor suppressor role in several cancers through its deubiquitinase activity, thereby regulating target gene transcription, cell cycle control, DNA damage repair, and cellular differentiation.[7] Inactivation mutations of the *BAP1* gene, including insertion, deletion, frameshift, nonsense, and missense mutations, have also been reported.[8]

The germline mutation in the *BAP1* gene is inherited in an autosomal dominant pattern.[9] Affected individuals inherit a non-functional *BAP1* allele, as observed with other tumor suppressors, and the remaining functional allele is inactivated later in life. There is a high risk for developing tumors, including atypical Spitz tumors, uveal melanoma, cutaneous melanoma, epithelioid malignant mesothelioma, and ccRCC.[10] *BAP1* germline mutations are associated with poor prognosis in uveal melanoma, cutaneous melanoma, and ccRCC.[10] Sporadic *BAP1* mutations have also been identified in several tumors, including uveal melanoma,[11] malignant mesothelioma,[12] and ccRCC. The loss of *BAP1* expression in mesothelial cells in effusion cytology specimens is an indicator of possible mesothelioma.[13] Nearly half of the investigated uveal melanoma tumors harbor an inactivating *BAP1* mutation, which was strongly associated with the loss of BAP1 nuclear staining and other aggressive prognostic features.[14] Furthermore, several studies have revealed the association between inactivating *BAP1* mutation and high grade ccRCC,[6] sarcomatoid

pISSN 2383-7837
eISSN 2383-7845

transformation, and poor prognosis in patients with ccRCC,[15] especially in those with low-grade RCC.[16] The loss of BAP1 expression in immunohistochemical staining has been reported as a highly reliable method for the detection of *BAP1* mutation.[6] Although *BAP1* mutations are frequently observed in ccRCC, limited data are available on the expression of BAP1 in other RCC types.

Therefore, we evaluated the loss of BAP1 nuclear expression in several subtypes of RCC, including ccRCC, papillary RCC, and chromophobe RCC, and analyzed its relationship with clinicopathological characteristics of patients.

MATERIALS AND METHODS

Patient selection

A total of 371 samples were retrospectively obtained from Hanyang University Hospital (247 cases, 2005–2017) and Soonchunhyang University Bucheon Hospital (124 cases, 2001–2013). Formalin-fixed, paraffin-embedded tissue samples obtained from surgically resected primary tumors at the time of initial diagnosis were collected. The pathologist in each institution reviewed the slides and selected a representative block for each case, and 3.0 mm of core tissue microarray (TMA) blocks were constructed, with two representative cores for each case. The patient and tumor characteristics, including age, type of surgery, histological type, histological grade, and follow-up data, were acquired. The histological subtypes were classified according to the 2016 World Health Organization (WHO) Tumor Classification. We graded ccRCC and papillary RCC according to the 2013 WHO/International Society of Urological Pathology (ISUP) grading system.[17,18] Chromophobe RCC was graded according to the published parameters.[19] All cases were reviewed by two pathologists for tumor type and WHO/ISUP grade. This study was approved by the Institutional Review Board of the Hanyang University Hospital (HYUH 2018-05-005), and the requirement for informed consent was waived.

Immunohistochemistry for BAP1 expression

Sections from the TMA blocks were immunostained using the Bond-max Automated immunohistochemistry (IHC)/*in situ* hybridization stainer (Leica Biosystems, Nussloch, Germany) according to the manufacturer's protocol. Sections (4-μm thickness) were immunostained with a primary antibody against BAP1 (1:100, sc-28383, mouse monoclonal, Santa Cruz Biotechnology, Santa Cruz, CA, USA). BAP1 expression level was evaluated according to the extent of nuclear staining in the tumor cells. The staining was scored as negative (no expression or expression in < 10% of tumor cells) or positive (expression in ≥ 10% of tumor cells).

Statistical analysis

All of the statistical analyses were performed using SPSS ver. 24.0 (IBM Corp., Armonk, NY, USA). The relationships between the groups were compared using the chi-square test, Fisher exact test, or Student's t test. Cancer-specific survival (CSS) was defined as the time interval between the date of surgical resection

Table 1. Histological and clinical characteristics

Characteristic	Value (n = 371)
Tumor type	
Clear cell RCC	300 (80.9)
Chromophobe RCC	26 (7.0)
Papillary RCC, type 1	13 (3.5)
Papillary RCC, type 2	23 (6.2)
Others	9 (2.4)
Age (yr)	60.0 (13–90)
Sex	
Male	246 (66.3)
Female	125 (33.7)
Tumor size	3.77 (0.7–15)
WHO/ISUP grade (clear and papillary RCC)	
1	33 (9.8)
2	160 (47.6)
3	113 (33.6)
4	30 (8.9)
Chromophobe grade (chromophobe RCC)	
1	19 (73.1)
2	7 (26.9)
Vascular invasion[a]	
Absent	323 (87.1)
Present	48 (12.9)
Tumor necrosis	
Absent	219 (84.2)
Present	41 (15.8)
Sarcomatoid feature	
Absent	350 (94.3)
Present	21 (5.7)
Lymph node metastasis	
Absent	362 (97.6)
Present	9 (2.4)
pT category	
1	258 (69.5)
2	36 (9.7)
3	74 (19.9)
4	3 (0.8)

Values are presented as number (%) or median (range).
RCC, renal cell carcinoma; WHO, World Health Organization; ISUP, International Society of Urological Pathology.
[a]Vascular invasion includes microscopic tumor invasion into small or large vessels and gross renal vein tumor thrombus.

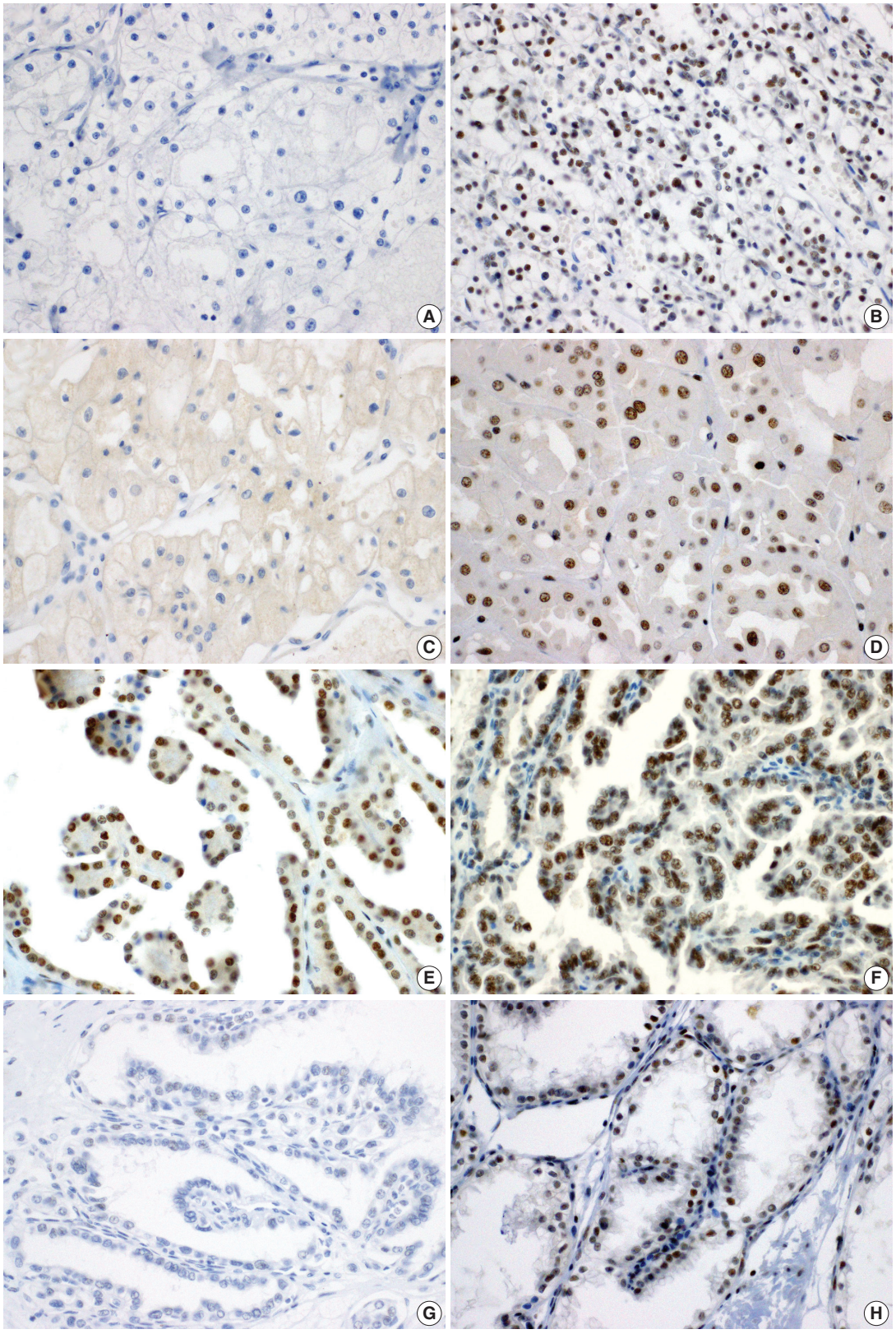

Fig. 1. Immunohistochemical staining of BRCA1-associated protein 1 in clear cell renal cell carcinoma (A, negative; B, positive), chromophobe renal cell carcinoma (RCC) (C, negative; D, positive), papillary RCC type 1 (E, positive), papillary RCC type 2 (F, positive), and clear cell papillary RCC (G, negative; H, positive).

https://doi.org/10.4132/jptm.2018.09.21

and the date of death due to RCC. Recurrence-free survival (RFS) was defined as the time interval between surgical resection and the date of any recurrence. The Kaplan-Meier method with the log-rank test and the Cox proportional hazard regression model were used for survival analyses. Two-sided p-values of < .05 were considered to indicate statistically significant differences.

RESULTS

Patient characteristics

The clinicopathological characteristics of the patients are summarized in Table 1. Among 371 RCC cases, the most common subtype was ccRCC (300 cases, 80.9%). The other subtypes included in this study comprised 36 cases of papillary RCC (13 type 1 and 23 type 2 papillary RCC, 9.7%), 26 cases of chromophobe RCC (7.0%), four cases of clear cell papillary RCC, four cases of acquired cystic disease-associated RCC, and one case of collecting duct carcinoma. The age of the patients ranged from 13 to 90 years, with a median of 60 years. The median follow-up period for the patients in this study was 66 months (range, 0.1 to 167.6 months). Of the 371 patients, 11 (3.0%) had metastatic disease at the time of initial diagnosis (i.e., nephrectomy), 30 (8.1%) had experienced metastasis or relapse during the follow-up period, and 34 (9.2%) had died due to RCC by

Table 2. Correlation between BAP1 expression and tumor type (n = 371)

	Negative (n = 63)	Positive (n = 308)
Clear cell RCC	56 (18.7)	244 (81.3)
Chromophobe RCC	6 (23.1)	20 (76.9)
Papillary RCC type 1	0	13 (100)
Papillary RCC type 2	0	23 (100)
Clear cell papillary RCC	1 (25)	3 (75)
Acquired cystic disease-associated RCC	0	4 (100)
Collecting duct carcinoma	0	1 (100)

Values are presented as number (%).
BAP1, BRCA1-associated protein 1; RCC, renal cell carcinoma.

Table 3. Correlations between BAP1 expression and clinicopathological features

	Clear cell RCC (n = 300)			Chromophobe RCC (n = 26)		
	Negative (n = 56)	Positive (n = 244)	p-value	Negative (n = 6)	Positive (n = 20)	p-value
Sex			.046			.664
Male	32 (15.6)	173 (84.4)		3 (27.3)	8 (72.7)	
Female	24 (25.3)	71 (74.7)		3 (20.0)	12 (80.0)	
WHO/ISUP grade			.002			
1	0	25 (100)				
2	20 (14.1)	122 (85.9)				
3	27 (25.7)	78 (74.3)				
4	9 (32.1)	19 (67.9)				
Chromophobe grade						.146
1				6 (31.6)	13 (68.4)	
2				0	7 (100)	
Vascular invasion			.664			.231
Absent	49 (19.1)	203 (80.9)		5 (20.0)	20 (80.0)	
Present	7 (16.3)	36 (83.7)		1 (100)	0	
Tumor necrosis			.437			
Absent	28 (16.8)	139 (83.2)		6 (23.1)	20 (76.9)	
Present	8 (22.2)	28 (77.7)				
Sarcomatoid feature			.346			
Absent	51 (18.1)	231 (81.9)		6 (23.1)	20 (76.9)	
Present	5 (27.8)	13 (72.2)				
pT category[a]			.037			.606
pT1	35 (16.9)	172 (83.1)		3 (18.8)	13 (81.3)	
pT2	10 (37.0)	17 (63.0)		2 (40.0)	3 (60.0)	
pT3/4	11 (16.7)	55 (83.3)		1 (20.0)	4 (80.0)	
pN category[a]			.899			> .999
pN0	55 (18.7)	239 (81.3)		6 (24.0)	19 (76.0)	
pN1	1 (16.7)	5 (83.3)		0	1 (100)	

Values are presented as number (%).
BAP1, BRCA1-associated protein 1; RCC, renal cell carcinoma; WHO, World Health Organization; ISUP, International Society of Urological Pathology.
[a]AJCC eighth edition.

the time of analysis.

BAP1 expression and tumor type evaluation

A total of 371 successfully stained cases with adequate clinical follow-up were classified as either BAP1 negative (n = 63, 17.0%) or BAP1 positive (n = 308, 83.0%). Representative images of BAP1 staining are shown in Fig. 1. Loss of BAP1 expression was frequently observed in ccRCC (18.7%) and chromophobe RCC (23.1%), while we failed to observe BAP1 expression loss in other renal tumor subtypes, including papillary RCC, acquired cystic disease-associated RCC, and collecting duct carcinoma. In clear cell papillary RCC, one case showed loss of BAP1 expression (Table 2).

BAP1 expression and clinicopathological features of patients with ccRCC and chromophobe RCC

In ccRCC, loss of BAP1 expression was significantly associated with female sex (p = .046) and high WHO/ISUP grade (p = .002). Furthermore, BAP1 expression loss was more frequent in pT2 than in pT1 category (Table 3). Other clinicopathological parameters such as vascular invasion, tumor necrosis, sarcomatoid feature, and lymph node status showed no significant association with BAP1 expression (Table 3).

In chromophobe RCC, no significant correlation was observed between BAP1 expression and clinicopathological parameters (Table 3).

BAP1 expression and survival in ccRCC

Of 300 patients with ccRCC, 10 (3.3%) had metastatic disease at the time of initial diagnosis (i.e., nephrectomy), 23 (7.7%) had experienced metastasis or relapse during the follow-up period, and 26 (8.7%) had died due to RCC by the time of analysis.

Kaplan-Meier analysis and Cox regression analysis were applied to evaluate the prognostic value of BAP1 loss. Univariate analysis revealed that high WHO/ISUP grade, vascular invasion, tumor necrosis, sarcomatoid feature, high pT category, and lymph node metastasis predicted a poor outcome in ccRCC (Table 4). However, BAP1 expression showed no association with CSS and RFS (Fig. 2A, B). Even in cases with low pT (pT1/2) ccRCC, loss of BAP1 expression showed no statistically significant correlation with CSS and RFS (Fig. 2C, D).

DISCUSSION

In this study, we demonstrated the loss of BAP1 nuclear expression in chromophobe RCC and clear cell papillary RCC as well as ccRCC. Furthermore, the loss of BAP1 nuclear expression was associated with adverse clinicopathological features such as

Table 4. Univariate Cox regression analyses for cancer-specific survival and recurrence-free survival in patients with clear cell RCC

Variable	Cancer-specific survival			Recurrence-free survival		
	HR	95% CI	p-value	HR	95% CI	p-value
BAP1						
Positive vs negative	1.076	0.405–2.859	.884	1.125	0.462–2.740	.795
Sex						
Female vs male	2.140	0.807–5.676	.118	1.879	0.814–4.334	.139
WHO/ISUP grade						
1–2	1			1		
3	3.401	1.138–10.165	.028	2.484	0.997–6.185	.051
4	20.883	7.323–59.550	<.001	16.202	6.749–38.890	<.001
Vascular invasion						
Absent vs present	9.386	4.306–20.460	<.001	8.219	4.130–16.355	<.001
Tumor necrosis						
Absent vs present	18.216	5.713–58.079	<.001	16.980	5.953–48.428	<.001
Sarcomatoid feature						
Absent vs present	13.933	6.283–30.896	<.001	10.823	5.103–22.957	<.001
pT category						
pT1	1			1		
pT2	6.298	1.409–28.145	.016	8.249	2.387–28.509	.001
pT3 and pT4	18.200	6.185–53.557	<.001	18.733	7.103–49.404	<.001
Lymph node metastasis						
Absent vs present	32.885	10.417–103.815	<.001	18.940	6.203–57.828	<.001

RCC, renal cell carcinoma; HR, hazard ratio; CI, confidence interval; BAP1, BRCA1-associated protein 1; WHO, World Health Organization; ISUP, International Society of Urological Pathology.

https://doi.org/10.4132/jptm.2018.09.21

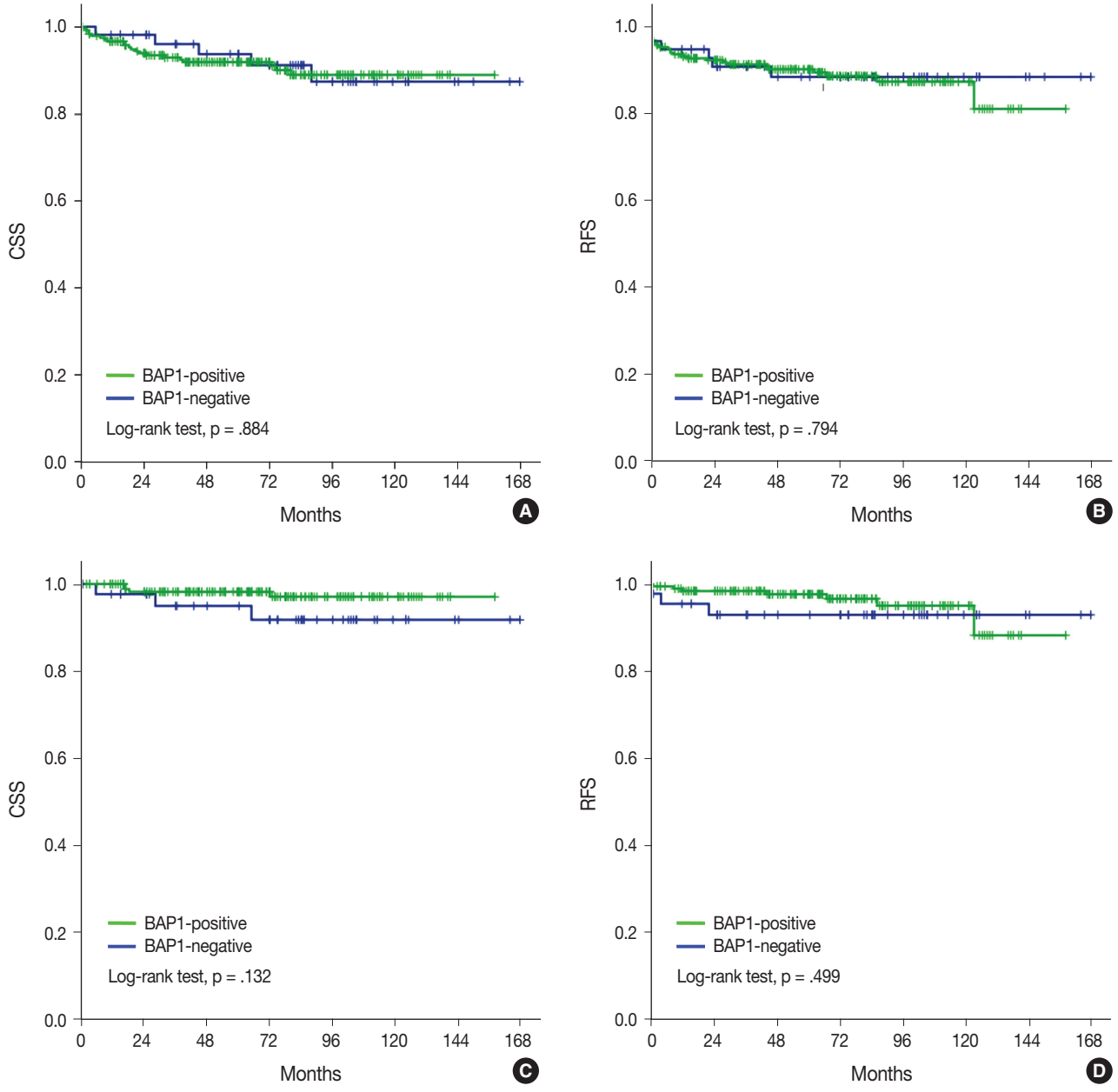

Fig. 2. Kaplan-Meier analysis of cancer-specific survival (CSS) and recurrence-free survival (RFS) in clear cell renal cell carcinoma (A, CSS; B, RFS) and pT1/2 ccRCC (C, CSS; D, RFS). BAP1, BRCA1-associated protein 1.

high WHO/ISUP grade in ccRCC but showed no relationship with CSS or RFS in patients with ccRCC.

The Cancer Genome Atlas (TCGA) research network recently reported the molecular characterization of RCC and included 488 ccRCC, 160 papillary type 1 RCC, 70 papillary type 2 RCC, and 81 chromophobe RCC. *BAP1* mutation, a chromatin remodeling gene mutation, was reported in ccRCC (11.0%) and papillary RCC (5.6%) but not in chromophobe RCC.[20] *BAP1* mutation was also shown to be correlated with decreased survival in ccRCC.[20]

The ratio of BAP1 loss in the present study (18.7%) was similar to that reported in previous studies.[21,22] We also found that the loss of BAP1 expression was significantly common in female sex (p = .046). *BAP1* mutation was more frequent in female patients as per TCGA data.[20,23] We observed that BAP1 nuclear expression loss was associated with high WHO/ISUP grade in ccRCC and showed no correlation with CSS and RFS. In several studies, loss of BAP1 expression served as an independent

marker of prognosis in patients with ccRCC and low-grade ccRCC.[24,25] On the other hand, in other studies, no significant association was reported between BAP1 loss and CSS or RFS, although BAP1 loss significantly correlated with poor clinicopathological parameters.[16,21] Differences in the prognostic associations may be related to differences in cohorts among studies. Our cohort had relatively low-grade RCC and a short follow-up period; therefore, overall cancer-specific death rate was lower than that recorded in the previous TGCA report (8% vs 33%).[20]

Among non-ccRCC, papillary RCC, chromophobe RCC, clear cell papillary RCC, acquired cystic disease-associated RCC, and collecting duct carcinoma were evaluated for BAP1 expression. We observed the loss of BAP1 expression in 23.1% of chromophobe RCC (6/26) cases and in one clear cell papillary RCC case. No significant association was detected between BAP1 expression and adverse clinicopathological parameters in chromophobe RCC. Unfortunately, the number of patients with chromophobe RCC and clear cell papillary RCC was too small to evaluate proper clinical relevance. In addition, during the follow-up period, one patient died due to chromophobe RCC; therefore, survival analysis could not be performed. An additional analysis is needed to further elucidate the role of BAP1 and the relationship between loss of BAP1 expression in IHC and *BAP1* mutation in chromophobe RCC and clear cell papillary RCC.

In conclusion, we revealed that BAP1 expression is associated with high WHO/ISUP grade in patients with ccRCC and that BAP1 expression loss is also observed in chromophobe RCC and clear cell papillary RCC. Further studies are needed to assess larger cohorts and associated pathological features.

ORCID

Su-Jin Shin: https://orcid.org/0000-0001-9114-8438

Conflicts of Interest

No potential conflict of interest relevant to this article was reported.

Acknowledgments

This work was supported by the research fund of Hanyang University (HY-2016).

REFERENCES

1. Rini BI, Campbell SC, Escudier B. Renal cell carcinoma. Lancet 2009; 373: 1119-32.
2. Dalgliesh GL, Furge K, Greenman C, *et al*. Systematic sequencing of renal carcinoma reveals inactivation of histone modifying genes. Nature 2010; 463: 360-3.
3. Guo G, Gui Y, Gao S, *et al*. Frequent mutations of genes encoding ubiquitin-mediated proteolysis pathway components in clear cell renal cell carcinoma. Nat Genet 2011; 44: 17-9.
4. Varela I, Tarpey P, Raine K, *et al*. Exome sequencing identifies frequent mutation of the SWI/SNF complex gene *PBRM1* in renal carcinoma. Nature 2011; 469: 539-42.
5. Hakimi AA, Ostrovnaya I, Reva B, *et al*. Adverse outcomes in clear cell renal cell carcinoma with mutations of 3p21 epigenetic regulators *BAP1* and *SETD2*: a report by MSKCC and the KIRC TCGA research network. Clin Cancer Res 2013; 19: 3259-67.
6. Peña-Llopis S, Vega-Rubín-de-Celis S, Liao A, *et al*. BAP1 loss defines a new class of renal cell carcinoma. Nat Genet 2012; 44: 751-9.
7. White AE, Harper JW. Cancer: emerging anatomy of the BAP1 tumor suppressor system. Science 2012; 337: 1463-4.
8. Bhattacharya S, Hanpude P, Maiti TK. Cancer associated missense mutations in *BAP1* catalytic domain induce amyloidogenic aggregation: a new insight in enzymatic inactivation. Sci Rep 2015; 5: 18462.
9. Murali R, Wiesner T, Scolyer RA. Tumours associated with *BAP1* mutations. Pathology 2013; 45: 116-26.
10. Rai K, Pilarski R, Cebulla CM, Abdel-Rahman MH. Comprehensive review of BAP1 tumor predisposition syndrome with report of two new cases. Clin Genet 2016; 89: 285-94.
11. Harbour JW, Onken MD, Roberson ED, *et al*. Frequent mutation of *BAP1* in metastasizing uveal melanomas. Science 2010; 330: 1410-3.
12. Bott M, Brevet M, Taylor BS, *et al*. The nuclear deubiquitinase BAP1 is commonly inactivated by somatic mutations and 3p21.1 losses in malignant pleural mesothelioma. Nat Genet 2011; 43: 668-72.
13. Andrici J, Sheen A, Sioson L, *et al*. Loss of expression of BAP1 is a useful adjunct, which strongly supports the diagnosis of mesothelioma in effusion cytology. Mod Pathol 2015; 28: 1360-8.
14. Koopmans AE, Verdijk RM, Brouwer RW, *et al*. Clinical significance of immunohistochemistry for detection of *BAP1* mutations in uveal melanoma. Mod Pathol 2014; 27: 1321-30.
15. Oka S, Inoshita N, Miura Y, *et al*. The loss of BAP1 protein expression predicts poor prognosis in patients with nonmetastatic clear cell renal cell carcinoma with inferior vena cava tumor thrombosis. Urol Oncol 2018; 36: 365.e9-e14.
16. Minardi D, Lucarini G, Milanese G, Montironi R, Di Primio R. Prognostic role of BAP1 in pT1 clear cell carcinoma in partial nephrectomy specimens. Virchows Arch 2017; 471: 99-105.
17. Eble JN, Sauter G, Epstein JI, Sesterhenn IA. World Health Organization classification of tumors: pathology and genetics of tumours

of the urinary system and male genital organs. Lyon: IARC Press, 2016.
18. Delahunt B, Cheville JC, Martignoni G, *et al*. The International Society of Urological Pathology (ISUP) grading system for renal cell carcinoma and other prognostic parameters. Am J Surg Pathol 2013; 37: 1490-504.
19. Paner GP, Amin MB, Alvarado-Cabrero I, *et al*. A novel tumor grading scheme for chromophobe renal cell carcinoma: prognostic utility and comparison with Fuhrman nuclear grade. Am J Surg Pathol 2010; 34: 1233-40.
20. Ricketts CJ, De Cubas AA, Fan H, *et al*. The Cancer Genome Atlas comprehensive molecular characterization of renal cell carcinoma. Cell Rep 2018; 23: 3698.
21. Kim SH, Park WS, Park EY, *et al*. The prognostic value of BAP1, PBRM1, pS6, PTEN, TGase2, PD-L1, CA9, PSMA, and Ki-67 tissue markers in localized renal cell carcinoma: a retrospective study of tissue microarrays using immunohistochemistry. PLoS One 2017; 12: e0179610.
22. da Costa WH, da Cunha IW, Fares AF, *et al*. Prognostic impact of concomitant loss of PBRM1 and BAP1 protein expression in early stages of clear cell renal cell carcinoma. Urol Oncol 2018; 36: 243.e1-e8.
23. Ricketts CJ, Linehan WM. Gender specific mutation incidence and survival associations in clear cell renal cell carcinoma (CCRCC). PLoS One 2015; 10: e0140257.
24. Joseph RW, Kapur P, Serie DJ, *et al*. Loss of BAP1 protein expression is an independent marker of poor prognosis in patients with low-risk clear cell renal cell carcinoma. Cancer 2014; 120: 1059-67.
25. Kapur P, Christie A, Raman JD, *et al*. BAP1 immunohistochemistry predicts outcomes in a multi-institutional cohort with clear cell renal cell carcinoma. J Urol 2014; 191: 603-10.

Journal of Pathology and Translational Medicine 2018; 52: 386-395
https://doi.org/10.4132/jptm.2018.10.02

ORIGINAL ARTICLE

Multiplicity of Advanced T Category–Tumors Is a Risk Factor for Survival in Patients with Colorectal Carcinoma

Hye Eun Park[1] · Seungyeon Yoo[1]
Jeong Mo Bae[1] · Seorin Jeong[2]
Nam-Yun Cho[2] · Gyeong Hoon Kang[1,2]

[1]Department of Pathology, Seoul National University Hospital, Seoul National University College of Medicine, Seoul; [2]Laboratory of Epigenetics, Cancer Research Institute, Seoul National University College of Medicine, Seoul, Korea

Received: August 14, 2018
Revised: September 12, 2018
Accepted: October 2, 2018

Corresponding Author
Gyeong Hoon Kang, MD, PhD
Department of Pathology, Seoul National University College of Medicine, 103 Daehak-ro, Jongno-gu, Seoul 03080, Korea
Tel: +82-2-740-8263
Fax: +82-2-765-5600
E-mail: ghkang@snu.ac.kr

Background: Previous studies on synchronous colorectal carcinoma (SCRC) have reported inconsistent results about its clinicopathologic and molecular features and prognostic significance. **Methods:** Forty-six patients with multiple advanced tumors (T2 or higher category) who did not receive neoadjuvant chemotherapy and/or radiotherapy and who are not associated with familial adenomatous polyposis were selected and 99 tumors from them were subjected to clinicopathologic and molecular analysis. Ninety-two cases of solitary colorectal carcinoma (CRC) were selected as a control considering the distributions of types of surgeries performed on patients with SCRC and T categories of individual tumors from SCRC. **Results:** SCRC with multiple advanced tumors was significantly associated with more frequent nodal metastasis (p = .003) and distant metastasis (p = .001) than solitary CRC. *KRAS* mutation, microsatellite instability, and CpG island methylator phenotype statuses were not different between SCRC and solitary CRC groups. In univariate survival analysis, overall and recurrence-free survival were significantly lower in patients with SCRC than in patients with solitary CRC, even after adjusting for the extensiveness of surgical procedure, adjuvant chemotherapy, or staging. Multivariate Cox regression analysis revealed that tumor multiplicity was an independent prognostic factor for overall survival (hazard ratio, 4.618; 95% confidence interval, 2.126 to 10.030; p < .001), but not for recurrence-free survival (p = .151). **Conclusions:** Findings suggested that multiplicity of advanced T category–tumors might be associated with an increased risk of nodal metastasis and a risk factor for poor survival, which raises a concern about the guideline of American Joint Committee on Cancer's tumor-node-metastasis staging that T staging of an index tumor determines T staging of SCRC.

Key Words: Synchronous colorectal carcinoma; Multiple colorectal carcinoma; Clinical outcome; T category

Colorectal carcinoma (CRC) is the third most common cancer in men and the second most common in women. CRC has been reported to occur more commonly in the western countries, but over the past few decades, the incidence of CRC has increased in many Asian countries including South Korea, with about 610,000 Asian patients newly diagnosed in 2012.[1] Synchronous CRC (SCRC) refers to more than one CRC detected in a single patient at the time of diagnosis. Unlike what is expected, little is known about the clinicopathologic features of SCRC. With a handful of previous studies addressing the issue, the only consensus seems to be the male predominance; most of the previous studies reported that SCRC was observed more frequently in men.[2-6] The reported incidence of SCRCs varies from 1.1% to 8.1%,[3,5,7-15] with the narrower range of 3.1% to 3.9% in three large-scale studies performed on a population larger than 10,000 patients.[3,12,13] While some studies concluded that the average age at diagnosis was higher in patients with SCRC than in patients with solitary CRC,[10,13,16] others failed to demonstrate a significant difference between them.[5,12,15,17] Some studies reported that SCRC preferentially affects the distal colon,[5,18-20] but others, including large-scale studies, concluded that the proximal colon was more frequently involved by SCRC.[21,22]

Research has mainly focused on single factors such as microsatellite instability (MSI) for the underlying molecular mechanisms of SCRC. Some studies have reported that MSI-high (MSI-H) phenotype was more common in SCRC than in solitary CRC and the incidence of MSI-H phenotype was upto 30% in SCRC.[23-25] In particular, Nosho *et al*.[26] found that not only MSI-H phenotype but also *BRAF* mutation and CpG island methylator phenotype (CIMP)-high (CIMP-H) phenotype were more common in SCRC than in solitary CRC, suggesting that SCRC may arise through the serrated neoplasia pathway. A similar finding has been reported by Gonzalo *et al*.[27] who found that CIMP-H was more frequent in SCRC than in solitary CRC and

pISSN 2383-7837
eISSN 2383-7845

suggested a close association between tumor multiplicity and CIMP-H phenotype. However, one study reported that MSI occurs only in 10% of SCRCs.[28] Besides MSI, long interspersed nuclear element-1 (LINE-1) hypomethylation in colonic epithelial cells has been suggested to be a possible risk factor for the occurrence of metachronous or SCRC based on finding that LINE-1 methylation of non-neoplastic colonic epithelial cells was lower in SCRC than in solitary CRC.[29] Some studies found that *KRAS* and *TP53* may show discordant mutation statuses between individual tumors of SCRCs,[30,31] but correlations between SCRC and various clinicopathological or molecular parameters still remain unclear.

It seems plausible that a patient with multiple tumors at the time of diagnosis would show poorer prognosis than one with a solitary tumor. Strikingly, this has not been proved with the sufficient level of confidence in CRC, which is the reason that the current TNM staging of CRC does not reflect tumor multiplicity unlike other cancers such as intrahepatic cholangiocarcinoma.[32] In fact, the prognostic effect of tumor multiplicity at the time of diagnosis has been inconsistent among studies; with only a few studies reporting significantly worse prognosis,[26,33] many failed to demonstrate significant differences in survival between patients with solitary CRC and SCRC and some researchers even concluded that SCRC was associated with favorable prognosis.[10,22] Therefore, the current TNM staging guideline for SCRC advises that the lesion with the most advanced pathologic staging is designated to be an index lesion and it is assumed that the survival of the patients with SCRC follows the stage of the index lesions.[5,22] In this scheme, patients with SCRC with the index lesion of pT3 category would show similar survival to those with solitary pT3 CRC.

The purpose of the current study is to address all the inconsistency and to draw clearer conclusion on the prognostic effect of the tumor multiplicity at the time of diagnosis. To do so, we identified a group of patients with SCRCs with advanced T categories, examined their clinicopathologic and molecular features and compared their survival to those with the comparable group of patients with solitary CRC.

MATERIALS AND METHODS

Tissue collection

Two thousand eight hundred thirty-four CRC patients who underwent surgery at Seoul National University Hospital, Seoul, Korea, from January 2007 to December 2010 were reviewed. Among them, 2,701 were solitary CRC patients and 133 were diagnosed as SCRC. From the 133 patients, we excluded patients with familial adenomatous polyposis (FAP) (n = 3) and those who received neoadjuvant chemo- and/or radiotherapy (n = 8). In order to focus on patients with advanced stages, we further excluded patients with intramucosal carcinoma (n = 37) and T1-category lesions (n = 39). As a result, 46 cases with multiple advanced tumors (T2 or higher category) were selected for this study (Fig. 1). Of the 46 patients, 16 underwent extensive surgery including total colectomy and subtotal colectomy, and 30 had a relatively simple procedure (8 cases of anterior resection, 14 cases of ultra-low or low anterior resection, 4 cases of right or left hemicolectomy, and 4 cases of extended right hemicolectomy). Considering the distributions of pT categories of individual tumors and types of surgeries performed on patients with SCRC, we selected 92 cases of solitary CRC with similar distributions of pT categories (Table 1) and types of surgeries (35 cases of anterior resection, 31 cases of low anterior resection, 12 cases of right or left hemicolectomy, and 14 cases of extended right hemicolectomy). However, we could not retrieve patients with solitary CRC who received extensive surgery. This study was approved by the Institutional Review Board (IRB No. 1101-007-345). IRB exempted the informed consent due to the retrospective nature of the study.

Clinicopathologic data

Clinical and histopathologic data from the 46 patients with SCRC (99 tumors) and 92 patients with solitary CRC (92 tumors) were collected through the electronic medical record and a microscopic examination. The parameters of the clinicopathologic data included patient age, sex, overall survival (OS), recurrence-free survival (RFS), tumor location, tumor multiplicity, American Joint Committee on Cancer (AJCC)/Union for International Cancer Control (UICC) tumor-node-metastasis (TNM) category, tumor differentiation, lymphovascular invasion, and perineural invasion.

KRAS mutation and MSI analysis

Through histological examination, representative tumor portions were marked and then subjected to manual microdissection. The dissected tissues were collected into microtubes containing lysis buffer and proteinase K and were incubated at 55°C for upto 2 days. DNA from paraffin-embedded tissues was extracted, and polymerase chain reaction was performed. Mutations in *KRAS* codons 12 and 13 were analyzed in each case using direct sequencing. The MSI status of each tumor was determined through the evaluation of five microsatellite markers (BAT25, BAT26, D2S123, D5S346, and D17S250) as standardized by the National Cancer Institute. MSI-H status was defined as when tumor DNA

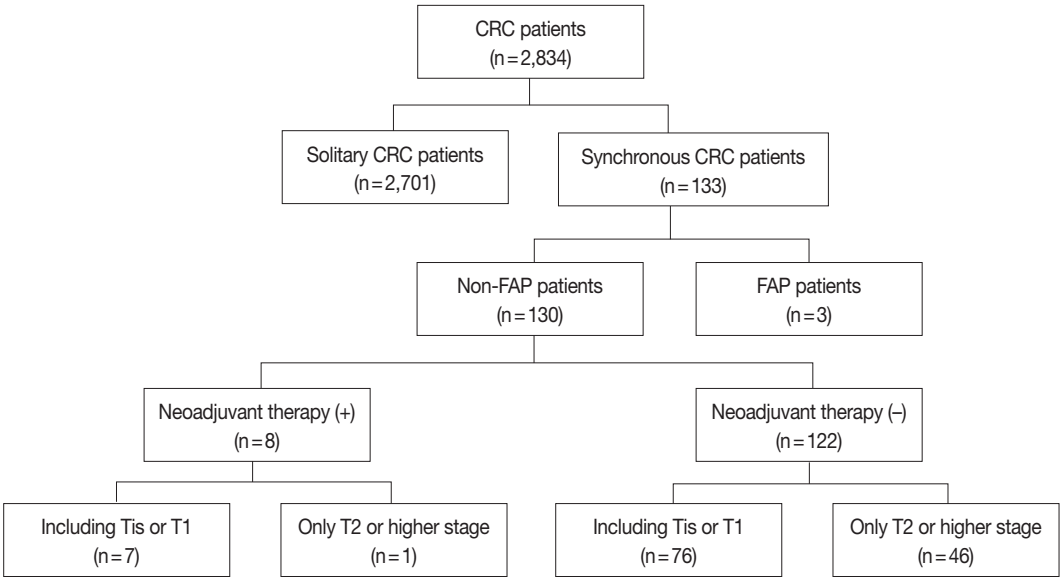

Fig. 1. Schematic diagram for selection of patients with synchronous colorectal cancer (CRC). FAP, familial adenomatous polyposis.

had altered alleles compared to normal DNA in two or more markers. MSI-low status was defined as when tumor DNA had altered allele compared to normal DNA in one marker. Microsatellite-stable was defined as when no altered allele was present in tumor DNA. We performed immunohistochemistry (IHC) for DNA mismatch repair proteins (MLH1 and MSH2) to assess MSI status for tumors that were not evaluated for MSI status using polymerase chain reaction-coupled capillary electrophoresis (50 individual tumors from SCRCs and 3 solitary CRCs). IHC was performed using antibodies against MLH1 (Ventana Medical Systems, Tucson, AZ, USA), MSH2 (Invitrogen, Camarillo, CA, USA) and automated immunostainers (Ventana BenchMark XT for MLH1; Bond-III, Leica Biosystems, Novocastra, Newcastle-upon-Tyne, UK for MSH2).

Analysis of CIMP

The CIMP status of individual tumors was analyzed using a real-time methylation-specific quantitative polymerase chain reaction method (MethyLight) and eight CIMP-specific markers (*CACNA1G*, *CDKN2A*, *CRABP1*, *IGF2*, *MLH1*, *NEUR0G1*, *RUNX3*, and *S0CS1*). We classified CRCs into CIMP-0 (no methylated marker), CIMP-low (1–4 methylated markers), and CIMP-H (5 or more methylated markers).

Statistical analysis

In this study, statistical analysis was performed using SPSS ver. 23 (IBM Corp., Armonk, NY, USA). Comparison between categorical variables was conducted with the chi-square test or Fisher exact test. Survival analysis using OS and RFS data was performed using the Kaplan-Meier method with the log-rank test. Hazard ratios (HRs) were calculated using the Cox proportional hazard model. All variables that were associated with OS with a $p < .10$ were entered into the model. These variables were reduced by backward elimination. All p-values were two-sided and p-values of $< .05$ were considered to be statistically significant.

RESULTS

Clinicopathologic features

The detailed clinicopathologic features are summarized in Table 1 and Fig. 2. SCRC with multiple advanced tumors was associated with more frequent nodal metastasis ($p = .003$) and advanced TNM category ($p = .003$). SCRC exhibited a tendency toward male predominance with marginal significance ($p = .050$). Metachronous metastasis was significantly more frequent in SCRCs with multiple advanced tumors than in solitary CRCs ($p = .001$). However, there were no significant differences in terms of lymphatic and vascular invasion between two groups. In addition, *KRAS* mutation and MSI status did not show any significant difference between the two groups. In CIMP analysis for SCRC, CIMP-H phenotype was observed in four of 46 patients (8.7%), which was quite lower compared with results of previous studies (35% in Nosho *et al.*'s study[26] and 66.6% in Gonzalo *et al.*'s study[27]). However, the frequency of CIMP-H in terms of individual tumors was 5.1% (5 of 99 tumors) which was not different from the frequency of CIMP-H in solitary CRCs (6.5%) of the

 https://doi.org/10.4132/jptm.2018.10.02

Table 1. Clinicopathologic and molecular characteristics of CRCs according to tumor multiplicity

Variable	Solitary CRCs (92 patients, 92 tumors)	Synchronous CRCs (46 patients, 99 tumors)	p-value
Age (yr)	63.5 (33–82)	66.0 (43–88)	.087
Sex			.050
Male	59 (64.1)	37 (80.4)	
Female	33 (35.9)	9 (19.6)	
Location			.247
Proximal	18 (19.6)	29 (29.3)	
Distal	48 (52.2)	42 (42.4)	
Rectum	26 (28.3)	28 (28.3)	
Gross type			.114
Polypoid	11 (12.0)	22 (22.2)	
Ulcerofungating	61 (66.3)	53 (53.5)	
Ulceroinfiltrative	20 (21.7)	24 (24.2)	
T category			.548
T2	12 (13.0)	18 (18.2)	
T3	73 (79.3)	72 (72.7)	
T4	7 (7.6)	9 (9.1)	
N category			.003
N0	49 (53.3)	12 (26.1)	
N1, N2	43 (46.7)	34 (73.9)	
M category			.001
M0	73 (79.3)	23 (50.0)	
Synchronous M1	7 (7.6)	12 (26.1)	
Metachronous M1	12 (13.0)	11 (23.9)	
Stage			.003
I	9 (9.8)	1 (2.2)	
II	40 (43.5)	11 (23.9)	
III	36 (39.1)	22 (47.8)	
IV	7 (7.6)	12 (26.1)	
Surgery			< .001
Simple	92	30 (65.2)	
Extensive	0	16 (34.8)	
Chemotherapy			1.000
Treated	80 (87.0)	40 (87.0)	
Non-treated	12 (13.0)	6 (13.0)	
Differentiation			.722[a]
Well	9 (9.8)	9 (9.1)	
Moderately	78 (84.8)	87 (87.9)	
Poorly	5 (5.4)	3 (3.0)	
Lymphatic invasion			.068
Absent	73 (79.3)	67 (67.7)	
Present	19 (20.7)	32 (32.3)	
Venous invasion			.086
Absent	86 (93.5)	85 (85.9)	
Present	6 (6.5)	14 (14.1)	
Perineural invasion			.986
Absent	80 (87.0)	86 (86.9)	
Present	12 (13.0)	13 (13.1)	
MSI			0.740[a]
MSS/MSI-low	87 (94.6)	95 (96.0)	
MSI-high	5 (5.4)	4 (4.0)	
KRAS mutation			.908
Wild type	55 (59.8)	60 (60.6)	
Mutant	37 (40.2)	39 (39.4)	
CIMP			.761
CIMP-0, low	86 (93.5)	94 (94.9)	
CIMP-high	6 (6.5)	5 (5.1)	

CRC, colorectal carcinoma; MSI, microsatellite instability; MSS, microsatellite-stable; CIMP, CpG island methylator phenotype.
[a]Fisher exact test.

present study and those of previous Korean CRC studies.[34,35] Nodal and distant metastasis showed significant differences between SCRC and solitary CRC when we restricted comparative analyses to CRC cases with non-extensive surgery or cases with R0 surgery (Table 2).

Prognostic implication of tumor multiplicity in CRCs

In order to examine the prognostic effect of tumor multiplicity per se, we sought to focus on subgroups where compounding variables were adjusted. Firstly, we performed Kaplan-Meier survival analysis on patients who had no metastasis at the time of diagnosis and hence underwent curative surgery (85 patients with solitary CRC and 34 patients with SCRC). As a result, SCRC patients with multiple advanced tumors showed worse OS and RFS than the respective ones of patients with solitary CRC (Fig. 3A, B). Since it cannot be excluded a possibility that the extensiveness of surgery itself might affect the survival of patients with SCRC, survival analysis was conducted in 85 solitary CRC and 22 SCRC patients with exclusion of patients who underwent the extensive surgical procedures such as total colectomy and subtotal colectomy, which revealed significant associations between SCRC and poor OS or RFS (Fig. 3C, D). When we further excluded patients who did not receive adjuvant chemotherapy to adjust for the effect of adjuvant chemotherapy, univariate survival analysis in 36 patients with solitary CRC and 13 patients with SCRC revealed that the prognosis of SCRC with multiple advanced tumors tended to be worse than that of solitary CRC patients (Fig. 3E, F). To validate these results, we selected 24 SCRC cases with an index tumor of T3 category and recruited another independent set of patients with solitary CRC of T3 category (n = 120) on the criteria of R0 surgery and adjuvant chemotherapy. Because SCRC cases were composed of nine N0, seven N1, and eight N2 cases, 45 solitary CRC cases of N0 category, 35 of N1 category, and 40 of N2 category were recruited.

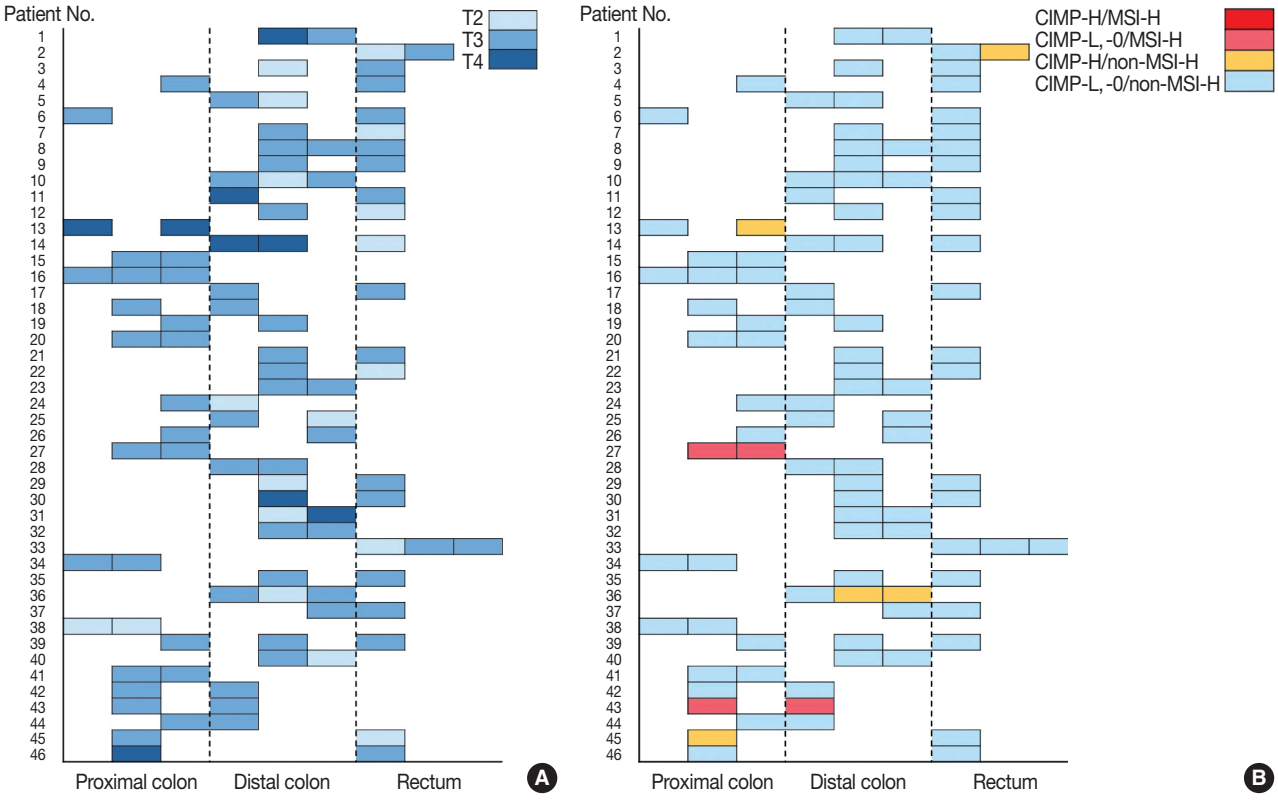

Fig. 2. Distribution of tumor location with specification of T category (A) and molecular features (B) for individual tumors of synchronous colorectal cancer. CIMP, CpG island methylator phenotype; CIMP-H, CIMP-high; CIMP-L, CIMP-low; CIMP-0, no methylated marker; MSI, microsatellite instability; MSI-H, MSI-high.

Kaplan-Meier survival analysis showed that patients with SCRC still had worse OS compared with patients with solitary CRC group that matched T and N category, but not for RFS (Fig. 3G, H). In multivariate Cox regression analysis, tumor multiplicity was found to be an independent prognostic factor for OS (HR, 4.618; 95% confidence interval, 2.126 to 10.030; $p < .001$), but not for RFS ($p = .151$) (Tables 3, 4).

DISCUSSION

In this study, we investigated the clinicopathologic and molecular characteristics of SCRC as well as the prognostic implication of the tumor multiplicity at the time of diagnosis. The reported incidence of SCRC in the literature varies from 1.1% to 8.1%.[3,5,7-15] This variance might be attributable to the difference in the definition of SCRC; whether FAP or intramucosal carcinoma is included or not in the definition of SCRC can make a significant difference.[20] In this study, we excluded SCRC associated with FAP (n = 3). The incidence of SCRC was 4.6% (n = 130) when intramucosal carcinomas were included and 3.2% (n = 91) when excluded, in line with the previous studies. Of these patients (n = 91), we excluded those patients who received neoadjuvant chemo- and/or radiotherapy (n = 6) or T1-category lesion (n = 39). We only selected SCRCs in which all the individual tumors were of pT2 or higher category and resultantly, 46 patients were included in the present study.

The median age at diagnosis of SCRC with multiple advanced tumors was higher than that of solitary CRC, but the difference did not reach a statistical significance in this study. Several studies have reported that the mean age of patients with SCRC is significantly higher than that of patients with solitary CRC.[10,13,16] However, in Oya *et al.*'s study,[5] age difference failed to reach the statistical significance, and Latournerie *et al.*[12] conducted a large-scale study to discover that there was no significant difference. Regarding sex distribution, previous studies reported that SCRC is more common in men,[2-6] but this study confirmed this tendency only with the marginal significance. Previous studies have reported inconsistent results on the sidedness of SCRC. Finan *et al.*[18] reported that SCRC is more common in the distal part of colon, the same with the solitary CRC in general, but Lam *et al.*[22] showed that SCRC more commonly affects the proximal colon than solitary CRC does. In the present study, SCRC showed a ten-

https://doi.org/10.4132/jptm.2018.10.02

Table 2. Differences in clinicopathologic characteristics according to subgroup analysis

Variable	Total cases of CRC		CRC cases with R0 resection		CRC cases with non-extensive surgery	
	Solitary CRC (n=92)	SCRC (n=46)	Solitary CRC (n=85)	SCRC (n=34)	Solitary CRC (n=92)	SCRC (n=30)
Age (yr)	63.5 (33–82)	66.0 (43–88)	63.0 (33–82)	66.0 (48–79)	63.5 (33–82)	66.0 (43–88)
p-value	.087		.150		.168	
Sex						
Male	59 (64.1)	37 (80.4)	56 (65.9)	25 (73.5)	59 (64.1)	24 (80.0)
Female	33 (35.9)	9 (19.6)	29 (34.1)	9 (26.5)	33 (35.9)	6 (20.0)
p-value	.050		.419		.106	
T category						
T2	12 (13.0)	18 (18.2)	12 (14.1)	13 (17.8)	12 (13.0)	13 (20.3)
T3	73 (79.3)	72 (72.7)	68 (80.0)	52 (71.2)	73 (79.3)	42 (65.6)
T4	7 (7.6)	9 (9.1)	5 (5.9)	8 (11.0)	7 (7.6)	9 (14.1)
p-value	.548		.374		.154	
N category						
N0	49 (53.3)	12 (26.1)	49 (57.6)	12 (35.3)	49 (53.3)	8 (26.7)
N1, N2	43 (46.7)	34 (73.9)	36 (42.4)	22 (64.7)	43 (46.7)	22 (73.3)
p-value	.003		.028		.011	
M category						
M0	73 (79.3)	23 (50.0)	73 (85.9)	23 (67.6)	73 (79.3)	14 (46.7)
Synchronous M1	7 (7.6)	12 (26.1)	-	-	7 (7.6)	8 (26.7)
Metachronous M1	12 (13.0)	11 (23.9)	12 (14.1)	11 (32.4)	12 (13.0)	8 (26.7)
p-value	.001		.023		.002	
Lymphatic invasion						
Absent	73 (79.3)	67 (67.7)	69 (81.2)	53 (72.6)	73 (79.3)	37 (57.8)
Present	19 (20.7)	32 (32.3)	16 (18.8)	20 (27.4)	19 (20.7)	27 (42.2)
p-value	.068		.200		.004	
Venous invasion						
Absent	86 (93.5)	85 (85.9)	81 (95.3)	65 (89.0)	86 (93.5)	55 (85.9)
Present	6 (6.5)	14 (14.1)	4 (4.7)	8 (11.0)	6 (6.5)	9 (14.1)
p-value	.086		.139		.116	

Values are presented as median (range) or number (%).

dency toward the right colon, but with no statistical significance.

In line with several previous studies which showed that the proportion of advanced stage is higher in SCRC than in solitary CRC,[12,19,20,22] we discovered that SCRC cases tended to be more advanced than solitary cases. Lymphatic and venous invasions tended to be more frequent in individual tumors of SCRC than in solitary CRC. Although our findings indicated that nodal metastasis was significantly more common in SCRC with multiple advanced tumors than in solitary CRC, a concern is that selection of solitary CRC might be biased toward collection of solitary CRC with less frequent nodal metastasis. To exclude such a possibility, we analyzed the frequency of nodal metastasis in 593 cases of solitary T3 CRC. The frequency of N0 was significantly higher in solitary T3 CRC than in SCRC with an index tumor of T3 category (45.5% vs. 26.3%, p = .027). This finding suggests that multiplicity of advanced T category–tumors might be a risk factor for nodal metastasis.

Molecular analysis performed in this study revealed that the prevalence of MSI and *KRAS* mutation in the SCRC were not different from the respective ones of the solitary CRC. Out of the 99 individual tumors from 46 SCRC patients, only four tumors from two patients were MSI-H. The analysis of CIMP status for these tumors showed that these MSI-H tumors were negative for *MLH1* methylation and not CIMP-H, which suggests the possibility that these SCRC patients with multiple MSI-H tumors might be patients with Lynch syndrome. In fact, both of these patients had first-degree relatives with CRC as well as SCRC with MSI-H phenotype, and could be diagnosed as hereditary nonpolyposis colon cancer. However, in previous studies, exploration on MSI status of SCRC showed a higher proportion of MSI-H phenotype in SCRC than in solitary CRC.[23-25] Nosho *et al*.[26] found that SCRC was more likely to be *BRAF*-mutated, CIMP-H and MSI-H, suggesting that MSI-H phenotype in SCRC is likely to be sporadic rather than hereditary. Such a discrepancy between previous studies and the present study might be attributable to the fact that we excluded tumors of Tis or T1 category or the fact

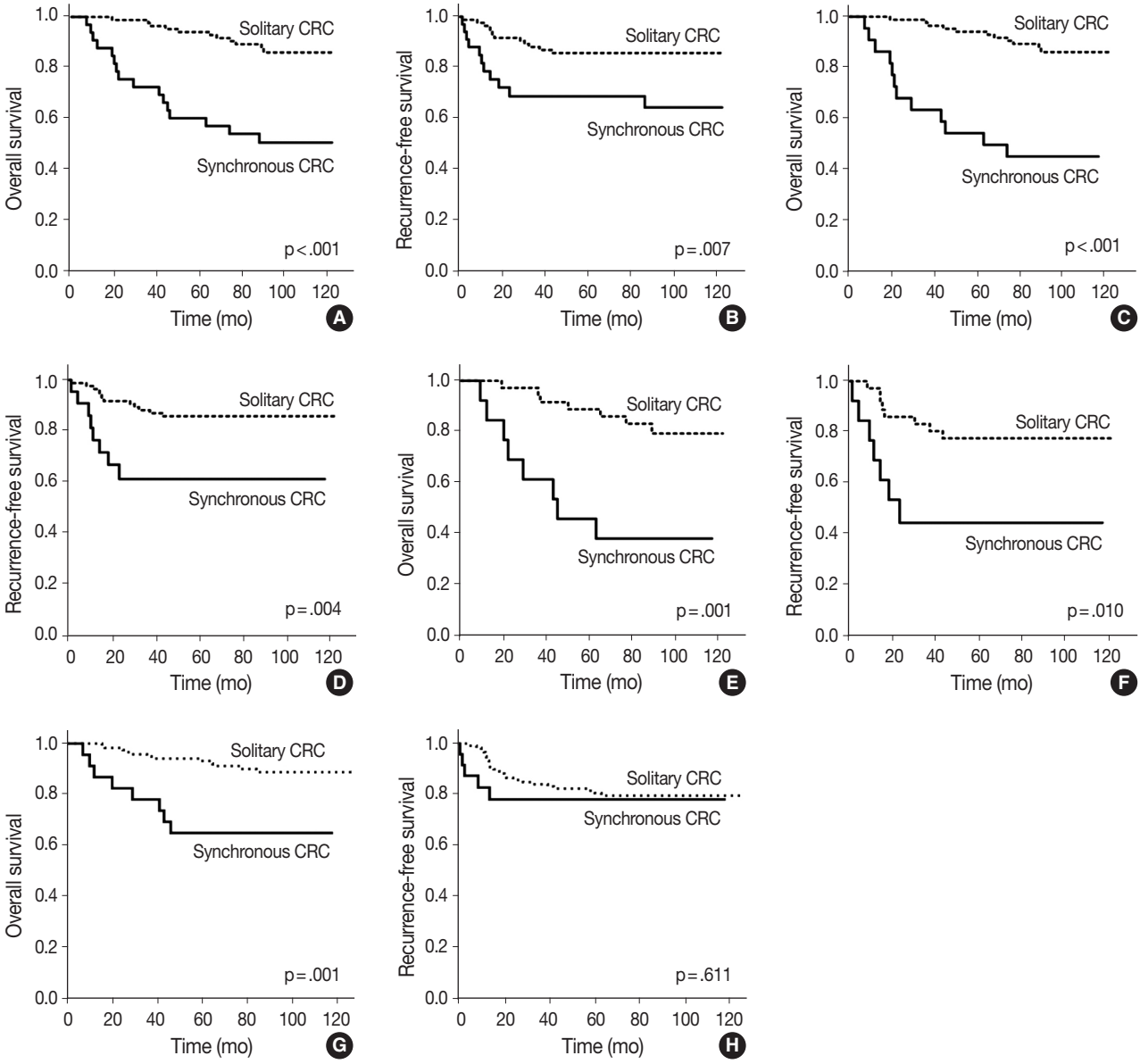

Fig. 3. Kaplan-Meier survival curves for overall survival and recurrence-free survival according to the tumor multiplicity in colorectal cancer (CRC) patients with curative surgery (n=119) (A, B), in CRC patients with curative and non-extensive surgery (85 patients with solitary CRC and 22 patients with synchronous CRC) (C, D), in CRC patients with curative and non-extensive surgery and adjuvant chemotherapy (36 patients with solitary CRC and 13 patients with synchronous CRC) (E, F), and in stage-matched CRC patients with R0 surgery and adjuvant chemotherapy (120 patients with solitary CRC and 24 patients with synchronous CRC) (G, H).

that the frequency of CIMP-H phenotype is lower in CRCs from Korean patients than those from western people.[36]

Most of the previous studies reported that the survival of the patients with SCRC was not significantly different from that of patients with solitary CRC and only depended on the pathologic staging of the index cancer.[22] Even Hu *et al*.[10] suggested that patients with SCRC might have survival benefit. Only a few studies have discovered that patients with SCRC had worse prognosis than that of patients with solitary CRC.[26,33] It should be pointed out that previous studies which reported no difference in survival between SCRC and solitary CRC were conducted on a population of SCRC in which SCRC with Tis or T1 tumor as a non-index tumor comprise approximately 46% and 30% of the study cases, respectively.[16,22] In accordance with the hypothesis that patients with multiple advanced tumors would indeed have more tumor burden, we only selected SCRC cases in which all the individual tumors were of T2 or higher categories. Kaplan-Meier survival analysis showed that SCRC patients with multi-

https://doi.org/10.4132/jptm.2018.10.02

Table 3. Univariate and multivariate Cox analysis for overall survival (n=119)

Variable	Univariate		Multivariate	
	HR	p-value	HR	p-value
Age (≥65 yr/<65 yr)	4.088 (1.728–9.673)	.001	4.041 (1.703–9.587)	.002
Sex (male/female)	1.051 (0.472–2.347)	.902	-	-
Multiplicity (synchronous/solitary)	5.075 (2.350–10.960)	<.001	4.618 (2.126–10.030)	<.001
T category (T3, 4/T2)	3.487 (0.473–25.709)	.220	-	-
N category (N1, 2/N0)	3.617 (1.528–8.564)	.003	3.072 (1.291–7.309)	.011
Vascular invasion (present/absent)	2.373 (0.897–6.273)	.082	-	.159
Lymphatic invasion (present/absent)	2.836 (1.326–6.065)	.007	-	.122
Perineural invasion (present/absent)	1.617 (0.612–4.270)	.333	-	-
Tumor location (including right colon/left colon only)	0.907 (0.397–2.072)	.817	-	-
Chemotherapy (treated/not-treated)	1.088 (0.376–3.147)	.876	-	-
Surgery (extensive/simple)	1.837 (0.635–5.314)	.262	-	-
MSI (MSI-H/MSS, MSI-L)	0.045 (0.000–33.308)	.357	-	-
KRAS (mutant/wild type)	2.337 (1.049–5.204)	.038	-	-

HR, hazard ratio; MSI, microsatellite instability; MSI-H, MSI-high; MSS, microsatellite-stable; MSI-L, MSI-low.

Table 4. Univariate and multivariate Cox analysis for recurrence-free survival (n=119)

Variable	Univariate		Multivariate	
	HR	p-value	HR	p-value
Age (≥65 yr/<65 yr)	1.803 (0.791–4.114)	.161	2.163 (0.905–5.171)	.083
Sex (male/female)	1.672 (0.733–3.815)	.222	-	-
Multiplicity (synchronous/solitary)	2.939 (1.294–6.674)	.010	-	.151
T category (T3, 4/T2)	2.993 (0.403–22.224)	.284	-	-
N category (N1, 2/N0)	4.378 (1.623–11.805)	.004	3.943 (1.457–10.670)	.007
Vascular invasion (present/absent)	3.658 (1.440–9.294)	.006	4.114 (1.527–11.081)	.005
Lymphatic invasion (present/absent)	3.096 (1.365–7.025)	.007	-	.225
Perineural invasion (present/absent)	2.417 (0.952–6.136)	.063	-	-
Tumor location (including right colon/left colon only)	1.370 (0.509–3.690)	.534	-	-
Chemotherapy (treated/not-treated)	0.555 (0.130–2.369)	.427	-	-
Surgery (extensive/simple)	1.535 (0.456–5.169)	.489	-	-
MSI (MSI-H/MSS, MSI-L)	0.045 (0.000–63.182)	.401	-	-
KRAS (mutant/wild type)	1.776 (0.768–4.105)	.179	-	-

HR, hazard ratio; MSI, microsatellite instability; MSI-H, MSI-high; MSS, microsatellite-stable; MSI-L, MSI-low.

ple advanced tumors had worse survival than that of patients with solitary CRC. We performed a subgroup analysis in order to adjust for the effect of adjuvant chemotherapy, extensive surgical procedure such as total colectomy or subtotal colectomy, or T and N categories, and discovered that tumor multiplicity was an independent prognostic factor for OS in multivariate analysis. The reason why SCRC patients with multiple advanced tumors pursue worse clinical outcome than patients with solitary CRC is related to the fact that SCRC was associated with more frequent nodal metastasis and metachronous metastasis.

In conclusion, we selected SCRC with all the individual tumors of T2 or higher category and compared various characteristics between SCRC and solitary CRC of similar T category–distribution. We found that SCRC was featured with higher incidence of nodal metastasis and metachronous metastasis and shortened OS time compared with solitary CRC. Based on the finding that multiplicity of advanced T category–tumors was an independent prognostic parameter heralding poor overall survival, the current staging of SCRC with multiple advanced tumors according to the tumor-node-metastasis guideline of AJCC that an index tumor of advanced T category determines the T category of SCRC, is likely to evaluate better than actual prognosis. More studies would be needed to validate this finding and discover the underlying mechanism of it.

ORCID

Hye Eun Park: https://orcid.org/0000-0003-1048-2827
Jeong Mo Bae: https://orcid.org/0000-0003-0462-3072
Gyeong Hoon Kang: https://orcid.org/0000-0003-2380-6675

Conflicts of Interest

No potential conflict of interest relevant to this article was reported.

Acknowledgments

This work was supported by a grant from the National Research Foundation (NRF) funded by the Korean Ministry of Science, ICT and Future Planning (2016M3A9B6026921) and a grant from the Korea Health Technology R&D Project through the Korea Health Industry Development Institute funded by the Korean Ministry of Health and Welfare (HI14C1277).

REFERENCES

1. Ferlay J, Soerjomataram I, Dikshit R, *et al*. Cancer incidence and mortality worldwide: sources, methods and major patterns in GLOBOCAN 2012. Int J Cancer 2015; 136: E359-86.
2. Ghiringhelli F, Hennequin A, Drouillard A, Lepage C, Faivre J, Bouvier AM. Epidemiology and prognosis of synchronous and metachronous colon cancer metastases: a French population-based study. Dig Liver Dis 2014; 46: 854-8.
3. Kaibara N, Koga S, Jinnai D. Synchronous and metachronous malignancies of the colon and rectum in Japan with special reference to a coexisting early cancer. Cancer 1984; 54: 1870-4.
4. Lam AK, Chan SS, Leung M. Synchronous colorectal cancer: clinical, pathological and molecular implications. World J Gastroenterol 2014; 20: 6815-20.
5. Oya M, Takahashi S, Okuyama T, Yamaguchi M, Ueda Y. Synchronous colorectal carcinoma: clinico-pathological features and prognosis. Jpn J Clin Oncol 2003; 33: 38-43.
6. Yang J, Peng JY, Chen W. Synchronous colorectal cancers: a review of clinical features, diagnosis, treatment, and prognosis. Dig Surg 2011; 28: 379-85.
7. Cunliffe WJ, Hasleton PS, Tweedle DE, Schofield PF. Incidence of synchronous and metachronous colorectal carcinoma. Br J Surg 1984; 71: 941-3.
8. Evers BM, Mullins RJ, Matthews TH, Broghamer WL, Polk HC Jr. Multiple adenocarcinomas of the colon and rectum: an analysis of incidences and current trends. Dis Colon Rectum 1988; 31: 518-22.
9. Fukatsu H, Kato J, Nasu JI, *et al*. Clinical characteristics of synchronous colorectal cancer are different according to tumour location. Dig Liver Dis 2007; 39: 40-6.
10. Hu H, Chang DT, Nikiforova MN, Kuan SF, Pai RK. Clinicopathologic features of synchronous colorectal carcinoma: a distinct subset arising from multiple sessile serrated adenomas and associated with high levels of microsatellite instability and favorable prognosis. Am J Surg Pathol 2013; 37: 1660-70.
11. Kimura T, Iwagaki H, Fuchimoto S, Hizuta A, Orita K. Synchronous colorectal carcinomas. Hepatogastroenterology 1994; 41: 409-12.
12. Latournerie M, Jooste V, Cottet V, Lepage C, Faivre J, Bouvier AM. Epidemiology and prognosis of synchronous colorectal cancers. Br J Surg 2008; 95: 1528-33.
13. Mulder SA, Kranse R, Damhuis RA, *et al*. Prevalence and prognosis of synchronous colorectal cancer: a Dutch population-based study. Cancer Epidemiol 2011; 35: 442-7.
14. Ueno M, Muto T, Oya M, Ota H, Azekura K, Yamaguchi T. Multiple primary cancer: an experience at the Cancer Institute Hospital with special reference to colorectal cancer. Int J Clin Oncol 2003; 8: 162-7.
15. Wang HZ, Huang XF, Wang Y, Ji JF, Gu J. Clinical features, diagnosis, treatment and prognosis of multiple primary colorectal carcinoma. World J Gastroenterol 2004; 10: 2136-9.
16. Kato T, Alonso S, Muto Y, *et al*. Clinical characteristics of synchronous colorectal cancers in Japan. World J Surg Oncol 2016; 14: 272.
17. Chen HS, Sheen-Chen SM. Synchronous and "early" metachronous colorectal adenocarcinoma: analysis of prognosis and current trends. Dis Colon Rectum 2000; 43: 1093-9.
18. Finan PJ, Ritchie JK, Hawley PR. Synchronous and 'early' metachronous carcinomas of the colon and rectum. Br J Surg 1987; 74: 945-7.
19. Kim YJ, Kim NK, Lee KY, Sohn SK, Min JS. Clinicopathological characteristics of multiple primary colorectal cancer. J Korean Soc Coloproctol 2002; 18: 343-8.
20. Kang JG, Kim DH, Kim CH, Lee SH, Choi YJ. Clinical characteristics of synchronous multiple colorectal cancer. J Korean Soc Coloproctol 2006; 22: 418-23.
21. Welch JP. Multiple colorectal tumors: an appraisal of natural history and therapeutic options. Am J Surg 1981; 142: 274-80.
22. Lam AK, Carmichael R, Gertraud Buettner P, Gopalan V, Ho YH, Siu S. Clinicopathological significance of synchronous carcinoma in colorectal cancer. Am J Surg 2011; 202: 39-44.
23. Pedroni M, Tamassia MG, Percesepe A, *et al*. Microsatellite instability in multiple colorectal tumors. Int J Cancer 1999; 81: 1-5.
24. Norrie MW, Hawkins NJ, Todd AV, Meagher AP, O'Connor TW, Ward RL. The role of hMLH1 methylation in the development of synchronous sporadic colorectal carcinomas. Dis Colon Rectum 2002; 45: 674-80.
25. Dykes SL, Qui H, Rothenberger DA, García-Aguilar J. Evidence of a preferred molecular pathway in patients with synchronous colorectal cancer. Cancer 2003; 98: 48-54.
26. Nosho K, Kure S, Irahara N, *et al*. A prospective cohort study shows unique epigenetic, genetic, and prognostic features of synchronous

colorectal cancers. Gastroenterology 2009; 137: 1609-20.e1-3.
27. Gonzalo V, Lozano JJ, Alonso-Espinaco V, *et al*. Multiple sporadic colorectal cancers display a unique methylation phenotype. PLoS One 2014; 9: e91033.
28. Brueckl WM, Limmert T, Brabletz T, *et al*. Mismatch repair deficiency in sporadic synchronous colorectal cancer. Anticancer Res 2000; 20: 4727-32.
29. Kamiyama H, Suzuki K, Maeda T, *et al*. DNA demethylation in normal colon tissue predicts predisposition to multiple cancers. Oncogene 2012; 31: 5029-37.
30. Eguchi K, Yao T, Konomoto T, Hayashi K, Fujishima M, Tsuneyoshi M. Discordance of p53 mutations of synchronous colorectal carcinomas. Mod Pathol 2000; 13: 131-9.
31. Giannini R, Lupi C, Loupakis F, *et al*. *KRAS* and *BRAF* genotyping of synchronous colorectal carcinomas. Oncol Lett 2014; 7: 1532-6.
32. Ronnekleiv-Kelly SM, Pawlik TM. Staging of intrahepatic cholangiocarcinoma. Hepatobiliary Surg Nutr 2017; 6: 35-43.
33. Enker WE, Dragacevic S. Multiple carcinomas of the large bowel: a natural experiment in etiology and pathogenesis. Ann Surg 1978; 187: 8-11.
34. Bae JM, Kim JH, Cho NY, Kim TY, Kang GH. Prognostic implication of the CpG island methylator phenotype in colorectal cancers depends on tumour location. Br J Cancer 2013; 109: 1004-12.
35. Oh HJ, Bae JM, Wen XY, Cho NY, Kim JH, Kang GH. Overexpression of POSTN in tumor stroma is a poor prognostic indicator of colorectal cancer. J Pathol Transl Med 2017; 51: 306-13.
36. Bae JM, Kim JH, Kang GH. Molecular subtypes of colorectal cancer and their clinicopathologic features, with an emphasis on the serrated neoplasia pathway. Arch Pathol Lab Med 2016; 140: 406-12.

Journal of Pathology and Translational Medicine 2018; 52: 396-403
https://doi.org/10.4132/jptm.2018.10.03

■ ORIGINAL ARTICLE ■

The Prognostic Impact of Synchronous Ipsilateral Multiple Breast Cancer: Survival Outcomes according to the Eighth American Joint Committee on Cancer Staging and Molecular Subtype

Jinah Chu · Hyunsik Bae
Youjeong Seo · Soo Youn Cho
Seok-Hyung Kim · Eun Yoon Cho

Department of Pathology and Translational Genomics, Samsung Medical Center, Sungkyunkwan University School of Medicine, Seoul, Korea

Received: July 31, 2018
Revised: September 27, 2018
Accepted: October 2, 2018

Corresponding Author
Eun Yoon Cho, MD, PhD
Department of Pathology and Translational Genomics, Samsung Medical Center, Sungkyunkwan University School of Medicine, 81 Irwon-ro, Gangnam-gu, Seoul 06351, Korea
Tel: +82-2-3410-2796
Fax: +82-2-3410-0025
E-mail: eunyoon.cho@samsung.com

Seok-Hyung Kim, PhD
Department of Pathology and Translational Genomics, Samsung Medical Center, Sungkyunkwan University School of Medicine, 81 Irwon-ro, Gangnam-gu, Seoul 06351, Korea
Tel: +82-2-3410-2898
Fax: +82-2-3410-0025
E-mail: parmenides.kim@samsung.com

Background: In the current American Joint Committee on Cancer staging system of breast cancer, only tumor size determines T-category regardless of whether the tumor is single or multiple. This study evaluated if tumor multiplicity has prognostic value and can be used to subclassify breast cancer. **Methods:** We included 5,758 patients with invasive breast cancer who underwent surgery at Samsung Medical Center, Seoul, Korea, from 1995 to 2012. **Results:** Patients were divided into two groups according to multiplicity (single, n=4,744; multiple, n=1,014). Statistically significant differences in lymph node involvement and lymphatic invasion were found between the two groups (p<.001). Patients with multiple masses tended to have luminal A molecular subtype (p<.001). On Kaplan-Meier survival analysis, patients with multiple masses had significantly poorer disease-free survival (DFS) (p=.016). The prognostic significance of multiplicity was seen in patients with anatomic staging group I and prognostic staging group IA (p=.019 and p=.032, respectively). When targeting patients with T1-2 N0 M0, hormone receptor–positive, and human epidermal growth factor receptor 2 (HER2)–negative cancer, Kaplan-Meier survival analysis also revealed significantly reduced DFS with multiple cancer (p=.031). The multivariate analysis indicated that multiplicity was independently correlated with worse DFS (hazard ratio, 1.23; 95% confidence interval, 1.03 to 1.47; p=.025). The results of this study indicate that tumor multiplicity is frequently found in luminal A subtype, is associated with frequent lymph node metastasis, and is correlated with worse DFS. **Conclusions:** Tumor multiplicity has prognostic value and could be used to subclassify invasive breast cancer at early stages. Adjuvant chemotherapy would be necessary for multiple masses of T1–2 N0 M0, hormone-receptor-positive, and HER2-negative cancer.

Key Words: Breast neoplasms; Multiplicity; Disease-free survival; Prognosis; Molecular subtype

Several studies have been conducted on the multiplicity of breast cancer over the past decades. Multiplicity in breast cancer is a concept that includes multifocality and multicentricity. The term multifocality is used when there are two or more invasive tumors within the same breast quadrant, while the term multicentricity is used to denote the existence of tumors in different quadrants.[1] The reported incidence of multiple breast cancers ranges from less than 10% to 70%.[2-4] Multiplicity in breast cancer has been reported to correlate with a higher frequency of lymphovascular invasion and lymph node involvement.[3,5-15] However, the clinical significance of multiplicity and its influence on prognosis are controversial. Therefore, the current edition of the tumor, node, and metastasis (TNM) classification in breast cancer uses only the dimension of the largest tumor focus when the tumor demonstrates multiplicity. In light of this fact, the present research analyzed, via a large retrospective study of breast cancer patients uniformly treated at a single institution, the impact of multiple breast cancers on disease-specific survival in relation to other clinicopathological factors.

MATERIALS AND METHODS

Study population

We identified 5,758 patients with invasive breast cancer who

pISSN 2383-7837
eISSN 2383-7845

underwent conserving breast surgery or total mastectomy at Samsung Medical Center in Seoul, Korea, from 1995 to 2012. For inclusion in the study, patients needed to meet the following criteria: no distant metastasis at the time of diagnosis, no neoadjuvant therapy prior to surgery, and a follow-up period longer than 36 months. The mean age of the patients was 47 years (age range, 21 to 86 years), and the median follow-up period was 64 months. This study was approved by the Institutional Review Board (IRB) of Samsung Medical Center (IRB No. 2018-06-098-001). Formal written informed consent was not required due to a waiver by the appropriate IRB.

Clinicopathological evaluation

Clinicopathological information, including multiplicity, age, tumor size, axillary nodal status, and histological grade, was obtained from electronic medical records or surgical pathology reports. According to the eighth edition of the American Joint Committee on Cancer (AJCC) staging, a patient with multiple breast cancer was defined if two or more separate masses were grossly or microscopically identified in a resection specimen no matter whether they were present in the same or different quadrants. In some cases, through assistance of careful gross examination and correlation with imaging findings, we can determine multiple breast cancer. Pathological tumor stage was assessed according to the eighth AJCC TNM classification.[16] If an invasive carcinoma has been transected by vacuum-assisted biopsy or excisional biopsy, then the sizes in each fragment were not added together, and correlation with the size on breast imaging was helpful to determine the best size for classification. If there had been a prior core needle biopsy or incisional biopsy showing a larger area of invasion than in the excisional specimen, the largest dimension of the invasive carcinoma in the prior specimen should be used for T classification. Histological grade was evaluated according to the Scarff-Bloom-Richardson classification modified by Elston and Ellis.[16] The expression status of estrogen receptors (ER), progesterone receptors (PR), and human epidermal growth factor receptor 2 (HER2) were evaluated by immunohistochemistry based on the surgical specimen. For ER and PR, only nuclear (not cytoplasmic) staining was scored. A positive test was defined as positive staining greater than or equal to 1% of tumor cells. A negative test was defined as staining of less than 1% of tumor cells. HER2 was scored as 0, 1+, 2+, or 3+. Only membrane staining intensity and pattern were evaluated using the recommendations of the American Society of Clinical Oncology/College of American Pathologists.[17,18] A positive test was defined as a staining score of 3+. Tumors with a 2+ score were submitted for silver *in situ* hybridization. The tumor was considered positive for *HER2* amplification if the *HER2*/chromosome 17 probe signal ratio was greater than 2.0 and/or the average *HER2* copy number was greater than 6.0 signals per cell. Molecular subtypes of breast cancer were classified into luminal A, luminal B1, luminal B2, HER2, and triple-negative subtypes based on histological grade and the results of ER, PR, and HER2 immunochemistry as follows: luminal A (ER-positive and/or PR-positive, HER2-negative, and low histological grade [grade 1 or 2]); luminal B1 (ER-positive and/or PR-positive, and HER2-positive); luminal B2 (ER-positive and/or PR-positive, HER2-negative, and high histological grade [grade 3]), HER2-positive (ER-negative, PR-negative, and HER2-positive); and triple-negative (ER-negative, PR-negative, and HER2-negative).[19]

Statistical analysis

The primary outcome was disease-free survival (DFS), defined as the time interval from the date of surgery to the date of first recurrence, including local or distant. Survival curves were estimated using the Kaplan-Meier method, and survival differences were analyzed by log-rank test. The clinicopathological variables were analyzed in univariate and multivariate analyses of DFS with Cox proportional hazards model. Statistical analysis was performed using the R v3.5.1 (R Foundation for Statistical Computing, Vienna, Austria).

RESULTS

Patient characteristics

Patients were divided into two groups according to multiplicity. We found breast cancers involving a single mass in 4,744 cases (82.4%) and breast cancers involving multiple masses in 1,014 cases (17.6%). Table 1 shows the results of the comparison between patients with a single mass and patients with multifocal or multicentric masses.

Patients with multiple cancers were more likely to be young and have undergone total mastectomy. Statistically significant differences in lymph node positivity (single 38.0% vs multiple 47.3%, $p < .001$) and lymphatic invasion (single 24.7% vs multiple 32.6%, $p < .001$) were found between the two groups. In addition, multiplicity was associated with non–high histological grade ($p < .001$), ER positivity ($p < .001$), PR positivity ($p < .001$), and HER2 negativity ($p = .003$) of tumor. Therefore, breast cancers with multiple masses were more likely to have luminal A molecular subtype and less likely to be triple-negative subtype compared to those with a single mass ($p < .001$).

Disease-free survival

DFS was evaluated in patients with single breast mass and multiple masses. Kaplan-Meier survival analysis indicated that patients with multiple masses had significantly poorer DFS than did those with a single mass (5-year rate, 88.2% vs 85.2%; p = .016) (Fig. 1A). When patients were subclassified according to T-category, Kaplan-Meier survival analysis in the T1 category group revealed significantly worse DFS for multiple breast cancer (5-year rate, 91.3% vs 87.4%; p = .033) (Fig. 1B). There was no significant prognostic difference in T2 and T3 category groups (p = .093 and p = .619, respectively) (Fig. 1C, D). Using the anatomic stage group table in the AJCC eighth edition for tumor staging, breast cancer with multiplicity had poor prognosis in stage I (5-year rate, 92.7% vs 90.3%; p = .019) (Fig. 2A). When using the prognostic stage group table in the AJCC eighth edition, multiple breast masses were found to have significantly shorter DFS than single breast masses in stage group IA (5-year rate, 94.9% vs 88.7%; p = .032) (Fig. 2B). However, no significant difference was found between single and multiple tumors in the other stage groups (i.e., anatomic staging group II or III and prognostic staging group IB, II, or III) (Fig. 2C).

Patients were divided into five molecular subtypes (i.e., luminal A, B1, and B2; HER2-positive; and triple-negative). The prognostic significance of multiplicity was only seen in patients with luminal A and HER2-positive groups in terms of DFS (5-year rate, 92.8% vs. 88.6%; p = .013 and 5-year rate, 86.9% vs 77.8%; p = .003, respectively) (Fig. 3A, B). There was no significant difference among the luminal B1 and B2 and triple-negative subtypes (p = .937, p = .453, and p = .411, respectively) (Fig. 3C–E). In addition, when targeting patients with T1–2 N0 M0, hormone-receptor-positive, and HER2-negative cancer, Kaplan-Meier survival analysis revealed a significantly reduced DFS of multiple breast cancer (5-year rate, 95.2% vs 88.6%; p = .031) (Fig. 4).

Univariate analysis using Cox proportional hazard model indicated that high tumor stage (T3) (hazard ratio [HR], 2.44; 95% confidence interval [CI], 1.84 to 3.23; p < .001), positive lymph node metastasis (HR, 2.06; 95% CI, 1.8 to 2.36; p < .001), high anatomic staging group (i.e., stage III) (HR, 3.47; 95% CI, 2.89 to 4.18; p < .001), positive lymphatic emboli (HR, 2.16; 95% CI, 1.88 to 2.49; p < .001), high histological grade (i.e., grade 3) (HR, 1.52; 95% CI, 1.33 to 1.74; p < .001), negative ER status (HR, 1.23; 95% CI, 1.07 to 1.42; p < .001), positive HER2 status (HR, 1.21; 95% CI, 1.05 to 1.40; p = .004), and the presence of multiplicity (HR, 1.24; 95% CI, 1.04 to 1.48; p = .016) are significant variables associated with lower DFS (Table 2).

These significant factors in the univariate model were included in multivariate analysis, which demonstrated that tumor multiplicity correlated independently with worse DFS (adjusted HR,

Table 1. Distribution of clinicopathological factors in single and multiple breast cancers (n = 5,758)

Characteristic	Single (n = 4,744)	Multiple (n = 1,014)	p-value
Age (yr)			.001
<47	2,459 (51.8)	591 (58.3)	
≥47	2,285 (48.2)	423 (41.7)	
Operation			<.001
Partial	3,089 (65.1)	470 (46.4)	
Total	1,655 (34.9)	544 (53.6)	
Chemotherapy			.115
Not done	1,113 (23.5)	214 (21.1)	
Done	3,631 (76.5)	800 (78.9)	
Hormonal therapy			<.001
Not done	1,412 (29.8)	214 (21.1)	
Done	3,332 (70.2)	800 (78.9)	
Radiotherapy			<.001
Not done	1,241 (26.2)	426 (42.0)	
Done	3,503 (73.8)	588 (58.0)	
pT			.016
T1	2,720 (57.3)	618 (60.9)	
T2	1,827 (38.5)	370 (36.5)	
T3	197 (4.2)	26 (2.6)	
Lymph node			<.001
Negative	2,941 (62.0)	534 (52.7)	
Positive	1,803 (38.0)	480 (47.3)	
Anatomic stage group			.064
Stage I	2,014 (42.5)	390 (38.5)	
Stage II	2,089 (44.0)	479 (47.2)	
Stage III	641 (13.5)	145 (14.3)	
Lymphatic invasion			<.001
Negative	3,572 (75.3)	683 (67.4)	
Positive	1,172 (24.7)	331 (32.6)	
Histology grade			<.001
Grade 1, 2	3,089 (65.1)	737 (72.7)	
Grade 3	1,655 (34.9)	277 (27.3)	
ER status			<.001
Negative	1,430 (30.1)	232 (22.9)	
Positive	3,314 (69.9)	782 (77.1)	
PR status			<.001
Negative	1,789 (37.7)	278 (27.4)	
Positive	2,955 (62.3)	736 (72.6)	
HER2 status			.003
Negative	3,448 (72.7)	783 (77.2)	
Positive	1,296 (27.3)	231 (22.8)	
Molecular subtype			<.001
Luminal A	2,228 (47.0)	580 (57.2)	
Luminal B1	753 (15.9)	125 (12.3)	
Luminal B2	410 (8.6)	94 (9.3)	
HER2 positive	543 (11.4)	106 (10.5)	
Triple negative	810 (17.1)	109 (10.7)	

Values are presented as number (%).

https://doi.org/10.4132/jptm.2018.10.03

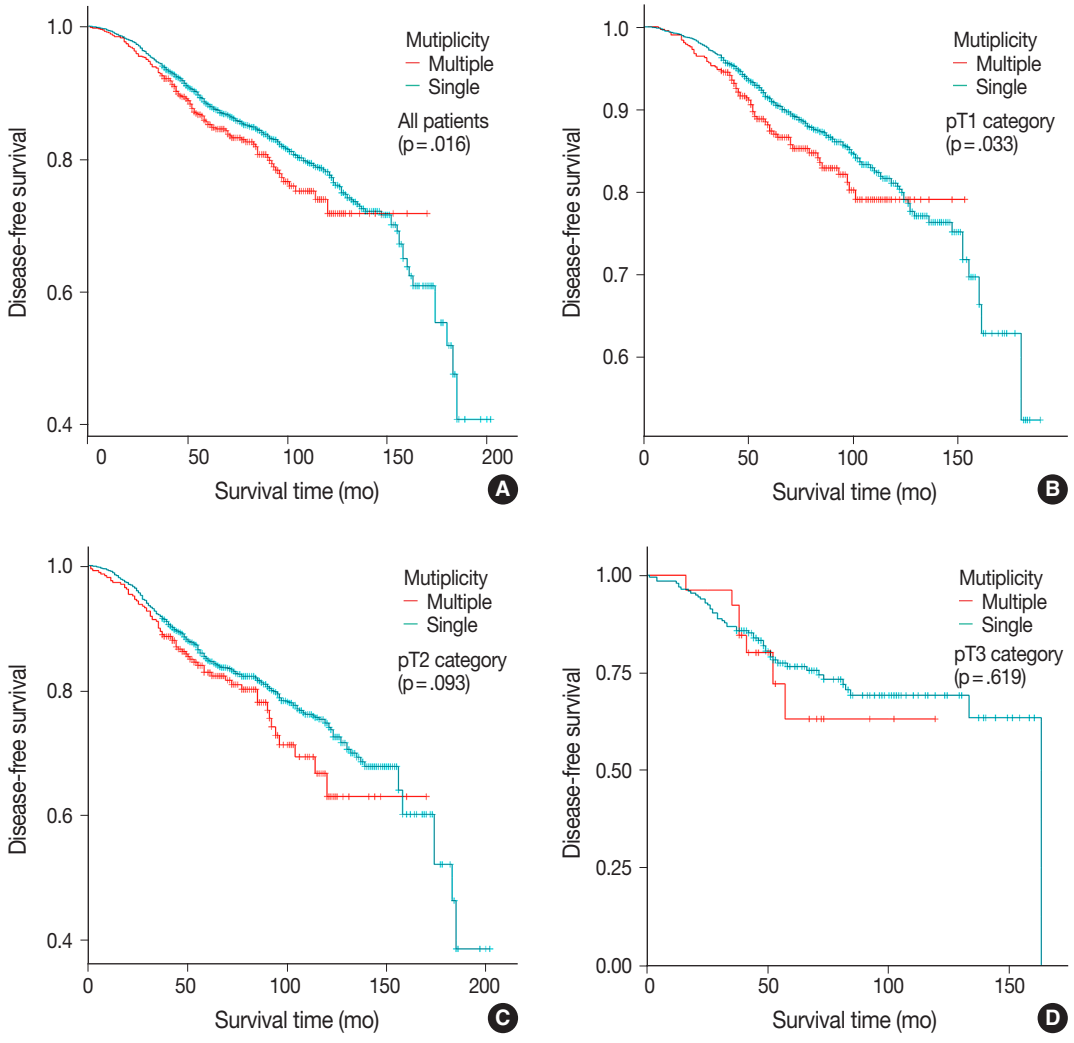

Fig. 1. The Kaplan-Meier curves for disease-free survival in patients with single and multiple masses according to T category. (A) Survival curve of all patients. (B) Survival curve of the T1 category. (C) Survival curve of the T2 category. (D) Survival curve of the T3 category. A significant difference is observed in the T1 category.

1.23; 95% CI, 1.05 to 1.47; p = .021). Other independent factors were high tumor stage (T3) (adjusted HR, 1.81; 95% CI, 1.35 to 2.41; p < .001), positive lymph node metastasis (adjusted HR, 1.84; 95% CI, 1.60 to 2.13; p < .001), and high histological grade (i.e., grade 3) (adjusted HR, 1.33; 95% CI, 1.14 to 1.55; p < .001) (Table 3).

DISCUSSION

In the present study, the 17.6% incidence of surgically removed breast cancer with multiplicity is in line with prior data series.[9,11,20-23] In previous studies, the incidence of multiple breast cancer had a wide range due to different definitions and inclusion criteria for multiple masses. Here, we used the term multiplicity if the cancer showed either multicentricity or multifocality. Many researchers have studied the characteristics of multicentric or multifocal breast cancer. In the literature, lymphovascular invasion and axillary nodal involvement were more frequent in multicentric or multifocal breast cancers.[3,5-15] The higher frequency of lymph node metastases could be due to the greater volume and surface area of multiple breast cancer or different biological behavior.[8] In agreement with reported series, patients in this study with multiple masses had a higher incidence of lymph node involvement than patients with single mass. In addition, multiplicity was associated with frequent lymphovascular invasion.

Theoretically, as breast cancers with multiplicity are more likely to have lymph node involvement and lymphovascular invasion, it could be inferred that prognosis would be worse than that of single mass breast cancers. Of course, many researchers have studied multiplicity as a prognostic factor in breast cancer. However,

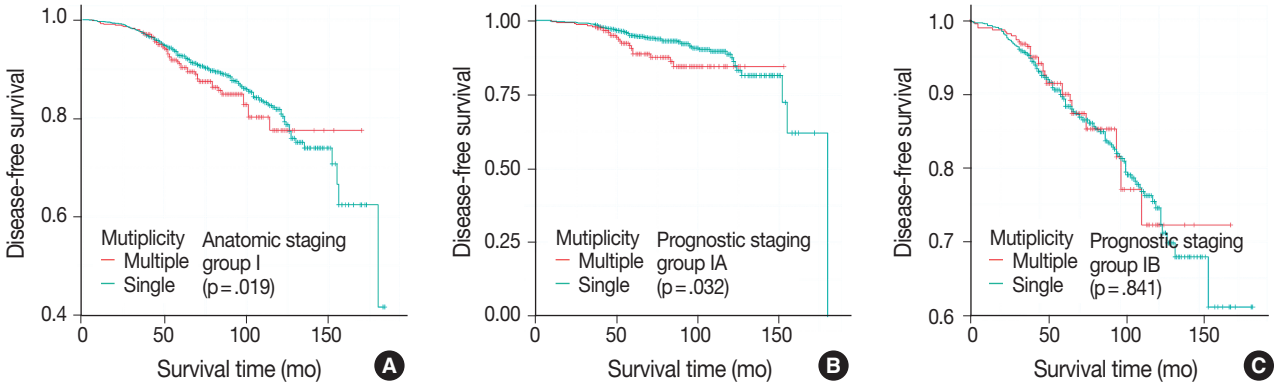

Fig. 2. The Kaplan-Meier survival curves for disease-free survival of patients with single and multiple masses in different Anatomic and prognostic staging groups. (A) Survival curve of the anatomic staging group I. (B) Survival curve of the prognostic staging group IA. (C) Survival curve of the prognostic staging group IB. The anatomic staging group I and prognostic staging group IA show a significant difference.

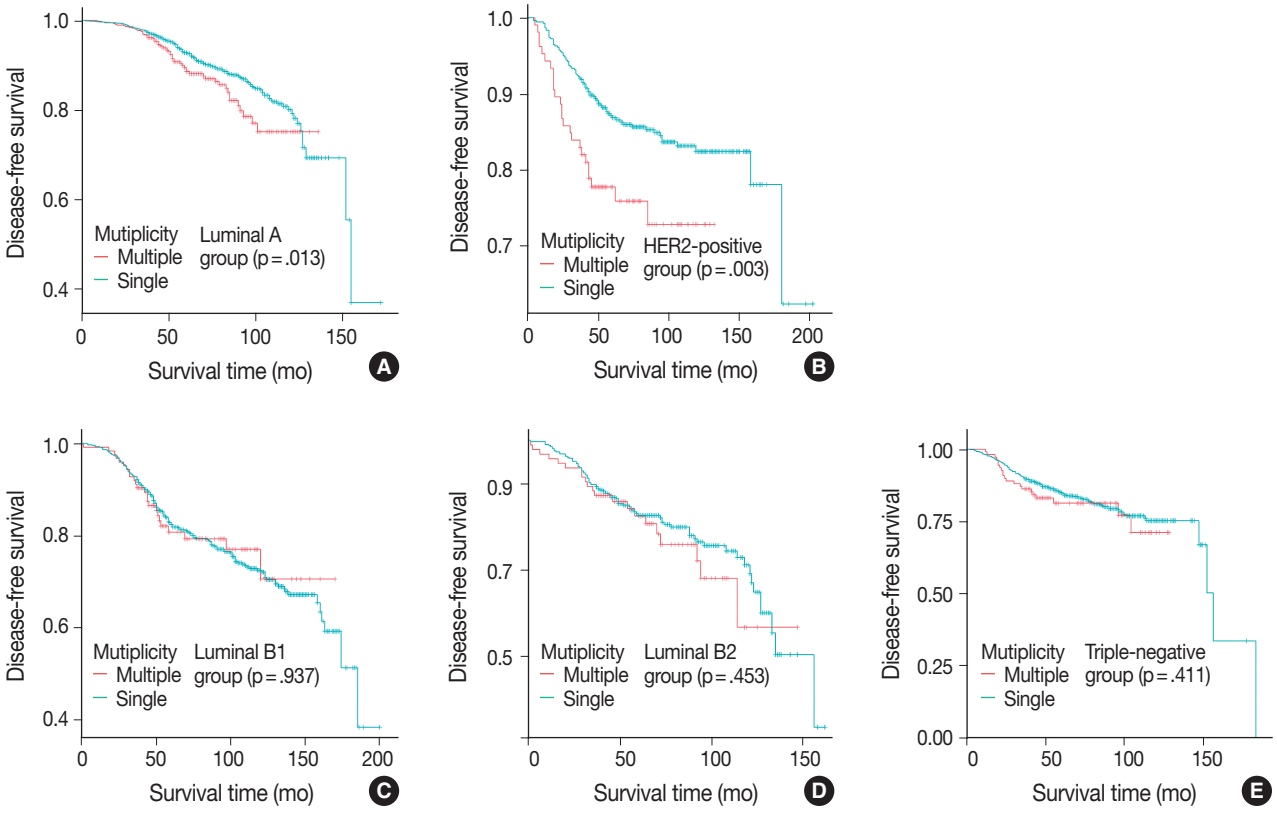

Fig. 3. Molecular subgroup analysis of the association between multiplicity and disease-free survival. The Kaplan-Meier survival curve of luminal A (A), human epidermal growth factor receptor 2 (HER2)–positive (B), luminal B1 (C), luminal B2 (D), and triple-negative groups (E). The difference is significant in patients of the luminal A and HER2-positive groups.

the biological and clinical significances of multiplicity are still debated.[3,7,9,11,12,14,20,21,24-26] Vlastos *et al.*[11] studied 284 patients with early-stage breast cancer and found that locoregional recurrence, distant metastasis, and disease-specific survival and DFS were not different between multicentric versus unicentric tumors. On the other hand, Yerushalmi *et al.*[3] analyzed 1,554 patients and found multicentric/multifocal tumors to be associated with worse breast cancer–specific survival. Additionally, Neri *et al.*[22] reported on 191 cases of breast cancer and found multifocal/multicentric breast cancer to be related to significantly worse prognosis with breast cancer–specific survival.

The results of our study suggest that multicentric and multi-

https://doi.org/10.4132/jptm.2018.10.03

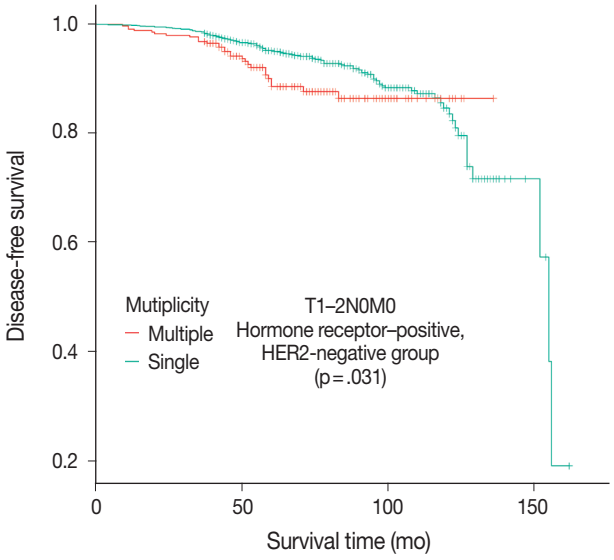

Fig. 4. The Kaplan-Meier survival curves for disease-free survival in patients with T1–2 N0 M0, hormone receptor–positive, and human epidermal growth factor receptor 2 (HER2)–negative cancer. Comparison between patients with single mass and multiple masses.

focal breast cancers may have different biological behaviors. Multiple masses were more likely to have non-high histology grade, ER positivity, PR positivity, and HER2 negativity compared with single mass cases. Interestingly, we found that breast cancers with multiplicity were associated with luminal A molecular subtype and non-high histology grade, which are known to have good prognosis. Additionally, multiple breast masses of the luminal A group were found to have a significantly shorter DFS than single breast masses in Kaplan-Meier survival analysis (p = .013). As with luminal A, multiplicity had prognostic significance in the HER2-positive group. According to our results, close observation during follow-up is needed, especially in patients of the luminal A and HER2-positive groups with multiple breast cancer. There have been conflicting reports about hormonal receptor status.[22,27] As in our study, Moon *et al*.[27] identified frequent ER positivity and HER2 negativity of multiple breast cancers in a series of 2,882 patients. Conversely, however, Neri *et al*.[22] reviewed 1,158 patients and found an association between multiplicity and ER-negative and HER2-positive status. On the other hand, Moon *et al*.[27] reported that the difference in overall survival was significant only in patients with the triple-negative subtype.

Our results show that breast cancer with multiplicity has a negative effect on DFS, especially in early-stage cancer. The results of multivariate analysis confirmed the independent prognostic value of multiplicity, and Kaplan-Meier survival curve showed significantly reduced DFS for patients with multiple masses in the T1 stage group (p = .033). The AJCC eighth edition presents the Prognostic Stage Group table in addition to the anatomic stage group table using the T, N, and M categories. The Prognostic Stage Group table includes the anatomical T, N, and M categories; tumor grade; and the status of ER, PR, and HER2 biomarkers. The prognostic significance of multiplicity in terms of DFS was only seen in patients with anatomic staging group I and prognostic staging group IA by Kaplan-Meier survival analysis (p = .019 and p = .032, respectively). Therefore, the negative prognostic impact of multiplicity could be considered for subclassification in at least early breast cancer patients.

The Oncotype Dx genomic test is now performed for consideration of adjuvant chemotherapy in patients with T1–2 N0 M0, hormone receptor–positive, and HER2-negative cancer.[28]

Table 2. Univariate Cox proportional hazards ratio analysis

	Hazard ratio	95% CI	p-value
Multiplicity			
Single	1		
Multiple	1.24	1.04–1.48	.016
Age (yr)			
≥ 47	1		
< 47	1.08	0.94–1.24	.258
pT			
T1	1		
T2	1.57	1.37–1.81	< .001
T3	2.44	1.84–3.23	< .001
Lymph node			
Negative	1		
Positive	2.06	1.80–2.36	< .001
Anatomic stage			
Stage I	1		
Stage II	1.65	1.40–1.95	< .001
Stage III	3.47	2.89–4.18	< .001
Lymphatic invasion			
Negative	1		
Positive	2.16	1.88–2.49	< .001
Histology grade			
Grade 1, 2	1		
Grade 3	1.52	1.33–1.74	< .001
ER status			
Positive	1		
Negative	1.23	1.07–1.42	.004
HER2 status			
Negative	1		
Positive	1.21	1.05–1.40	.009
Molecular Subtype			
Luminal A	1		
Luminal B1	1.8	1.49–2.18	< .001
Luminal B2	2.17	1.73–2.71	< .001
HER2 positive	1.37	1.09–1.73	.007
Triple negative	1.83	1.51–2.23	< .001

CI, confidence interval; ER, estrogen receptor; HER2, human epidermal growth factor receptor 2.

Table 3. Multivariate Cox proportional hazards ratio analysis

	Hazard ratio	95% CI	p-value
Multiplicity			
Single	1		
Multiple	1.23	1.05–1.47	.021
pT			
T1	1		
T2	1.27	1.09–1.47	.002
T3	1.81	1.35–2.41	<.001
Lymph node			
Negative	1		
Positive	1.84	1.60–2.13	<.001
Histology grade			
Grade 1, 2	1		
Grade 3	1.33	1.14–1.55	<.001
ER status			
Positive	1		
Negative	1.09	0.93–1.28	.255
HER2 status			
Negative	1		
Positive	1.1	0.95–1.28	.206

CI, confidence interval; ER, estrogen receptor; HER2, human epidermal growth factor receptor 2.

In this patient population in our study, multiple breast masses were found to have a significantly shorter DFS than single breast mass (p = .031). Based on the difference of prognosis, adjuvant chemotherapy would be necessary for multiple breast masses even without the Oncotype Dx test.

Our study has several limitations. First, this retrospective study had a relatively short-term follow-up period (median duration, 64 months). Second, molecular subtype was evaluated only using the largest among multiple masses. Because intertumoral heterogeneity could be a factor affecting survival, a further study should be conducted to investigate the relationship between intertumoral heterogeneity and survival in multiple breast cancer. Finally, patients with neoadjuvant therapy were not included. Therefore, the evaluation of advanced stage breast cancer was relatively limited.

In conclusion, the results of this study indicate that tumor multiplicity is frequently found in luminal A breast cancer, is associated with frequent lymph node metastasis, and is correlated with worse DFS. Tumor multiplicity has prognostic value and could be used to subclassify invasive breast cancer in the early stage. Adjuvant chemotherapy would be necessary for multiple breast masses of the T1–2 N0 M0, hormone-receptor-positive, and HER2-negative cancer groups.

ORCID

Jinah Chu: https://orcid.org/0000-0001-9050-084X
Hyunsik Bae: https://orcid.org/0000-0002-5347-466X
Youjeong Seo: https://orcid.org/0000-0003-4595-3836
Soo Youn Cho: https://orcid.org/0000-0001-9714-7575
Seok-Hyung Kim: https://orcid.org/0000-0001-6298-5958
Eun Yoon Cho: https://orcid.org/0000-0001-5849-3600

Conflicts of Interest

No potential conflict of interest relevant to this article was reported.

REFERENCES

1. Qualheim RE, Gall EA. Breast carcinoma with multiple sites of origin. Cancer 1957; 10: 460-8.
2. Bendifallah S, Werkoff G, Borie-Moutafoff C, *et al*. Multiple synchronous (multifocal and multicentric) breast cancer: clinical implications. Surg Oncol 2010; 19: e115-23.
3. Yerushalmi R, Kennecke H, Woods R, Olivotto IA, Speers C, Gelmon KA. Does multicentric/multifocal breast cancer differ from unifocal breast cancer? An analysis of survival and contralateral breast cancer incidence. Breast Cancer Res Treat 2009; 117: 365-70.
4. Egan RL. Multicentric breast carcinomas: clinical-radiographic-pathologic whole organ studies and 10-year survival. Cancer 1982; 49: 1123-30.
5. Tot T. Axillary lymph node status in unifocal, multifocal, and diffuse breast carcinomas: differences are related to macrometastatic disease. Ann Surg Oncol 2012; 19: 3395-401.
6. Duraker N, Caynak ZC. Axillary lymph node status and prognosis in multifocal and multicentric breast carcinoma. Breast J 2014; 20: 61-8.
7. Cabioglu N, Ozmen V, Kaya H, *et al*. Increased lymph node positivity in multifocal and multicentric breast cancer. J Am Coll Surg 2009; 208: 67-74.
8. Andea AA, Bouwman D, Wallis T, Visscher DW. Correlation of tumor volume and surface area with lymph node status in patients with multifocal/multicentric breast carcinoma. Cancer 2004; 100: 20-7.
9. Joergensen LE, Gunnarsdottir KA, Lanng C, Moeller S, Rasmussen BB. Multifocality as a prognostic factor in breast cancer patients registered in Danish Breast Cancer Cooperative Group (DBCG) 1996-2001. Breast 2008; 17: 587-91.
10. Coombs NJ, Boyages J. Multifocal and multicentric breast cancer: does each focus matter? J Clin Oncol 2005; 23: 7497-502.

11. Vlastos G, Rubio IT, Mirza NQ, *et al*. Impact of multicentricity on clinical outcome in patients with T1-2, N0-1, M0 breast cancer. Ann Surg Oncol 2000; 7: 581-7.
12. Rezo A, Dahlstrom J, Shadbolt B, *et al*. Tumor size and survival in multicentric and multifocal breast cancer. Breast 2011; 20: 259-63.
13. Lynch SP, Lei X, Chavez-MacGregor M, *et al*. Multifocality and multicentricity in breast cancer and survival outcomes. Ann Oncol 2012; 23: 3063-9.
14. Pedersen L, Gunnarsdottir KA, Rasmussen BB, Moeller S, Lanng C. The prognostic influence of multifocality in breast cancer patients. Breast 2004; 13: 188-93.
15. Tot T, Gere M, Pekár G, *et al*. Breast cancer multifocality, disease extent, and survival. Hum Pathol 2011; 42: 1761-9.
16. Giuliano AE, Edge SB, Hortobagyi GN. Eighth edition of the AJCC cancer staging manual: breast cancer. Ann Surg Oncol 2018; 25: 1783-5.
17. Hammond ME, Hayes DF, Dowsett M, *et al*. American Society of Clinical Oncology/College Of American Pathologists guideline recommendations for immunohistochemical testing of estrogen and progesterone receptors in breast cancer. J Clin Oncol 2010; 28: 2784-95.
18. Wolff AC, Hammond ME, Hicks DG, *et al*. Recommendations for human epidermal growth factor receptor 2 testing in breast cancer: American Society of Clinical Oncology/College of American Pathologists clinical practice guideline update. Arch Pathol Lab Med 2014; 138: 241-56.
19. Goldhirsch A, Wood WC, Coates AS, *et al*. Strategies for subtypes: dealing with the diversity of breast cancer: highlights of the St. Gallen International Expert Consensus on the Primary Therapy of Early Breast Cancer 2011. Ann Oncol 2011; 22: 1736-47.
20. Litton JK, Eralp Y, Gonzalez-Angulo AM, *et al*. Multifocal breast cancer in women < or =35 years old. Cancer 2007; 110: 1445-50.
21. Boyages J, Jayasinghe UW, Coombs N. Multifocal breast cancer and survival: each focus does matter particularly for larger tumours. Eur J Cancer 2010; 46: 1990-6.
22. Neri A, Marrelli D, Megha T, *et al*. "Clinical significance of multifocal and multicentric breast cancers and choice of surgical treatment: a retrospective study on a series of 1158 cases". BMC Surg 2015; 15: 1.
23. O'Daly BJ, Sweeney KJ, Ridgway PF, *et al*. The accuracy of combined versus largest diameter in staging multifocal breast cancer. J Am Coll Surg 2007; 204: 282-5.
24. Weissenbacher TM, Zschage M, Janni W, *et al*. Multicentric and multifocal versus unifocal breast cancer: is the tumor-node-metastasis classification justified? Breast Cancer Res Treat 2010; 122: 27-34.
25. Ustaalioglu BO, Bilici A, Kefeli U, *et al*. The importance of multifocal/multicentric tumor on the disease-free survival of breast cancer patients: single center experience. Am J Clin Oncol 2012; 35: 580-6.
26. Fish EB, Chapman JA, Link MA. Assessment of tumor size for multifocal primary breast cancer. Ann Surg Oncol 1998; 5: 442-6.
27. Moon HG, Han W, Kim JY, *et al*. Effect of multiple invasive foci on breast cancer outcomes according to the molecular subtypes: a report from the Korean Breast Cancer Society. Ann Oncol 2013; 24: 2298-304.
28. Sparano JA, Gray RJ, Makower DF, *et al*. Prospective validation of a 21-gene expression assay in breast cancer. N Engl J Med 2015; 373: 2005-14.

Journal of Pathology and Translational Medicine 2018; 52: 404-410
https://doi.org/10.4132/jptm.2018.09.20

■ ORIGINAL ARTICLE ■

The Usefulness of Immunocytochemistry of CD56 in Determining Malignancy from Indeterminate Thyroid Fine-Needle Aspiration Cytology

Hyunseo Cha · Ju Yeon Pyo
Soon Won Hong

Department of Pathology, Gangnam Severance Hospital, Seoul, Korea

Received: July 6, 2018
Revised: September 13, 2018
Accepted: September 18, 2018

Corresponding Author
Soon Won Hong, MD
Department of Pathology, Gangnam Severance Hospital, 211 Eonju-ro, Gangnam-gu, Seoul 06273, Korea
Tel: +82-2-2019-3540
Fax: +82-2-3463-2103
E-mail: SOONWONH@yuhs.ac

Background: Fine-needle aspiration cytology serves as a safe, economical tool in evaluating thyroid nodules. However, about 30% of the samples are categorized as indeterminate. Hence, many immunocytochemistry markers have been studied, but there has not been a single outstanding marker. We studied the efficacy of CD56 with human bone marrow endothelial cell marker-1 (HBME-1) in diagnosis in the Bethesda System for Reporting Thyroid Cytopathology (TBSRTC) category III. **Methods:** We reviewed ThinPrep liquid-based cytology (LBC) samples with Papanicolaou stain from July 1 to December 31, 2016 (2,195 cases) and selected TBSRTC category III cases (n=363). Twenty-six cases were histologically confirmed as benign (six cases, 23%) or malignant (20 cases, 77%); we stained 26 LBC slides with HBME-1 and CD56 through the cell transfer method. For evaluation of reactivity of immunocytochemistry, we chose atypical follicular cell clusters. **Results:** CD56 was not reactive in 18 of 20 cases (90%) of malignant nodules and showed cytoplasmic positivity in five of six cases (83%) of benign nodules. CD56 showed high sensitivity (90.0%) and relatively low specificity (83.3%) in detecting malignancy (p=.004). HBME-1 was reactive in 17 of 20 cases (85%) of malignant nodules and was not reactive in five of six cases (83%) of benign nodules. HBME-1 showed slightly lower sensitivity (85.0%) than CD56. The specificity in detecting malignancy by HBME-1 was similar to that of CD56 (83.3%, p=.008). CD56 and HBME-1 tests combined showed lower sensitivity (75.0% vs 90%) and higher specificity (93.8% vs 83.3%) in detecting malignancy compared to using CD56 alone. **Conclusions:** Using CD56 alone showed relatively low specificity despite high sensitivity for detecting malignancy. Combining CD56 with HBME-1 could increase the specificity. Thus, we suggest that CD56 could be a useful preoperative marker for differential diagnosis of TBSRTC category III samples.

Key Words: Biopsy, fine-needle; Thyroid fine-needle aspiration; Immunohistochemical staining; CD56; HBME-1

Thyroid nodules, composed of non-neoplastic and neoplastic lesions, are found in the general population at a rate of about 5%.[1] In Korea, as of 2011, the diagnosis of thyroid carcinoma has increased as much as 15 times compared to 1993.[2] One of the reasons for this increase is thought to be from development of the fine-needle aspiration cytology (FNAC) technique, which is fast and accurate. FNAC plays a crucial role in treating thyroid carcinoma, such as in predicting a malignant nodule or in helping physicians make reasonable choices between surgery and safe follow-up treatment.[3] For all the benefits of FNAC, the cytopathology reports are often either ambiguous or difficult to interpret. The words "atypical," "indeterminate," or "cannot be excluded" may cause confusion in patient management and diagnosis.[4] The Bethesda System for Reporting Thyroid Cytopathology (TBSRTC) was developed to report FNA and to provide a unified terminology and diagnostic criteria for associating these cytological diagnoses with clinical management.[5,6]

Papillary thyroid carcinoma (PTC) is the most common malignant lesion representing 70%–85% of all thyroid cancer and is usually diagnosed by its morphologic features such as papillary structures, ground glass nuclei, nuclear grooves, and nuclear inclusions.[7-16] But, when a sample has a small amount of follicular cells, it is too difficult to make a correct diagnosis.[17-19] Hence, many studies have advocated the use of immunocytochemistry markers and ancillary techniques that use a molecular panel in the purifying process.[20-30] Many types of single or multiple panels of immunohistochemical markers were studied to determine the optimal marker of malignancy; human bone marrow endothelial cell marker-1 (HBME-1), galectine-3, and cytokeratin-19 were shown to have high diagnostic accuracy.[24-36] We studied the application of CD56 immunocytochemistry with liquid-based cytology (LBC) for samples that had been diagnosed as TBSRTC category

pISSN 2383-7837
eISSN 2383-7845

III. Additionally, we evaluated the efficacy of the marker CD56 with HBME-1.

MATERIALS AND METHODS

Patients and samples

We conducted a prospective study from July 2016 to December 2016 and archived 2,195 Papanicolaou (Pap)-stained slides retrieved from the pathology department. Each author had access to the patient profiles. The thyroid nodules were examined initially by ultrasonography; the size varied from 4 to 25 mm. Cytologic cases of the baseline period were classified according to the TBSRTC classification. The cytology results were distributed accordingly: TBSRTC I, 8.3%; TBSRTC II, 28%; TBSRTC III, 16.5%; TBSRTC IV, 1%; TBSRTC V, 12.5%; and TBSRTC VI, 33.7%. The aim of our study was to evaluate the diagnostic value of CD56 in indeterminate cytology cases. All cases that belonged to TBSRTC category III (n = 363) were studied. All cases were handled through the LBC method and with the help of a ThinPrep 5000 processor (Hologic Co., Marlborough, MA, USA). The LBC slides were fixed using methanol and later stained with Pap. Leftover materials were stored using PreservCyt for possible future studies, including immunocytochemistry. Twenty-six cases were histologically confirmed as either benign (6 cases, 23%) or malignant (20 cases, 77%); we stained 26 LBC slides with HBME-1 and CD56 through the cell transfer method.

Cell transfer and immunocytochemistry

The Pap-stained slide of FNAC and the area of the smeared atypical cell were marked by a pathologist. Atypical clusters could be selected for staining from each LBC slide by the cell transfer method. The previously described cell delivery technique was performed at the marked spot on the slide.[37-39] The cover slip was separated from the Pap-stained smear slide, overlaid with Malinol (Muto Chemical, Tokyo, Japan), and heated overnight at 70°C–80°C. They were then incubated for 1 hour in a warm container at 50°C–60°C to lighten the Malinol films. We stripped the Malinol film containing the cells from the slide and cut the marked spots covered in the Malinol film into pieces concordant to the evident spot from the primary slide. The Malinol film was moved to another glass slide, incubated at 70°C for about 2 hours, and removed using xylene.[37-39]

Immunocytochemistry uses the following immune staining markers: HBME-1 (1:100, Dako, Glustrup, Denmark) and CD56 (1:100, Ventana, Tucson, AZ, USA). Positive immunohistochemical staining showed moderate or more cytoplasmic positivity for at least 30% of epithelial-follicular cells in all cytological cases. Histological diagnosis and a 30% immunocytochemistry cutoff were applied to reduce false-positive or false-negative outcomes.[34,35]

We did not distinguish between moderately positive or strongly positive in levels of immunostaining, and designated both moderate positive and strongly positive as benign in whole. While CD56 stained the cytoplasm, HBME-1 stained the cytoplasm and membrane. We identified mesothelial cells as the positive control with HBME-1 and histiocytes/macrophages for CD56 positive control. We identified lymphocytes as the negative control. We compared with paraffin blocks for immunohistochemistry. Immunohistochemistry analysis did not reveal cell-to-tissue mismatch yields; both cytology and specific histologic samples were coincident. We used buffered formaldehyde to fix the surgical samples. The paraffin blocks were cut into 5-μm-thick sections and stained with hematoxylin-eosin. All fibroadipose tissues that were adjacent to the thyroid were extensively searched to find lymph nodes.

We sought true papillary structure with nuclear characteristics to detect PTC and diagnosed follicular variant papillary thyroid carcinoma (FVPTC) when there were characteristics matching PTC in multiple sites.

Statistical analysis

The statistical data were analyzed using SPSS software ver. 23.0 (IBM Corp., Armonk, NY, USA) and Fisher exact test; p-values less than .05 were acknowledged as statistically significant.

All procedures performed in the current study were approved by institutional review board (IRB) in Gangnam Severance Hospital (local IRB number: 3-2018-0096, May 21, 2018) in accordance with the 1964 Helsinki declaration and its later amendments. Formal written informed consent was not required with a waiver by the appropriate IRB.

RESULTS

As emphasized earlier in the materials and methods section, during our study period from July 2016 to December 2016, we analyzed 2,195 samples from thyroid FNAC and selected 363 samples of TBSRTC category III using an immunocytochemistry panel composed of HBME-1 and CD56 (Fig. 1). Among 353 cases of indeterminate thyroid nodules with category III, 26 patients who had been surgically treated were selected. Three male and 23 female patients were included; the median age was

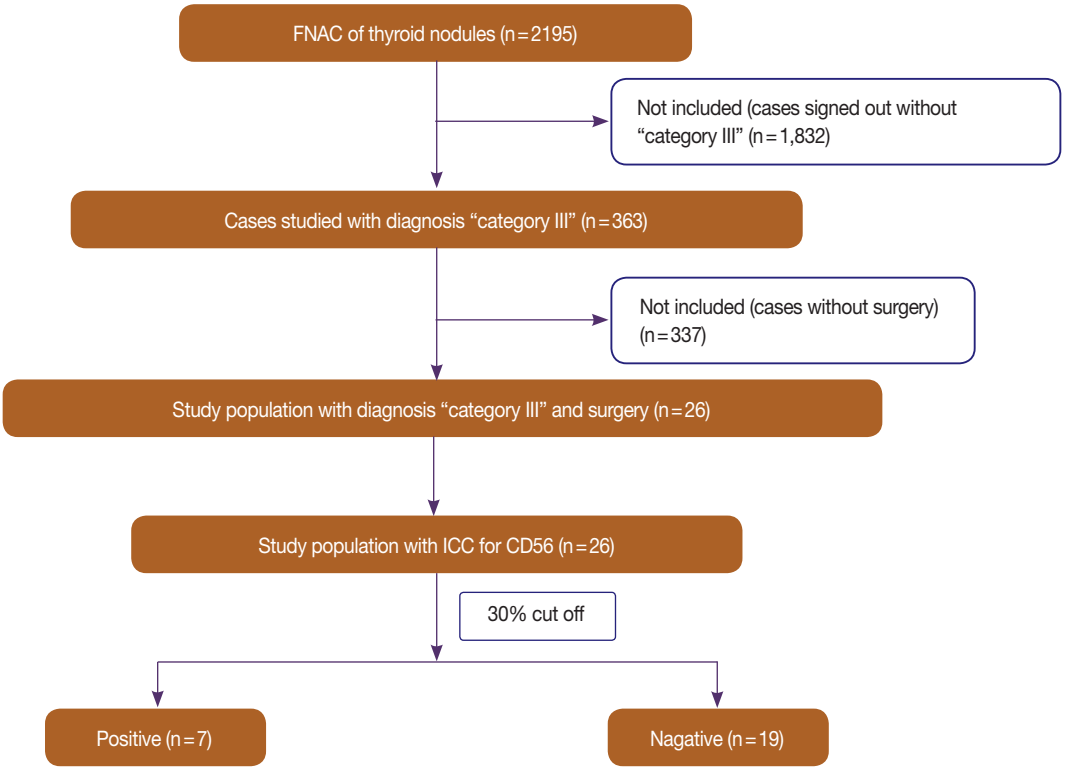

Fig. 1. Flow diagram of the study population. FNAC, fine-needle aspiration cytology; ICC, immunocytochemistry.

50 years. The surgically acquired category III samples were histologically confirmed as 10 non-malignant nodules and five adenomatous hyperplasia. Twenty nodules were malignant and 10 were conventional type PTC. Five cases were FVPTC. One case was diffuse sclerosing variant papillary thyroid carcinoma. Fig. 2 depicts the characteristics of the patients and their clinical and pathological features. We considered all FVPTC as infiltrative FVPTC.

Table 1 shows how immunostaining is expressed in two categories. In 18 of 20 cases (90%), the malignant nodules were completely negative to CD56 (Fig. 3A, B), and two cases of FVPTC showed focal weak positivity (5%). In contrast, five of six cases of benign nodules (83%) stained with CD56 showed cytoplasmic and membranous positivity (Fig. 4A, B). The sensitivity was 90% and specificity was 83.3% with diagnostic accuracy of 88.4%. The CD56 results were statistically meaningful (p = .004). HBME-1 was positive in 17 of 20 cases with 85% sensitivity and 83.3% specificity and diagnostic accuracy of 84% (p = .008). HBME-1 showed slightly lower sensitivity (85.0%) than that of CD56. The specificity in detecting malignancy by HBME-1 was similar to that of CD56 (83.3%, p = .008).

We analyzed the outcome using both CD56 and HBME-1 (Table 2). Combined CD56 and HBME-1 tests showed lower

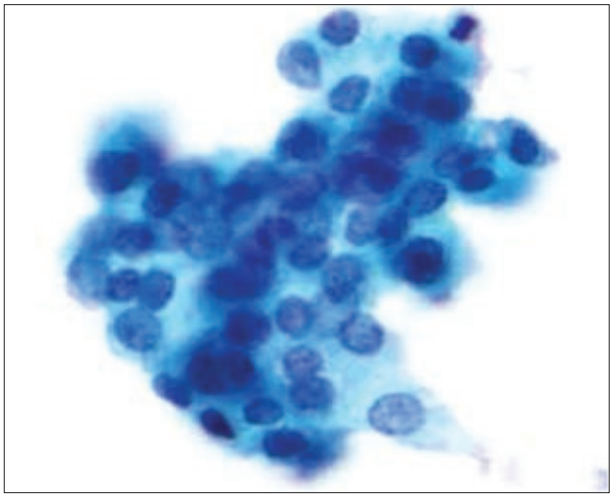

Fig. 2. A thyroid lesion diagnosed as category III on liquid-based cytology (Papanicolaou, ×400).

Table 1. CD56 and HBME-1 staining scores in the six benign nodules and 20 malignant nodules with histological follow-up

	CD56		HBME-1	
	Positive	Negative	Positive	Negative
Benign (n=6)	5 (83)	1 (17)	1 (17)	5 (83)
Malignant (n=20)	2 (10)	18 (90)	17 (85)	3 (15)

Values are presented as number (%).
HBME-1, human bone marrow endothelial cell marker-1.

https://doi.org/10.4132/jptm.2018.09.20

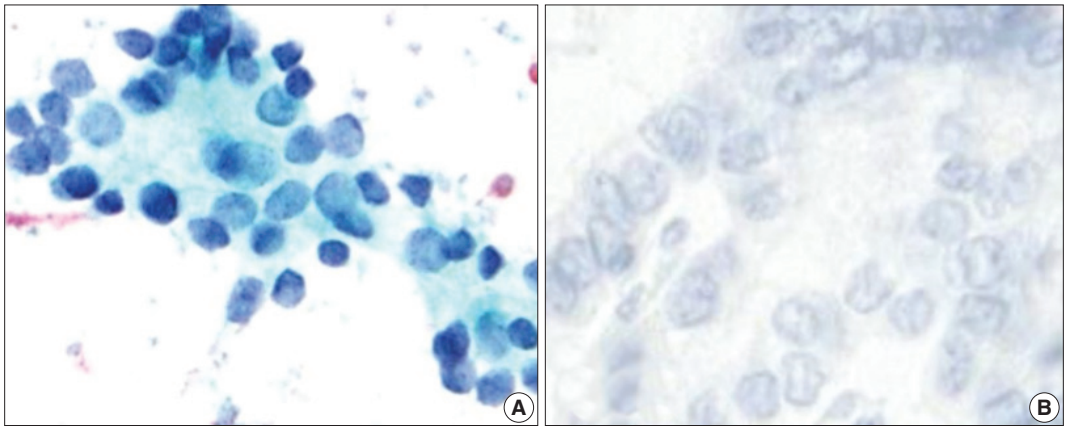

Fig. 3. (A) CD56 negativity in the case in Fig. 1 (avidin-biotin-peroxidase complex, ×400). (B) Negative CD56 expression on the histochemical sample for the same case (avidin-biotin-peroxidase complex, ×400).

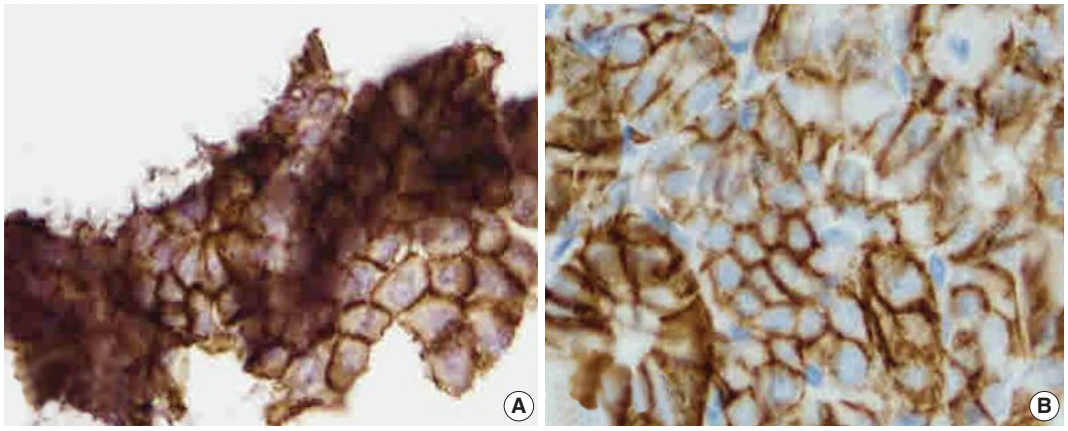

Fig. 4. (A) Cytoplasm-membranous CD56 positivity in a thyroid lesion diagnosed as category III on liquid-based cytology but diagnosed as benign goiter on the histological sample (avidin-biotin-peroxidase complex, ×400). (B) Diffuse cytoplasmic and membranous CD56 positivity on the histological sample for the same case (avidin-biotin-peroxidase complex, ×400).

Table 2. Descriptive statistics for each immunocytochemical marker in the cytohistological series

	Sensitivity	Specificity	Diagnostic accuracy	OR (95% CI)	p-value
CD56	90.0	83.3	88.4	45.0 (3.3–604)	.004
HBME-1	95.0	83.3	84.6	28.3 (2.3–336)	.008

A p-value less than .05 is considered significant.
OR, odds ratio; CI, confidence interval; HBME-1, human bone marrow endothelial cell marker-1.

sensitivity (75.0% vs 90%) and higher specificity (93.8% vs 83.3%) in detecting malignancy compared to using CD56 alone (Table 3). Also the diagnostic accuracy was 90.0% in detecting malignancy when compared to using CD 56 or HBME-1 alone.

DISCUSSION

As we predicted, CD56 showed high sensitivity (90%) and relatively high diagnostic accuracy in diagnoses in category III thyroid cytology. Therefore, we believe CD56 is a very effective screening marker. CD56 has been recognized as an effective marker in previous studies as well. Many studies showed that CD56 is less prominent in PTC samples. In our study, we showed that CD56 is a useful marker in thyroid cytology, which differs from previous studies in which CD56 was used in thyroid tissue samples.

Recent studies have examined the efficacy of CD56 immunostaining and the role of CD56 when used as a panel for HBME-1 immunostaining and for determination of thyroid FNAC positivity and malignancy.[34,35]

Samples showing fewer papillary structures, pseudo-inclusion in the nucleus, focal nuclear pleomorphism, and atypia can be confusing and might lead to a diagnostic dilemma. Any morphological similarity between benign lesions and PTC may be

Table 3. Staining with a double immunocytochemistry combination of CD56 and HBME-1

	CD56/HBME-1 (n=20)	
	$CD56^-/HBME\text{-}1^+$	$CD56^+/HBME\text{-}1^-$
Benign	1 (5)	3 (15)
Malignant	15 (75)	1 (5)

Values are presented as number (%).
HBME-1, human bone marrow endothelial cell marker-1.

the cause of misdiagnosis between FNAC and histological surgical specimens. For example, when Hashimoto's thyroiditis has nuclear atypia, empty chromatin, or nuclear groove, this can be confusing and might result in misdiagnosis.[26]

The relatively low specificity of FNAC can be further improved by applying an ancillary technique (e.g., immunocytochemistry and molecular marker). For this reason, effective dye markers (HBME-1, galatin-3) are attracting attention.[35,37]

HBME-1 displayed high sensitivity and high specificity in detecting PTC in many cases.[34] Additional reports suggest that mixed panels of immunostaining markers would provide more accurate diagnoses.[12-16,20,22,25,26,33,36]

Many studies were aimed at finding a sole maker for identifying malignancy accurately. CD56 was one of the most preferred markers for thyroid epithelial neoplasm in an immunohistochemistry panel.[21-26,37] While the exact mechanism is not well known, CD56 is noted in multiple sites (e.g., neuron, mesenchymal tissue, and endocrine cells).[21-26] Some studies correlated different CD56 expression with tumor cell migrations.[29] In previous studies of thyroid histological samples, CD56 was seen as a promising immunostaining marker expressed in most normal thyroid tissues including goiter, Grave disease, and Hashimoto thyroiditis. CD56 showed a negative staining pattern in PTC tissues including variants of PTC.[27,29,34,40-42] Indeed, in one study, the low expression of CD56 in PTC was shown to be highly specific in both single-use and dyed panel applications.[29,34]

Although the data of El Demellawy *et al*.[40] showed that CD56 was expressed in all benign lesions, our study showed slightly less (83%) positive expression of CD56 in benign lesions. Interestingly, all but one malignant lesion showed negative CD56 expression. We also compared CD56 with HBME-1 because HBME-1 is a preferred marker in building an immunocytochemistry panel, which could improve diagnostic accuracy. Our study is the first we know of that reveals the diagnostic usefulness of CD56 immunostaining for Bethesda's category III samples using thyroid cytology.

CD56 is usually studied in formalin-fixed and paraffin-embedded material.[29,34,41,42] We demonstrated the usefulness of immunodiffusion with cells that are thought of as atypical when using the cell transfer method. The positive features of FNAC are cost effectiveness, time saving, and practicality; also, the test is not invasive.[35] An ancillary technique such as immunocytochemistry or molecular testing can add cost but can also save money in the end by avoiding unnecessary thyroidectomy or lifelong drug treatment.

One limitation of our study was the relatively small sample size. Further study conducted with a larger number of samples should bring about more definitive conclusions.

Instead of using the well-known cell-block technique, we immunostained LBC for two reasons. First, LBC showed reliable results in immunostaining. Second, fixation can cause the cell-block to show false positive or false-negative, a problem we did not encounter while using LBC immunostaining.[34,35]

Our preliminary results show that CD56 is likely to be a very effective and reliable marker for ruling out PTC. We also suggest that CD56 be used in FNA when it is difficult to confirm the diagnosis using HBME-1 alone. Also, its efficacy can be enhanced through combination with other immunostaining markers.

ORCID

Hyunseo Cha: https://orcid.org/0000-0003-0243-9589
Ju Yeon Pyo: https://orcid.org/0000-0002-9198-5065
Soon Won Hong: https://orcid.org/0000-0002-0324-2414

Conflicts of Interest

No potential conflict of interest relevant to this article was reported.

REFERENCES

1. American Thyroid Association (ATA) Guidelines Taskforce on Thyroid Nodules and Differentiated Thyroid Cancer, Cooper DS, Doherty GM, *et al*. Revised American Thyroid Association management guidelines for patients with thyroid nodules and differentiated thyroid cancer. Thyroid 2009; 19: 1167-214.
2. Ahn HS, Kim HJ, Kim KH, *et al*. Thyroid cancer screening in South Korea increases detection of papillary cancers with no impact on other subtypes or thyroid cancer mortality. Thyroid 2016; 26: 1535-40.
3. Cha YJ, Pyo JY, Hong S, *et al*. Thyroid fine-needle aspiration cytology practice in Korea. J Pathol Transl Med 2017; 51: 521-7.
4. Powsner SM, Costa J, Homer RJ. Clinicians are from Mars and pathologists are from Venus. Arch Pathol Lab Med 2000; 124: 1040-6.
5. Cibas ES, Ali SZ; NCI Thyroid FNA State of the Science Conference.

 https://doi.org/10.4132/jptm.2018.09.20

The Bethesda System For Reporting Thyroid Cytopathology. Am J Clin Pathol 2009; 132: 658-65.
6. Cibas ES, Ali SZ. The 2017 Bethesda System for Reporting Thyroid Cytopathology. Thyroid 2017; 27: 1341-6.
7. Jung CK, Hong S, Bychkov A, Kakudo K. The use of fine-needle aspiration (FNA) cytology in patients with thyroid nodules in Asia: a brief overview of studies from the Working Group of Asian Thyroid FNA Cytology. J Pathol Transl Med 2017; 51: 571-8.
8. Kang Y, Lee YJ, Jung J, Lee Y, Won NH, Chae YS. Morphometric analysis of thyroid follicular cells with atypia of undetermined significance. J Pathol Transl Med 2016; 50: 287-93.
9. Yoo C, Choi HJ, Im S, *et al*. Fine needle aspiration cytology of thyroid follicular neoplasm: cytohistologic correlation and accuracy. Korean J Pathol 2013; 47: 61-6.
10. Oosthuizen JL, Walker B, Todorovic E, Masoudi H, Wiseman SM. The presence of papillary features in thyroid nodules diagnosed as atypia of undetermined significance or follicular lesion of undetermined significance increases cancer risk and should influence treatment. Am J Surg 2018; 215: 819-23.
11. Yashaswini R, Suresh TN, Sagayaraj A. Cytological evaluation of thyroid lesions by nuclear morphology and nuclear morphometry. J Cytol 2017; 34: 197-202.
12. Vivero M, Renshaw AA, Krane JF. Adequacy criteria for thyroid FNA evaluated by ThinPrep slides only. Cancer Cytopathol 2017; 125: 534-43.
13. Rossi M, Lupo S, Rossi R, *et al*. Proposal for a novel management of indeterminate thyroid nodules on the basis of cytopathological subclasses. Endocrine 2017; 57: 98-107.
14. Satoh S, Yamashita H, Kakudo K. Thyroid cytology: The Japanese system and experience at Yamashita Thyroid Hospital. J Pathol Transl Med 2017; 51: 548-54.
15. Kim SJ, Roh J, Baek JH, *et al*. Risk of malignancy according to subclassification of the atypia of undetermined significance or follicular lesion of undetermined significance (AUS/FLUS) category in the Bethesda system for reporting thyroid cytopathology. Cytopathology 2017; 28: 65-73.
16. Misiakos EP, Margari N, Meristoudis C, *et al*. Cytopathologic diagnosis of fine needle aspiration biopsies of thyroid nodules. World J Clin Cases 2016; 4: 38-48.
17. Kholová I, Ludvíková M. Thyroid atypia of undetermined significance or follicular lesion of undetermined significance: an indispensable Bethesda 2010 diagnostic category or waste garbage? Acta Cytol 2014; 58: 319-29.
18. Shi Y, Ding X, Klein M, *et al*. Thyroid fine-needle aspiration with atypia of undetermined significance: a necessary or optional category? Cancer 2009; 117: 298-304.
19. Garg S, Naik LP, Kothari KS, Fernandes GC, Agnihotri MA, Gokhale JC. Evaluation of thyroid nodules classified as Bethesda category III on FNAC. J Cytol 2017; 34: 5-9.
20. Rossi ED, Martini M, Capodimonti S, *et al*. Diagnostic and prognostic value of immunocytochemistry and *BRAF* mutation analysis on liquid-based biopsies of thyroid neoplasms suspicious for carcinoma. Eur J Endocrinol 2013; 168: 853-9.
21. Fadda G, Rossi ED, Raffaelli M, *et al*. Follicular thyroid neoplasms can be classified as low- and high-risk according to HBME-1 and Galectin-3 expression on liquid-based fine-needle cytology. Eur J Endocrinol 2011; 165: 447-53.
22. Ohori NP, Nikiforova MN, Schoedel KE, *et al*. Contribution of molecular testing to thyroid fine-needle aspiration cytology of "follicular lesion of undetermined significance/atypia of undetermined significance". Cancer Cytopathol 2010; 118: 17-23.
23. Cochand-Priollet B, Dahan H, Laloi-Michelin M, *et al*. Immunocytochemistry with cytokeratin 19 and anti-human mesothelial cell antibody (HBME1) increases the diagnostic accuracy of thyroid fine-needle aspirations: preliminary report of 150 liquid-based fine-needle aspirations with histological control. Thyroid 2011; 21: 1067-73.
24. Abouhashem NS, Talaat SM. Diagnostic utility of CK19 and CD56 in the differentiation of thyroid papillary carcinoma from its mimics. Pathol Res Pract 2017; 213: 509-17.
25. Solmaz OA. Diagnostic importance of CD56 with fine-needle aspiration cytology in suspected papillary thyroid carcinoma cases. Cytojournal 2018; 15: 3.
26. Mokhtari M, Eftekhari M, Tahririan R. Absent CD56 expression in papillary thyroid carcinoma: A finding of potential diagnostic value in problematic cases of thyroid pathology. J Res Med Sci 2013; 18: 1046-50.
27. Nechifor-Boila A, Borda A, Sassolas G, *et al*. Immunohistochemical markers in the diagnosis of papillary thyroid carcinomas: the promising role of combined immunostaining using HBME-1 and CD56. Pathol Res Pract 2013; 209: 585-92.
28. Nechifor-Boilă A, Cătană R, Loghin A, Radu TG, Borda A. Diagnostic value of HBME-1, CD56, galectin-3 and cytokeratin-19 in papillary thyroid carcinomas and thyroid tumors of uncertain malignant potential. Rom J Morphol Embryol 2014; 55: 49-56.
29. Scarpino S, Di Napoli A, Melotti F, Talerico C, Cancrini A, Ruco L. Papillary carcinoma of the thyroid: low expression of NCAM (CD56) is associated with downregulation of VEGF-D production by tumour cells. J Pathol 2007; 212: 411-9.
30. Shahebrahimi K, Madani SH, Fazaeli AR, Khazaei S, Kanani M, Keshavarz A. Diagnostic value of CD56 and nm23 markers in papillary thyroid carcinoma. Indian J Pathol Microbiol 2013; 56: 2-5.
31. Huang L, Wang X, Huang X, *et al*. Diagnostic significance of CK19,

galectin-3, CD56, TPO and Ki67 expression and *BRAF* mutation in papillary thyroid carcinoma. Oncol Lett 2018; 15: 4269-77.
32. Muzafar A, Bukhari MH, Qureshi IU. A study of galactin-3 on fine needle aspiration as a diagnostic marker differentiating benign from malignant thyroid neoplasm. Pak J Med Sci 2017; 33: 726-31.
33. Golu I, Vlad MM, Dema A, *et al*. The absence of CD56 expression can differentiate papillary thyroid carcinoma from other thyroid lesions. Indian J Pathol Microbiol 2017; 60: 161-6.
34. Abd El Atti RM, Shash LS. Potential diagnostic utility of CD56 and claudin-1 in papillary thyroid carcinoma and solitary follicular thyroid nodules. J Egypt Natl Canc Inst 2012; 24: 175-84.
35. Ceyran AB, Şenol S, Şimşek BÇ, Sağıroğlu J, Aydın A. Role of cd56 and e-cadherin expression in the differential diagnosis of papillary thyroid carcinoma and suspected follicular-patterned lesions of the thyroid: the prognostic importance of e-cadherin. Int J Clin Exp Pathol 2015; 8: 3670-80.
36. Erdogan-Durmus S, Ozcan D, Yarikkaya E, Kurt A, Arslan A. CD56, HBME-1 and cytokeratin 19 expressions in papillary thyroid carcinoma and nodular thyroid lesions. J Res Med Sci 2016; 21: 49.
37. Oh EJ, Hong SW, Jeong HJ, Yoon SO. The diagnostic approach to fine-needle aspiration of malignant lymphoma: using cytomorphology and immunocytochemistry with cell transfer method. Diagn Cytopathol 2014; 42: 671-9.
38. Sherman ME, Jimenez-Joseph D, Gangi MD, Rojas-Corona RR. Immunostaining of small cytologic specimens: facilitation with cell transfer. Acta Cytol 1994; 38: 18-22.
39. Zu Y, Gangi MD, Yang GC. Ultrafast Papanicolaou stain and cell-transfer technique enhance cytologic diagnosis of Hodgkin lymphoma. Diagn Cytopathol 2002; 27: 308-11.
40. El Demellawy D, Nasr AL, Babay S, Alowami S. Diagnostic utility of CD56 immunohistochemistry in papillary carcinoma of the thyroid. Pathol Res Pract 2009; 205: 303-9.
41. Zeromski J, Bagnasco M, Paolieri F, Dworacki G. Expression of CD56 (NKH-1) differentiation antigen in human thyroid epithelium. Clin Exp Immunol 1992; 89: 474-8.
42. Ozolins A, Narbuts Z, Strumfa I, Volanska G, Stepanovs K, Gardovskis J. Immunohistochemical expression of HBME-1, E-cadherin, and CD56 in the differential diagnosis of thyroid nodules. Medicina (Kaunas) 2012; 48: 507-14.

 https://doi.org/10.4132/jptm.2018.09.20

Journal of Pathology and Translational Medicine 2018; 52: 411-415
https://doi.org/10.4132/jptm.2018.07.15

■ CASE STUDY ■

Squamous Metaplasia in Pleomorphic Adenoma: A Diagnostic and Prognostic Enigma

Swati Sharma · Monica Mehendiratta
Nivedita Chaudhary · Vineet Gupta
Maulshree Kohli · Anjana Arora[1]

Departments of Oral and Maxillofacial Pathology and Microbiology and [1]Oral Medicine and Radiology, I.T.S. Dental College, Hospital and Research Centre, Greater Noida, India

Received: April 27, 2018
Revised: June 20, 2018
Accepted: July 14, 2018

Corresponding Author
Swati Sharma, MDS
Department of Oral and Maxillofacial Pathology and Microbiology, I.T.S. Dental College, Hospital and Research Centre, Greater Noida, Uttar Pradesh 201308, India
Tel: +91-0120-2331089
Fax: +91-0120-2323702
E-mail: sharmaswatisharma86@gmail.com

Pleomorphic adenoma (PA) is the most common benign salivary gland tumor. Histologically, squamous metaplasia has been reported in PA, but has rarely been documented as being extensive enough to cause significant misdiagnosis. Here, we present an unusual case of PA in a 50-year-old female patient presenting with swelling on the postero-lateral aspect of the palate for a week. Histopathologically, the tumor exhibited the features of conventional PA with extensive squamous metaplasia and giant keratotic lamellae in cyst-like areas. Such exuberant squamous metaplasia and keratin can be a diagnostic and prognostic pitfall and lead to overtreatment of the patient.

Key Words: Squamous metaplasia; Pleomorphic adenoma; Pathology

Pleomorphic adenoma (PA) is the most common benign salivary gland tumor, accounting for 54%–76% of all salivary neoplasia. The parotid gland is the most common site of PA.[1] Approximately 8% of PA involve the minor salivary glands, whereas the palate is the most common site, accounting for 60%–65% of cases. Such tumors have been referred to by a great variety of names over the years (e.g., mixed tumors, enclavoma, branchioma, endothelioma, and enchondroma). The term "pleomorphic adenoma" suggested by Willis closely characterizes the unusual and varied histologic pattern of the lesion. PA demonstrates consistent cytogenetic abnormalities, chiefly involving the chromosome region 12q13-15. The putative PA gene is PLAG 1 and has been mapped to chromosome 8q 12. Being pleomorphic, it exhibits the ability to differentiate into epithelial (ductal and nonductal) cells and mesenchyme-like tissue (chondroid, myxoid and osseous).[2] Thus, it is composed of a mixture of glandular epithelium and myoepithelial cells within a mesenchyme-like tissue, and the proportion of each component varies widely among individual tumors.[1] The histomorphological variations are so extensive that in an incisional biopsy specimen, diagnosis can be challenging. The variations in epithelial and mesenchyme-like components with or without dysplasia add to this dilemma. The present case-study dealt with a massive PA of the palate with a misleading history of a week and an extensive squamous metaplasia with giant keratotic lamellae in cyst-like areas. This extensive squamous metaplasia and keratin brought this tumor's diagnosis close to intracapsular (*in situ*) PA, muco-epidermoid carcinoma, adenoid or adeno-squamous cell carcinoma, conventional squamous cell carcinoma (SCC), carcinoma ex PA, and necrotizing sialometaplasia. The patient granted consent and institutional ethical clearance was given for this case report (ITSCDSR/L/2018/086).

CASE REPORT

A 50-year-old female patient reported with a chief complaint of swelling on the right postero-lateral aspect of the palate for the past 1 week. Intraorally, a swelling associated with central ulceration and a fibrino-purulent membrane covering was present on the right side of the hard palate, with an approximate size of 5.0 × 5.0 × 1.5 cm^3 (Fig. 1). The swelling was firm in consistency,

pISSN 2383-7837
eISSN 2383-7845

non-tender, slightly movable and had an erythematous oedematous periphery. There were no associated palpable lymph nodes.

Further investigations were carried out, including hematological examination, computed tomography, aspiration cytology and biopsy. Hematological examination included complete blood count, prothrombin time, erythrocyte sedimentation rate, and routine blood sugar without any significant alarming result. Aspiration of the swelling did not yield much and was not helpful for evaluating the diagnosis. A subsequent cone beam computed tomography (CBCT) scan captured coronal sectional images revealing a well-defined dome-shaped soft tissue shadow measuring 2.19×2.42 cm^2, extending between the palatal aspect of 17 and 18, and mid-line of the palate medio-laterally. There was no evidence of bone resorption. The three dimensional image revealed an ill-defined posterior-most extent of this soft tissue swelling up to the oropharynx. No radiographic signs of malignancy such as invasive borders, irregular cortical boundary and aggressive bone destruction, root resorption, tooth displacement or periosteal reaction were evident (Fig. 2).

Wide local excision was conducted and the specimen was removed in toto in an uneventful surgery. Grossly, the tumor appeared well-encapsulated (Fig. 1), grayish-white, firm in consistency, smooth in texture and measured 2.6×2.9×1.7 cm^3. A provisional diagnosis of lymphadenopathy and palatal minor salivary gland tumor were made.

Hematoxylin and eosin–stained sections revealed a well-delin-

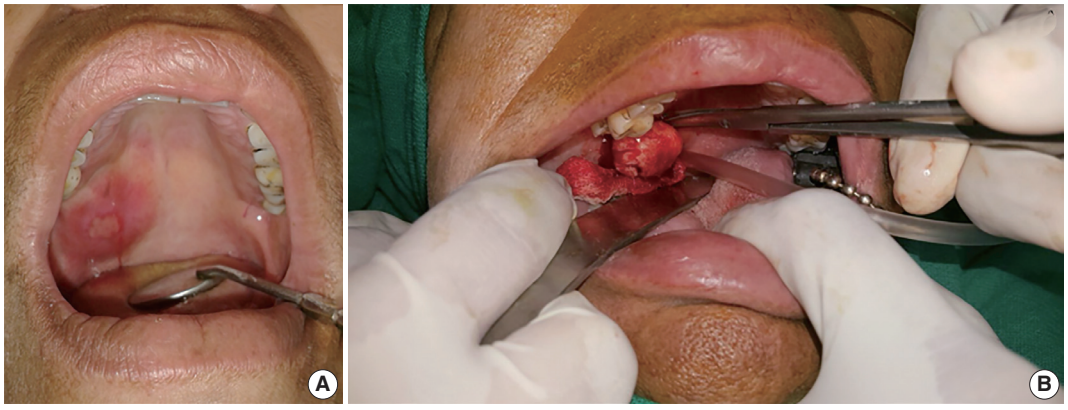

Fig. 1. (A) Swelling associated with central ulceration covered by a fibrino-purulent membrane and surrounded by palatal erythema can be seen on the right distal side of the hard palate, laterally. (B) A well-encapsulated tumor removed in toto from the palate.

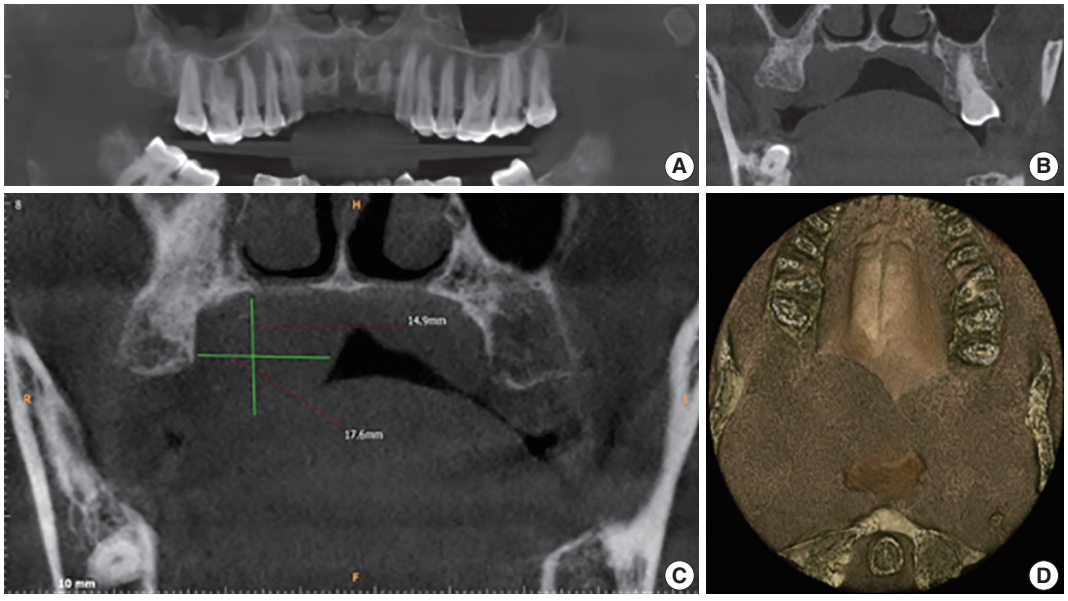

Fig. 2. (A) Reconstructed panoramic image shows the polyp at the level of the mid right maxillary sinus. (B) Axial section shows inflamed sinus lining involving the right maxillary sinus. (C) Cone beam computed tomography (CBCT) mid-coronal section of the right maxillary third molar (18) showing the soft tissue shadow palatally. (D) Two-three dimensional CBCT image showing the antero-posterior extent of the swelling.

https://doi.org/10.4132/jptm.2018.07.15

eated but partly encapsulated tumor mass flanked with abundant adipocytes. Under low magnification, the central pathology consisted of variably shaped, abundant ducts and massive squamous epithelium-lined cysts with extensive keratin in a myxoid and hyalinized stroma (Fig. 3). Under higher magnification, a classical bilayered ductal pattern with luminal cuboidal cells and variably-shaped, abluminal, myoepithelial cells was ascertained. The myoepithelial cell layers varied from a single layer to collar to an extensive collection, imparting the appearance of a swarm of bees. The other important feature of the lesion was florid squamous cells (50% of the tumor) arranged in nests, islands or in sheets with or without extensive cystic cavities containing massive keratotic lamellae and/or areas of degeneration. The cystic cavities were lined by 4–5 compressed layers of hyperchromatic, stratified squamous epithelium with hypergranulosis and sparse mitotic figures in the outer cells, but no evidence of atypia. The lining epithelium showed bud-shaped projections in the stromal tissue away from the cystic cavities (Fig. 3).

The stroma also revealed histogenetic diversity with extensive myxoid, fibrous to hyalinized areas with evidence of dystrophic calcification. The features were clearly suggestive of PA with florid squamous metaplasia and keratin-filled cysts. Post-operative healing of the patient was uneventful without any recurrence till 1.5 years after excision.

The presence of an extensive squamous component with keratin lamellae in the tumor background with ducts and variably shaped epithelial cells dispersed in a myxoid and hyalinized background created a multitude of differential diagnoses. The absence of frank mucous and intermediate cells as well as extensive mucin pooling helped distinguish from mucoepidermoid carcinoma. Conventional SCC was considered, as it may invade or entrap non-tumorous salivary glands, but was ultimately ruled out due to the presence of extensive morphological, epithelial and stromal diversity with no evidence of dysplasia. Adenoid SCC and adenosquamous cell carcinoma owing to the presence of squamous and glandular components were also considered as differentials, although the former malignancy does not show any true glands/ducts or intracytoplasmic mucins. The latter and other malignancies such as *in-situ* (intracapsular) PA and carcinoma ex-PA were ruled out for several reasons. First, the received tissue was in toto

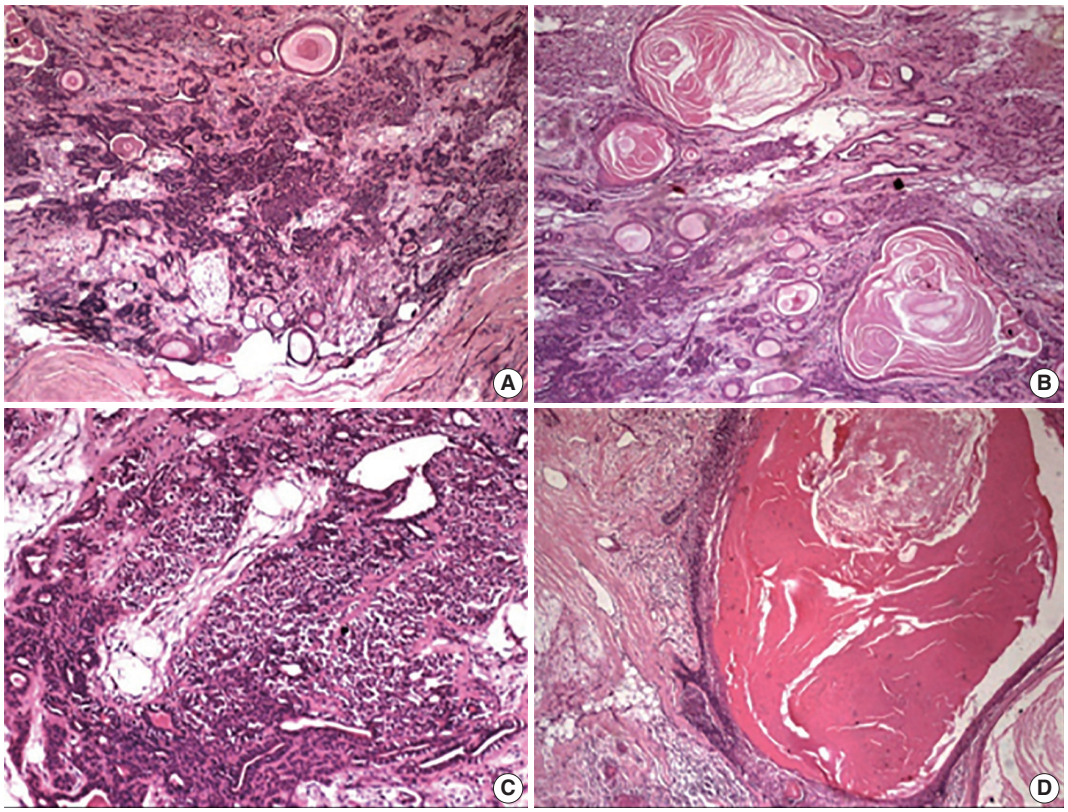

Fig. 3. (A) The periphery of the tumor with classical features of pleomorphic adenoma having abundant ducts dispersed in a myxoid and hyalinized background with multiple keratin-filled cystic areas. (B) Multitude of features, including variably shaped epithelial cells, ducts, and squames. Keratin-filled cysts dispersed in the myxoid stroma. (C) Abundant myoepithelial cells around the ducts giving the appearance of a swarm of bees. (D) Massive epithelial lined cysts with keratotic lamellae and the lining budding into the stroma.

and thoroughly examined for evidence of any atypical changes. Second, there was an absence of cellular and nuclear atypia, necrosis, capsular invasion, an aggressive growth pattern and nerve/surrounding tissue permeation.

Clinically, because the tumor was located on the palate with a short history of presentation, a diagnosis of necrotizing sialometaplasia or chronic sialadenitis was also considered, but ultimately ruled out due to the absence of necrosis and presence of rich morphological diversity consistent with the diagnosis of PA.

Another important feature of note in the present case was squamous metaplasia, which could have been the result of the fine needle aspiration cytology (FNAC) conducted prior to excision of the lesion. However, the exuberant amount of squamous metaplasia evident in the lesion did not appear to be correlated with a needle-induced change.

DISCUSSION

The present case is a classical case of PA without cytological atypia, but demonstrating extensive squamous metaplasia, which can be of serious concern. Squamous metaplasia is an incidental microscopic finding in various benign and malignant (*de-novo* or induced) tumors in humans or animal models. The origin is unknown and has been associated erratically with the intra-tumoral/tissue environment, like trauma, infarction/ischemia and repair following infarction.[3] Squamous metaplasia has been experimentally induced by arterial ligation in rat salivary glands by Dardick *et al*.,[4] and appears to have formed via the gradual dedifferentiation and hyperplasia of the acinar-intercalated duct system. Tonofilaments and desmosomes begin to appear in the luminal and abluminal myoepithelial cells, and thus keratinization of central cells materializes.[4] The varying degree of squamous metaplasia could be a consequence of the rapidity and ease of switch in the genetic programming of cytokeratin filaments induced by ischemia in the salivary glands, and so the most probable etiology for this change appears to be ischemia.[3] FNAC for diagnostic purposes has been shown to induce the same in tumors during histopathological evaluation.[5] FNAC was conducted in our case, but there was no evidence of necrosis/repair in the sections, and the amount of squamous metaplasia appeared to be correlated with the extent of injury induced by ischemia.

Foci of squamous cells are an integral feature of PA, but extensive squamous metaplasia is uncommon and can be easily misinterpreted as SCC, especially in FNAC and incisional biopsies due to the limited and selective sampling. In addition, diagnosis becomes challenging in the absence of chondro-myxoid stroma, making it imperative to understand this diagnostic pitfall.[6]

The presence of squamous metaplasia is also a prognostic pitfall, as its transition into SCC has been further emphasized by Takegawa *et al*.[7] in the submandibular glands of rats by the application of potassium iodide. Takegawa *et al*.[7] observed the development of squamous metaplasia in proliferative ductules and interlobular ducts that apparently transited to SCC, and emphasized that this occurred via a non-genotoxic, proliferation-dependent mechanism.[7]

To summarize, similar case reports have been provided by various authors with or without application of immunohistochemistry (IHC) markers. One case described a 32-year-old patient with 45% of the tumor consisting of squamous cells, wherein IHC helped distinguish the squamous metaplastic cells from SCC.[8] The presence of low molecular weight cytokeratin and p63 in squamous cells helps rule out SCC or even reactive squamous hyperplasia in such PA cases.[9] Multiple IHC markers are used to ascertain differences between glandular cells or metaplastically-formed squamous cells. Although no conclusive differences have been established using cytokeratin or even MIB-1[8] (a proliferative marker), Ki-67 as used by Goulart *et al*.[10] had a higher proliferative index in the epithelial lining of a large keratin cyst.

Diagnosis of PA requires physical examination, CBCT, cytology and histopathology. FNAC and incisional biopsy can help determine the proper management regimen, but must be thoroughly sampled to rule out any misdiagnosis, especially in cases of misleading short histories like our present case. Other supportive investigations like computed tomography scanning and magnetic resonance imaging can provide information on the location and size of the tumor and its extension into surrounding superficial and deep structures.

The treatment for PA is surgical excision, and although radiotherapy is not indicated, correct diagnosis is essential to avoid overtreatment.[2] The present case, to the best of our knowledge, is among the first 20 cases reported in the English language literature and thus a rarity. The misleading short history of one week, enormous size of $5.0 \times 5.0 \times 1.5$ cm^3 and massive squamous islands could have led to an incorrect diagnosis of malignancy. Thus, the thorough examination of samples, particularly in FNAC and incisional cases, is important.

ORCID

Swati Sharma: https://orcid.org/0000-0003-1124-568X
Monica Mehendiratta: https://orcid.org/0000-0001-6841-8591
Nivedita Chaudhary: https://orcid.org/0000-0001-9134-8835
Vineet Gupta: https://orcid.org/0000-0002-2333-1625

https://doi.org/10.4132/jptm.2018.07.15

Conflicts of Interest

No potential conflict of interest relevant to this article was reported.

REFERENCES

1. Neville B, Damm DD, Allen C, Bouquot J. Oral and maxillofacial pathology. 3rd ed. St. Louis: Elsevier; 2009; 473-506.
2. Rajendran R, Sivapathasundharam B. Shafer's text book of oral pathology. 7th ed. Noida: Elsevier, 2012; 223-57.
3. Kaveri H, Gopalkrishnana K, Venkatesh A. Cystic and florid squamous metaplasia in pleomorphic adenoma of palate: a diagnostic dilemma. Asian J Med Sci 2014; 5: 108-10.
4. Dardick I, Jeans MT, Sinnott NM, Wittkuhn JF, Kahn HJ, Baumal R. Salivary gland components involved in the formation of squamous metaplasia. Am J Pathol 1985; 119: 33-43.
5. Jaishankar HP, Hegde U, Nagpal B. Florid squamous metaplasia and keratin cyst formation in palatal minor salivary gland tumor: a diagnostic challenge. Int J Health Sci Res 2016; 6: 516-20.
6. Compagno J, Wong RT. Intranasal mixed tumors (pleomorphic adenomas): a clinicopathologic study of 40 cases. Am J Clin Pathol 1977; 68: 213-8.
7. Takegawa K, Mitsumori K, Onodera H, *et al*. Induction of squamous cell carcinomas in the salivary glands of rats by potassium iodide. Jpn J Cancer Res 1998; 89: 105-9.
8. Lam KY, Ng IO, Chan GS. Palatal pleomorphic adenoma with florid squamous metaplasia: a potential diagnostic pitfall. J Oral Pathol Med 1998; 27: 407-10.
9. Lim S, Cho I, Park JH, Lim SC. Pleomorphic adenoma with exuberant squamous metaplasia and keratin cysts mimicking squamous cell carcinoma in minor salivary gland. Open J Pathol 2013; 3: 113-6.
10. Goulart MC, Freitas-Faria P, Goulart GR, *et al*. Pleomorphic adenoma with extensive squamous metaplasia and keratin cyst formations in minor salivary gland: a case report. J Appl Oral Sci 2011; 19: 182-8.

Journal of Pathology and Translational Medicine 2018; 52: 416-419
https://doi.org/10.4132/jptm.2018.07.20

■ CASE STUDY ■

An Intrarenal Adrenocortical Carcinoma Arising in an Adrenal Rest

Ji Hee Lee · Young Deuk Choi[1]
Nam Hoon Cho

Departments of Pathology and [1]Urology, Severance Hospital, Yonsei University College of Medicine, Seoul, Korea

Received: May 23, 2018
Revised: July 2, 2018
Accepted: July 20, 2018

Corresponding Author
Nam Hoon Cho, MD
Department of Pathology, Severance Hospital, Yonsei University College of Medicine, 50-1 Yonsei-ro, Seodaemun-gu, Seoul 03722, Korea
Tel: +82-2-2228-1767
Fax: +82-2-2227-7939
E-mail: CHO1988@yuhs.ac

We describe a case of a 61-year-old Korean man who was diagnosed with renal cell carcinoma that was discovered on abdominopelvic computed tomography obtained after the patient complained of back pain. A radical nephrectomy was performed, and the surgical specimen showed a relatively well-circumscribed and yellowish lobulated hard mass. Microscopically, the tumor showed sheets and nests of hypercellular pleomorphic cells with thick fibrous septation, frequent mitoses, and areas of adrenal cortical-like tissue. Immunohistochemical staining revealed that the tumor cells were positive for inhibin-α, vimentin, synaptophysin, and melan A. It also revealed that the tumor cells were negative for pan-cytokeratin, epithelial membrane antigen, paired box 8, α-methylacyl-coenzyme A racemase, CD10, cytokeratin 7, carbonic anhydrase 9, c-Kit, renal cell carcinoma, transcription factor E3, human melanoma black 45, desmin, smooth muscle actin, S-100, chromogranin A, CD34, anaplastic lymphoma kinase, and integrase interactor 1. Based on these histopathological and immunohistochemical findings, we diagnosed the tumor as intrarenal adrenocortical carcinoma arising in an adrenal rest. Several cases of intrarenal adrenocortical carcinoma have been reported, although they are very rare. Due to its poor prognosis and common recurrence or metastasis, clinicians and pathologists must be aware of this entity.

Key Words: Adrenocortical carcinoma; Adrenal rest tumor; Carcinoma; Renal cell

Adrenocortical carcinoma is a rare and heterogeneous malignancy with a poor prognosis, the pathogenesis of which is not yet completely understood. Patients present with hormone excess or local mass effect.[1] An adrenal rest (ectopic adrenal tissue) can occur anywhere along the gonadal descent. This tissue usually has no clinical significance, but it may become hyperplastic or malignant in patients with primary or secondary adrenal pathology.[2] Most adrenal rest tumors are functional and diagnosed preoperatively. However, the less frequent nonfunctional adrenal rest tumors are discovered accidentally or postoperatively.[3] We described a patient with a nonfunctioning intrarenal adrenocortical carcinoma that arose from an adrenal rest.

CASE REPORT

This study was approved by the Institutional Review Board of Severance Hospital with a waiver of informed consent (IRB No. 4-2017-1044).

A 61-year-old man was evaluated for back pain that had persisted for 10 days. Abdominopelvic computed tomography (APCT) and magnetic resonance imaging were performed at a local clinic and revealed a 13-cm mass in his right kidney. The mass was causing an ureteropelvic junction obstruction that broadly contacted the second and third duodenal portions, psoas muscle, and inferior vena cava. All radiologic findings were consistent with renal cell carcinoma with multiple lung metastases. The patient was hospitalized at our institution, and the APCT was repeated and provided the same diagnosis (Fig. 1A).

The patient underwent radical nephrectomy without adrenalectomy. The right kidney weighed 1,135 g and measured 17×12×6 cm. The tumor had a smooth and bulging external surface. Cross sections revealed a well-circumscribed and yellowish lobulated hard mass (Fig. 1B) measuring 14×12×8 cm, present in the mid pole of the right kidney. The mass showed extensive necrosis (60%) and hemorrhage (30%).

Microscopically, the tumor had multilobulated nests divided by thick fibrous septations (Fig. 2A). The tumor was comprised of compact polygonal cells with distinct cell borders and granular cytoplasm. Sinusoidal vascular ingrowth was less distinct. Nuclei were round or ovoid, hyperchromatic with central prominent nucleoli, and contained frequent mitoses (40/50 high-power fields) (Fig. 2B) without raisinoid nuclei or perinuclear haloes. Some areas containing adrenal cortical-like tissues were identified (Fig. 2C). Necrosis and vascular invasion were also present. These

pISSN 2383-7837
eISSN 2383-7845

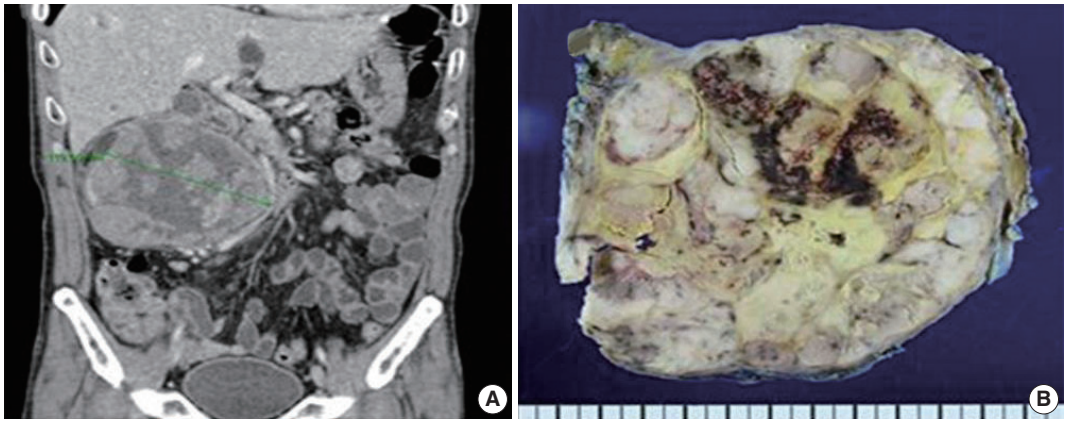

Fig. 1. Imaging and gross findings of adrenocortical carcinoma. (A) Abdominopelvic computed tomography reveals a 13 cm heterogeneous mass in the right kidney. (B) Bisected kidney specimen showing a lobulated hard mass with necrosis and hemorrhage.

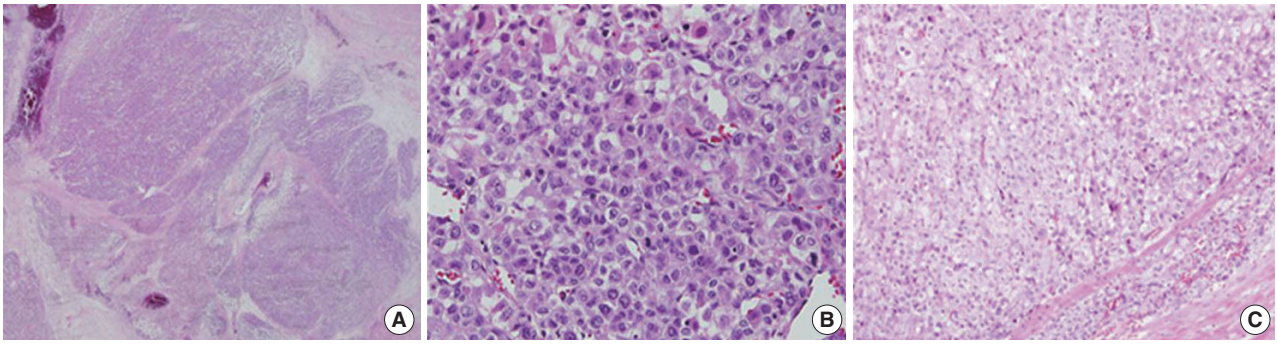

Fig. 2. Histologic findings of adrenocortical carcinoma. (A) Sheets and nests of hypercellular tumor cells with thick fibrous septation. (B) Pleomorphic cells with frequent mitoses. (C) Areas of adrenal cortical-like tissue.

results suggested against the diagnosis of renal cell carcinoma.

Immunohistochemical staining results are presented in Table 1 and Fig. 3. The results were consistent with adrenocortical carcinoma and excluded the possibility of renal cell carcinoma and specific variants of the kidney tumor.

DISCUSSION

Ectopic or accessory adrenal cells are often found postnatally along the path of gonadal descent because the adrenocortical primordium develops in close proximity to the urogenital ridge of the emerging gonad and migrates alongside the gonad.[4] Typically, these cells disappear within a few years of birth, and sometimes these cells linger without any event.

Ye *et al*.[4] reported seven cases of intrarenal adrenal tissue and two cases of renal-adrenal fusion. Except for one case identified within the kidney mid pole, all intrarenal lesions were found in the superior portion of the kidney. Our case reports a malignant tumor arising from the ectopic adrenal rest in the mid pole of the kidney. In all nine reported cases of Ye *et al*.,[4] the intrarenal

Table 1. Immunostaining results of adrenocortical carcinoma

Antigen	Tumor cell
Pan-cytokeratin	Negative
EMA	Negative
Inhibin-α	Positive
Vimentin	Positive
Melan A	Focal positive
Synaptophysin	Positive
Paired box 88	Negative
Calretinin	Negative
α-Methylacyl-coenzyme A racemase	Negative
CD10	Negative
Cytokeratin 7	Negative
Carbonic anhydrase 9	Negative
C-kit	Negative
Renal cell carcinoma	Negative
Transcription factor E3	Negative
Human melanoma black 45	Negative
Desmin	Negative
Smooth muscle actin	Negative
S-100	Negative
Chromogranin A	Negative
CD 34	Negative
Anaplastic lymphoma kinase	Negative
Integrase interactor 1	No loss

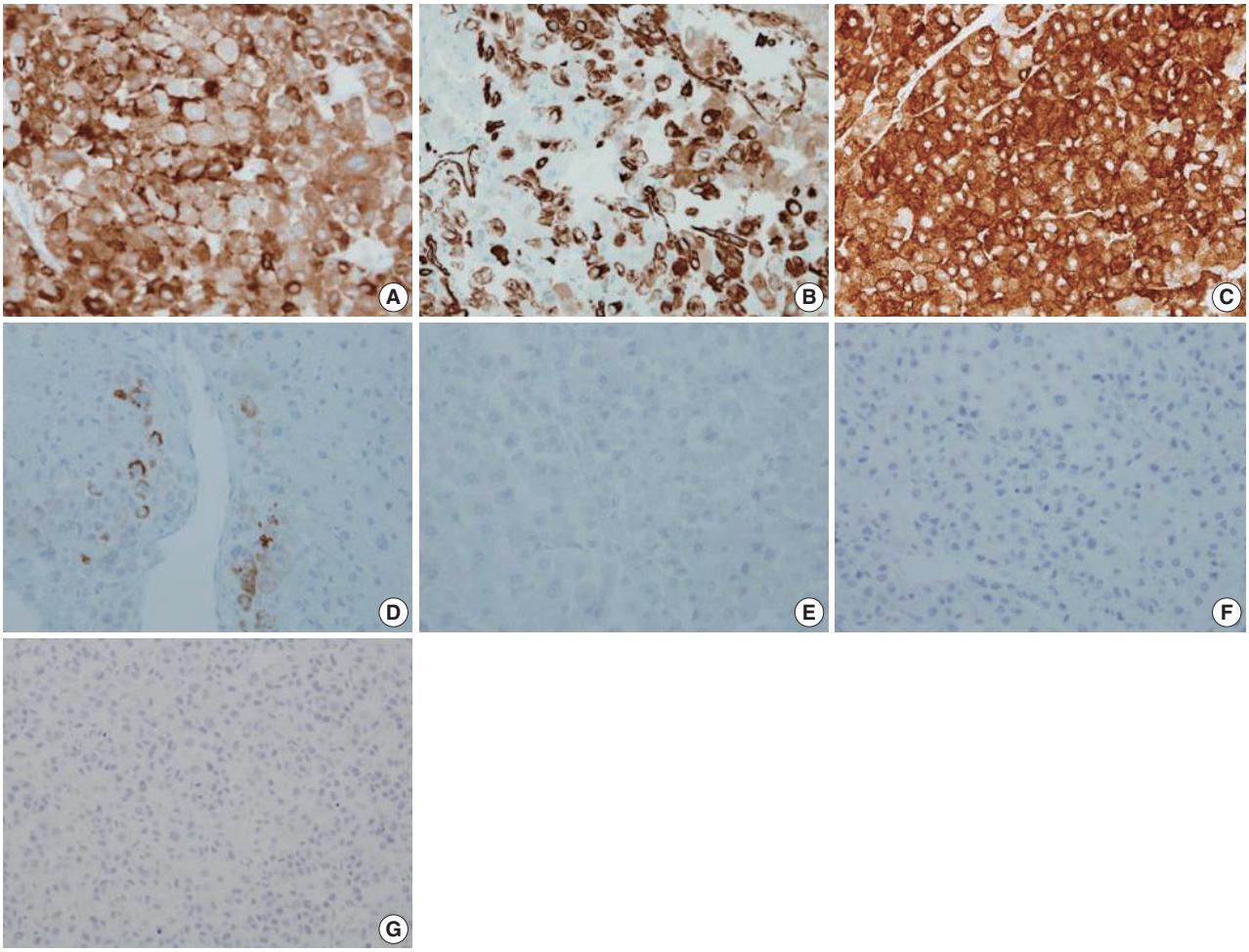

Fig. 3. Immunohistochemical staining results of adrenocortical carcinoma. The tumor cells were positive for inhibin-α (A), vimentin (B), synaptophysin (C), and melan A (D) and negative for epithelial membrane antigen (E), paired box 8 (F), and pan-cytokeratin (G).

adrenal tissues were composed of only adrenal cortical tissue with no adrenal medullary tissue present. There is a recent review of the literature about adrenocortical carcinoma arising in an adrenal rest. Reported malignant tumors arising from an ectopic adrenal rest are predominantly adrenocortical carcinomas of the retroperitoneum, gonad, liver, kidney, spinal cord, and pelvis.[5] Intrarenal adrenocortical carcinomas have been previously identified in the hilum[3] and in the mid pole of the kidney as in our case. Adrenocortical carcinomas that involve the gonads show relatively high rates of mortality.[6-8]

The microscopic features that favor the diagnosis of renal cell carcinoma over adrenocortical carcinoma are the presence of glands, particularly if they contain red blood cells, and abundant cytoplasmic glycogen. However, neither is pathognomonic and were present in the case. Among the nine histological parameters of the Weiss scoring system for histologic diagnosis of adrenocortical carcinoma (high nuclear grades [Fuhrman nuclear grades III and IV], mitotic rate > 5/50 high-power fields, atypical mitotic figures, clear tumor cell cytoplasm [less than 25% tumor cells], diffuse architecture [greater than 33% of tumor], necrosis, venous invasion, sinusoidal invasion, and capsular invasion), the present case met seven parameters, excluding sinusoidal invasion and capsular invasion. After the diagnosis of renal cell carcinoma was excluded by morphology and negative cytokeratin expression, we examined additional immunohistochemical stains to differentiate epithelioid angiomyolipoma, adrenocortical carcinoma, glomus tumor, or related mesenchymal tumors. Finally, we defined the tumor as adrenocortical carcinoma (pT2NxcM1).

Currently, radical surgery is the only curative approach, and it is recommended for all patients with resectable adrenocortical carcinoma tumors, including those patients with recurrent disease. There is no consensus concerning adjuvant therapy.[9] However, recent studies have reported that adjuvant mitotane may prolong recurrence-free survival in patients with radically resected adre-

https://doi.org/10.4132/jptm.2018.07.20

nocortical carcinoma.[10,11]

Our patient was treated with radical nephrectomy and adjuvant chemotherapy (VAP; vincristine, doxorubicin, and prednisolone) with mitotane. He has been healthy with no evidence of recurrence or metastasis for 3 months after the original diagnosis. Recent studies have reported the prevalence of adrenocortical carcinoma in Korea to be 2%–5%. In our institution, five cases of adrenocortical carcinoma were reported from 2000 to 2018. Among them, this is the only and first reported case of intrarenal adrenocortical carcinoma. We reported a rare case of intrarenal adrenocortical carcinoma arising from an ectopic adrenal rest as a mimicker of renal cell carcinoma in the kidney. Although the incidence of malignancy arising in an adrenal rest is low, clinicians and pathologists must be aware of the possibility because of its poor prognosis and common recurrence and metastasis.

ORCID

Ji Hee Lee: https://orcid.org/0000-0003-0054-7033
Nam Hoon Cho: https://orcid.org/0000-0002-0045-6441

Conflicts of Interest

No potential conflict of interest relevant to this article was reported.

REFERENCES

1. Allolio B, Fassnacht M. Clinical review: adrenocortical carcinoma: clinical update. J Clin Endocrinol Metab 2006; 91: 2027-37.
2. Barwick TD, Malhotra A, Webb JA, Savage MO, Reznek RH. Embryology of the adrenal glands and its relevance to diagnostic imaging. Clin Radiol 2005; 60: 953-9.
3. Goren E, Engelberg IS, Eidelman A. Adrenal rest carcinoma in hilum of kidney. Urology 1991; 38: 187-90.
4. Ye H, Yoon GS, Epstein JI. Intrarenal ectopic adrenal tissue and renal-adrenal fusion: a report of nine cases. Mod Pathol 2009; 22: 175-81.
5. Cornejo KM, Afari HA, Sadow PM. Adrenocortical carcinoma arising in an adrenal rest: a case report and review of the literature. Endocr Pathol 2017; 28: 165-70.
6. Engel FL, McPherson HT, Fetter BF, *et al*. Clinical, morphological and biochemical studies on a malignant testicular tumor. J Clin Endocrinol Metab 1964; 24: 528-42.
7. Morimoto Y, Hiwada K, Nanahoshi M, *et al*. Cushing's syndrome caused by malignant tumor in the scrotum: clinical, pathologic and biochemical studies. J Clin Endocrinol Metab 1971; 32: 201-10.
8. Jain SH, Sadow PM, Nosé V, Dluhy RG. A patient with ectopic cortisol production derived from malignant testicular masses. Nat Clin Pract Endocrinol Metab 2008; 4: 695-700.
9. Langer P, Bartsch D, Moebius E, Rothmund M, Nies C. Adrenocortical carcinoma: our experience with 11 cases. Langenbecks Arch Surg 2000; 385: 393-7.
10. Terzolo M, Angeli A, Fassnacht M, *et al*. Adjuvant mitotane treatment for adrenocortical carcinoma. N Engl J Med 2007; 356: 2372-80.
11. Berruti A, Grisanti S, Pulzer A, *et al*. Long-term outcomes of adjuvant mitotane therapy in patients with radically resected adrenocortical carcinoma. J Clin Endocrinol Metab 2017; 102: 1358-65.

Journal of Pathology and Translational Medicine 2018; 52: 420-424
https://doi.org/10.4132/jptm.2018.03.29

■ BRIEF CASE REPORT ■

Collagenous Spherulosis Associated with Lobular Carcinoma *In Situ* of the Breast: Two Case Reports

Ga-Eon Kim · Nah Ihm Kim · Ji Shin Lee · Min Ho Park[1]

Departments of Pathology and [1]Surgery, Chonnam National University Medical School, Gwangju, Korea

Collagenous spherulosis (CS) of the breast is an uncommon benign lesion, which is characterized by nodules of eosinophilic or basophilic basement membrane material enclosed in spherical spaces of cribriform architecture with myoepithelial and epithelial proliferation.[1-4] While CS is usually encountered as an incidental finding in association with other benign hyperplastic lesions, the presence of calcification or abnormal density on imaging studies attracts clinical attention.[2-4] CS is occasionally associated with lobular carcinoma *in situ* (LCIS).[3-6] Despite its benign nature, the diagnosis of CS is challenging because it shows a cribriform architecture mimicking adenoid cystic carcinoma on low power.[3,4,7,8] In addition, the diagnosis is especially difficult when associated with LCIS because it is often misdiagnosed as a cribriform pattern ductal carcinoma *in situ* (DCIS).[3-8] Recently, it is predicted that the incidence of CS will increase due to breast cancer screening programs, and the pathologists need to be aware of CS in order not to misdiagnose CS associated with LCIS as DCIS or other malignancy, especially on core needle biopsy specimens. Here, we report two cases of CS associated with LCIS of the breast. To the best of our knowledge, this is the first reported case of CS associated with LCIS of the breast in Korea.

CASE REPORT

The cases reported herein were consult cases, and this study was approved by the Institutional Review Board of Chonnam National University Hwasun Hospital with waiver of informed consents (CNUHH-EXP-2018-012).

Case 1 was an asymptomatic 51-year-old female with multiple small nodules on ultrasound examination of the right breast. Case 2 was a 47-year-old female with an incidentally detected lesion in the left breast presenting as an ill-defined nodule measuring 8 mm on ultrasound examination. Both patients underwent ultrasound-guided vacuum-assisted biopsy. The histology of the two cases was similar. Microscopically, the lesions showed enlarged lobules filled with neoplastic cells (Figs. 1A, 2A). The neoplastic cells of case 1 contained scant cytoplasm, and small, rounded, and bland nuclei without nucleoli (Fig. 1B). In case 2, the neoplastic cells showed more abundant cytoplasm than those seen in case 1, and larger, more pleomorphic nuclei with nucleoli (Fig. 2B). The neoplastic cells in both cases showed incohesive growth and negative E-cadherin immunoreactivity. Cases 1 and 2 represented classical and pleomorphic types of LCIS, respectively. In both cases, multiple spherules showing cribriform architecture lined by flattened epithelial cells were seen adjacent to the LCIS area (Figs. 1C, 2C). The space of the spherules contained faintly basophilic fibrillary substances. Overall, the spherules displayed microscopic characteristics typical of CS. A few spherules of CS had LCIS (Figs. 1D, 2D). E-cadherin-negative LCIS cells colonized several spherules of CS and replaced the luminal epithelial cells, which were positive for E-cadherin (Figs. 1E, 2E). The spherules were outlined by myoepithelial cells stained with p63 and calponin (Figs. 1F, 2F, G). The basophilic fibrillary materials within CS were positive for laminin (Fig. 1G). The cells of the spherules tested negative for c-Kit (Figs. 1H, 2H).

Corresponding Author
Ji Shin Lee, MD
Department of Pathology, Chonnam National University Hwasun Hospital,
322 Seoyang-ro, Hwasun 58128, Korea
Tel: +82-61-379-7072, Fax: +82-61-379-7079, E-mail: jshinlee@hanmail.net

Received: January 23, 2018 **Revised:** March 19, 2018
Accepted: March 27, 2018

pISSN 2383-7837
eISSN 2383-7845

DISCUSSION

CS is a rare breast lesion with well-characterized, structural, and histological alterations of unknown histogenesis.[1-4] Histologically, CS constitutes less than 1% of all breast biopsies.[2,4] Typically, CS is detected as an incidental microscopic finding in

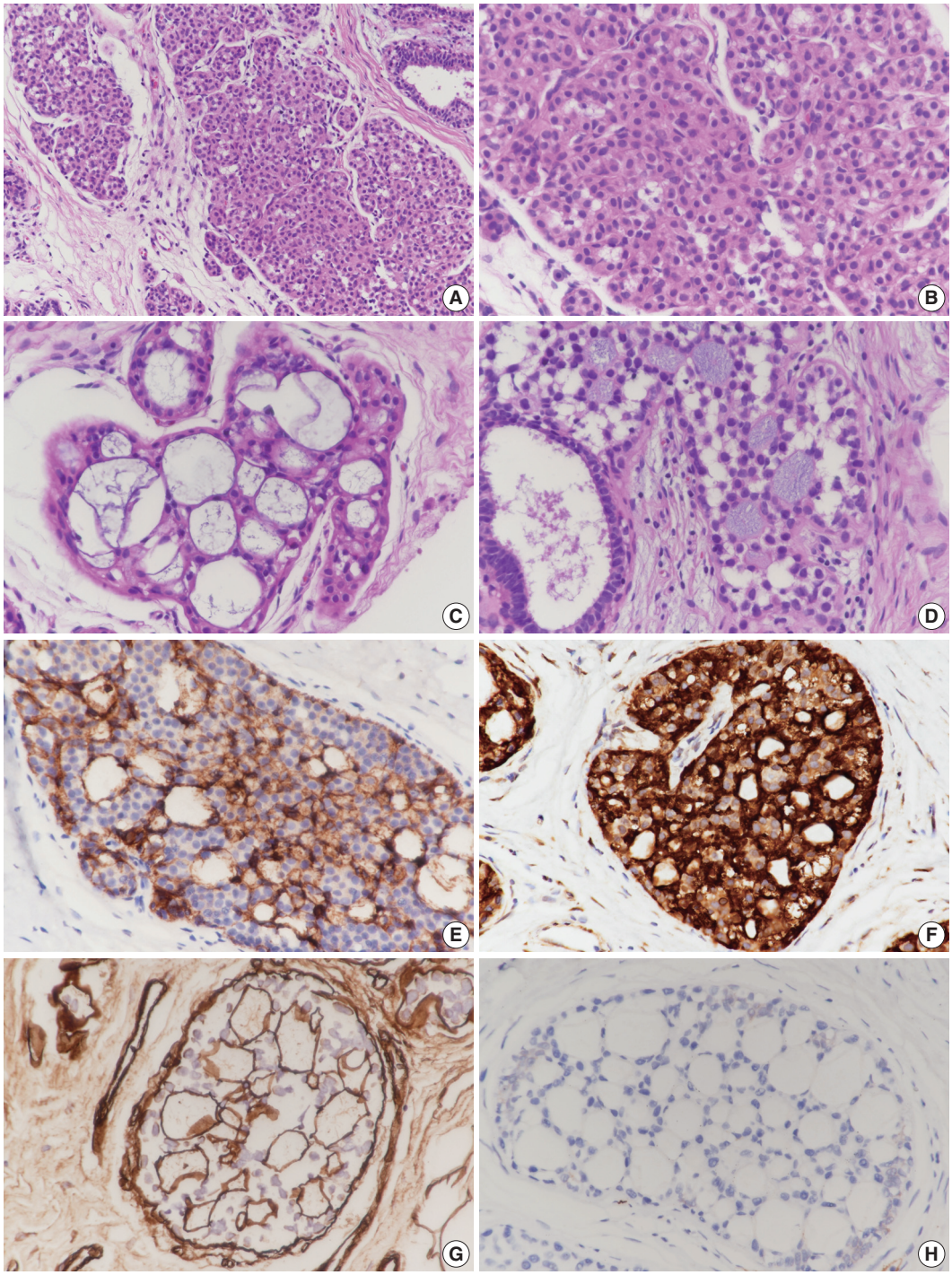

Fig. 1. Microscopic and immunohistochemical findings of case 1 collagenous spherulosis (CS) associated with lobular carcinoma *in situ* (LCIS), classical type. (A) In LCIS, enlarged lobules are seen. (B) The neoplastic cells of LCIS show loss of cohesion. (C) Cribriform proliferation with spherules containing cellular fibrillar components is seen. (D) LCIS cells colonize CS. (E) LCIS cells stain negative for E-cadherin, and the residual cells of CS stain positive. (F) Myoepithelial cells within CS with LCIS show calponin immunoreactivity. (G) Basement membrane-like components within spherules are highlighted by laminin immunostain. (H) CS with LCIS is negative for c-Kit.

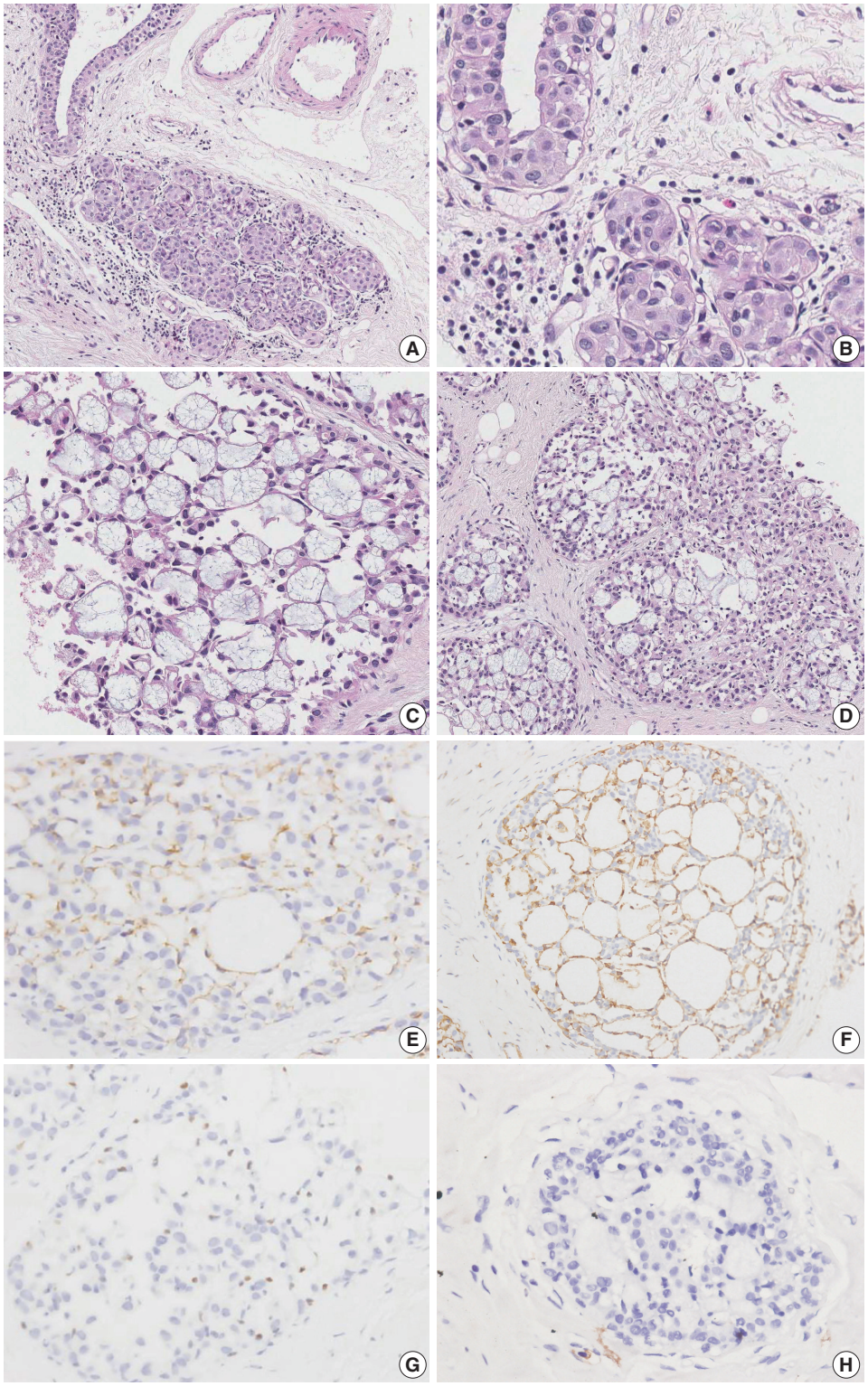

Fig. 2. Microscopic and immunohistochemical findings of case 2 collagenous spherulosis (CS) associated with lobular carcinoma *in situ* (LCIS), pleomorphic type. (A) The LCIS area shows enlarged lobular glands and intraepithelial growth pattern. (B) In contrast to case 1, the neoplastic cells contain more abundant cytoplasm and pleomorphic nuclei with occasional nucleoli. (C) A cribriform pattern of CS is characterized by cystic spaces containing basophilic fibrillar components. (D) CS with LCIS retains cribriform spaces, which contain cellular fibrillar components. (E) LCIS cells within the spherule show loss of E-cadherin expression. (F, G) The cells surrounding the spherules are positive for calpoinin and p63. (H) CS with LCIS is negative for c-Kit.

https://doi.org/10.4132/jptm.2018.03.29

surgical specimens of other lesions. CS can also be detected as calcifications or an abnormal density on imaging studies.[3,4] Benign proliferative lesions associated with CS include papillomas, ductal hyperplasia, radial scars, and complex sclerosing lesions.[3,4] CS is occasionally associated with LCIS.[3-6] The prognosis and treatment depend on the nature of the underlying lesion.

Eisenberg and Hoda[6] summarized the clinical and morphological features of 38 cases of CS diagnosed with LCIS at a single institution over a 12-year period. All the cases were submitted for consultation either for diagnostic assistance or with the mistaken interpretation of DCIS. The patients included women ranging in age from 41 to 75 years (mean age, 52 years). CS with LCIS was demonstrated in 22 core-needle biopsy specimens (58%), 15 excisional specimens (40%), and 1 mastectomy specimen (2%). Both breasts were equally involved and no case was bilateral. Thirty-four cases (89%) presented with mammographically detected abnormal density, with associated microcalcifications in 24 (63%). Histologically, CS with LCIS showed expanded ducts and glandular acini with relatively uniform cribriform spaces, which contained fibrillary or stellate basement membrane material. LCIS and CS were seen immediately adjacent to CS with LCIS. The constituent LCIS in CS with LCIS represented the classical type in 35 cases (92%), pleomorphic type in one (3%) and a mixture of classical and pleomorphic type in two cases (5%).[6]

To the best of our knowledge, the cases reported herein represent the first cases of CS with LCIS in Korea. Both of our patients were female, aged 47 and 51 years, and the lesions were detected incidentally by ultrasound screening. The lesions showed LCIS, one a classical type and the other a pleomorphic type.

With experience, the recognition of CS with LCIS may not be challenging, but it can still pose a diagnostic difficulty. The most common lesion for which CS with LCIS may be mistaken is adenoid cystic carcinoma.[3,4,7,8] Both lesions contain spherules with basement membrane materials. The spherules in CS with LCIS and adenoid cystic carcinoma are similar in composition; histochemical and immunohistochemical studies show components of basement membrane, including type IV collagen and laminin, in both lesions. Functional myoepithelial cells are known to generate basement membrane components, which form spherical masses. However, the two lesions can be distinguished by the growth pattern; CS with LCIS is not an infiltrative lesion while adenoid cystic carcinoma shows stromal invasion. In challenging cases, immunohistochemical stains can facilitate differential diagnosis.[4,7-10] Immunostaining for myoepithleial markers such as smooth muscle myosin heavy chain, p63, and calponin demonstrate the presence of a single layer of myoepithelial cells surrounding the spherules in CS. Variable expression of myoepithelial cell markers is reported due to the basal/myoepithelial phenotype of the tumor cells in adenoid cystic carcinoma,. Additionally, adenoid cystic carcinoma shows positive staining for c-Kit, unlike CS with LCIS.[9,10]

CS with LCIS imparts a regular, chiseled cribriform architecture with monotonous neoplastic cells, which can be mistaken for low grade DCIS of cribriform pattern.[3-8] Recognition of the incohesive growth and punctate cytoplasmic vacuoles of the LCIS cells also facilitates an accurate diagnosis. Immunostaining for E-cadherin in combination with myoepithelial cell makers can further differentiate CS with LCIS from DCIS. In CS with LCIS, E-cadherin is negative in the neoplastic LCIS cells and positive in the intermingled residual epithelial and myoepithelial cells of CS. Myoepithelial cell immunostaining demonstrates the presence of myoepithelial cells within the spherules. In DCIS, E-cadherin is positive in the neoplastic epithelial cells, and myoepithelial cell markers highlight the peripheral myoepithelial cell layer.

Lobular neoplasia includes atypical lobular hyperplasia and LCIS, and the distinction between the two is based on the degree of acinar involvement in a lobular unit. In core-needle biopsy specimens, CS involved by lobular neoplasia is a more appropriate diagnostic term.

We diagnosed CS with LCIS based on results of immunohistochemical studies. E-cadherin-negative LCIS cells colonized the spherules in CS, surrounded by a layer of myoepithelial cells stained with p63 and calponin. The tumor cells tested negative for c-Kit.

In conclusion, breast cancer screening programs may detect increased numbers of CS cases with LCIS or CS alone. The pathologist should be aware of this lesion to avoid erroneous diagnosis of malignancy, especially in core-needle biopsy specimens.

ORCID

Ji Shin Lee: https://orcid.org/0000-0003-4634-2228

Conflicts of Interest

No potential conflict of interest relevant to this article was reported.

REFERENCES

1. Clement PB, Young RH, Azzopardi JG. Collagenous spherulosis of the breast. Am J Surg Pathol 1987; 11: 411-7.
2. Mooney EE, Kayani N, Tavassoli FA. Spherulosis of the breast: a

spectrum of municous and collagenous lesions. Arch Pathol Lab Med 1999; 123: 626-30.
3. Resetkova E, Albarracin C, Sneige N. Collagenous spherulosis of breast: morphologic study of 59 cases and review of the literature. Am J Surg Pathol 2006; 30: 20-7.
4. Hoda SA, Brogi E, Koerner FC, Rosen PP, eds. Rosen's breast pathology. 4th ed. Philadelphia: Lippincott Williams & Wilkins, 2014; 143-7.
5. Sgroi D, Koerner FC. Involvement of collagenous spherulosis by lobular carcinoma *in situ*: potential confusion with cribriform ductal carcinoma *in situ*. Am J Surg Pathol 1995; 19: 1366-70.
6. Eisenberg RE, Hoda SA. Lobular carcinoma in situ with collagenous spherulosis: clinicopathologic characteristics of 38 cases. Breast J 2014; 20: 440-1.
7. Toll A, Joneja U, Palazzo J. Pathologic spectrum of secretory and mucinous breast lesions. Arch Pathol Lab Med 2016; 140: 644-50.
8. Torous VF, Schnitt SJ, Collins LC. Benign breast lesions that mimic malignancy. Pathology 2017; 49: 181-96.
9. Cabibi D, Giannone AG, Belmonte B, Aragona F, Aragona F. CD10 and HHF35 actin in the differential diagnosis between Collagenous spherulosis and adenoid-cystic carcinoma of the breast. Pathol Res Pract 2012; 208: 405-9.
10. Rabban JT, Swain RS, Zaloudek CJ, Chase DR, Chen YY. Immunophenotypic overlap between adenoid cystic carcinoma and collagenous spherulosis of the breast: potential diagnostic pitfalls using myoepithelial markers. Mod Pathol 2006; 19: 1351-7.

 https://doi.org/10.4132/jptm.2018.03.29

Journal of Pathology and Translational Medicine 2018; 52: 425-427
https://doi.org/10.4132/jptm.2018.04.16

■ BRIEF CASE REPORT ■

Follicular T-Cell Lymphoma with Concomitant Lennert Lymphoma

Seungkyu Choi · Jai-Hyang Go

Department of Pathology, Dankook University College of Medicine, Cheonan, Korea

Follicular T-cell lymphoma (FTCL) has recently been re-categorized by the World Health Organization as a member of the angioimmunoblastic T-cell lymphomas (AITLs) and other nodal lymphomas of T follicular helper (TFH) cell origin from peripheral T-cell lymphoma (PTCL) not otherwise specified (NOS).[1] Lennert lymphoma (LeL) is considered to be a variant of PTCL, NOS.[2] The coexistence of LeL with FTCL has not previously been reported. Herein, we describe an unusual case of FTCL with associated LeL, suggesting a possible relationship between these two entities as part of the TFH-derived lymphomas.

CASE REPORT

A 64-year-old male patient was admitted with a neck mass that had been present for 1 month. Computed tomography showed multiple enlarged lymph nodes along the left side of the neck from level I to V. An excisional biopsy of the neck mass was performed.

The architecture of the excised lymph nodes was completely effaced by multiple nodules of ill-defined small IgD+ mantle zone B cells (Fig. 1A, B). Within the B cell nodules, several aggregates of small to medium lymphoid cells with round nuclei and clear cytoplasm were present (Fig. 1C). Double immunostaining for BOB-1 and CD10 was performed. Most BOB-1 (–) atypical tumor cells were positive for CD3, CD4, CD10, PD-1, and BCL6 (Fig. 1D). These findings are compatible with FTCL with the growth pattern of progressive transformation of germinal center (PTGC). Focally, the area of LeL was intimately admixed with typical FTCL components (Fig. 2A). LeL components showed evenly distributed prominent clusters of epithelioid cells, which were surrounded by small to medium atypical cells (Fig. 2B). In double immunostaining for BOB-1 and CD10, many BOB-1 (–) atypical tumor cells were positive for CD10 (Fig. 2C, D), PD-1, and BCL6. No follicular dendritic cell (FDC) hyperplasia was noted in either the FTCL or LeL components. Analysis of T-cell γ gene (TCR-γ) rearrangement studies using BIOMED-2 –based polymerase chain reaction demonstrated clonal peaks at the same location generated using a DNA template from either the FTCL (Fig. 3A) or LeL components (Fig. 3B).

The Institutional Review Board of Dankook University Hospital (2018-03-007) approved this case report, and informed consent was waived.

DISCUSSION

We describe an unusual case of FTCL with associated LeL, suggesting a possible relationship between these two entities.

FTCL is a lymph node-based neoplasm of TFH cells with a predominantly follicular growth pattern and lacking characteristic features of AITL, such as proliferation of high endothelial venules or extrafollicular FDCs. Two distinct growth patterns are recognized: one that mimics follicular lymphoma and one that mimics PTGC.[1] While FTCL and AITL have some overlapping clinical and pathologic features,[2] FTCL seems to represent a peculiar stage of AITL in which neoplastic cells remain located within B-cell follicles.[2] In a limited number of cases in which consecutive biopsies from different times were studied, change in morphology from FTCL to typical AITL, or vice versa, has been observed.[1] Some cases of AITL relapse with FTCL and rare cases of FTCL with coexistent AITL have been reported.[3] These findings suggest that these two entities may constitute different morphologic representations of the same biological process.[1]

Corresponding Author
Jai-Hyang Go, MD
Department of Pathology, Dankook University College of Medicine, 119 Dandae-ro, Dongnam-gu, Cheonan 31116, Korea
Tel: +82-41-550-6972, Fax: +82-41-561-9127, E-mail: cyjy555@hanmail.net

Received: March 20, 2018 **Revised:** April 13, 2018
Accepted: April 16, 2018

pISSN 2383-7837
eISSN 2383-7845

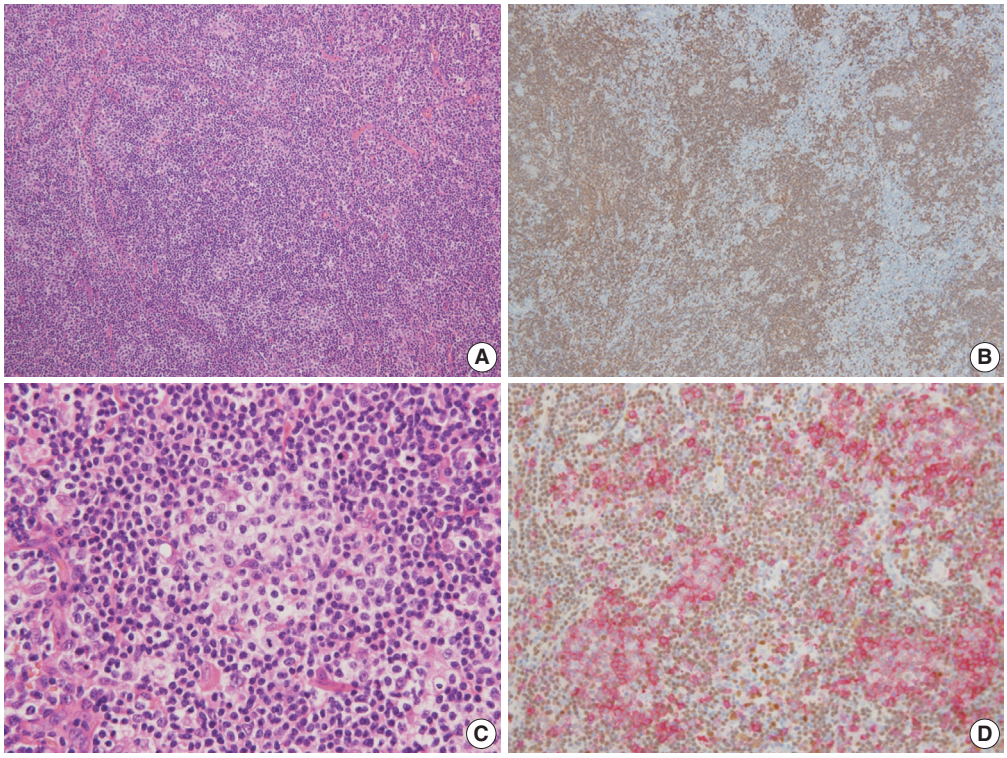

Fig. 1. (A) Lymph node architecture is totally effaced by multiple ill-defined nodules of small lymphocytes. (B) Most cells in the nodules are positive for CD20. (C) Within B-cell nodules, aggregates of small to medium atypical lymphoid cells with round nuclei and clear cytoplasm are present. (D) In double immunostaining for BOB-1 in brown (DAB) and CD10 in red (AEC), BOB-1 (–) tumor cells are diffusely positive for CD10.

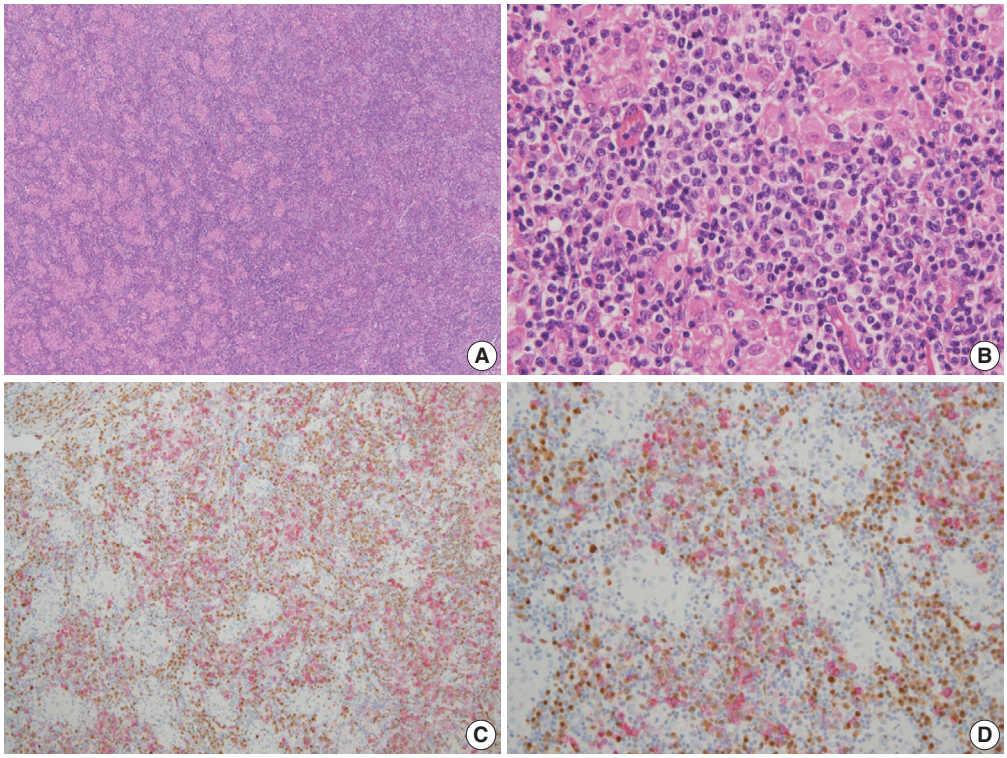

Fig. 2. (A, B) Prominent clusters of epithelioid cells surrounded by small to medium atypical cells are focally present. (C, D) In double immunostaining for BOB-1 in brown (DAB) and CD10 in red (AEC), many BOB-1 (–) tumor cells are positive for CD10.

https://doi.org/10.4132/jptm.2018.04.16

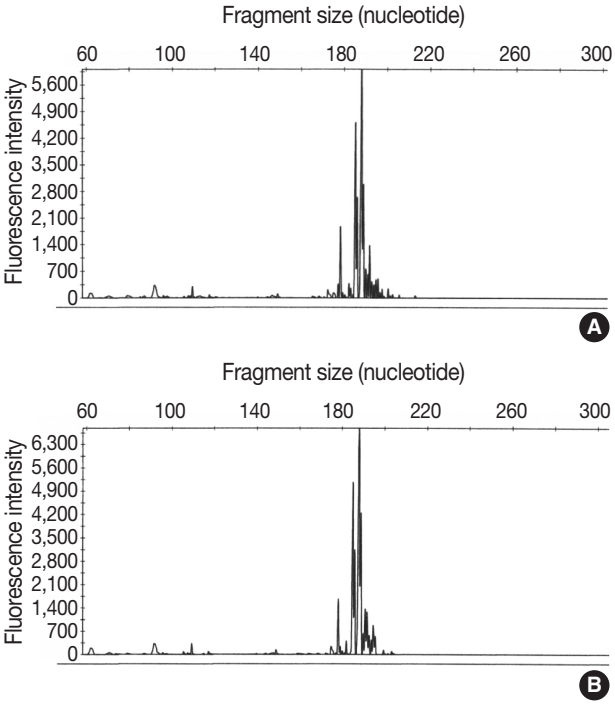

Fig. 3. Analysis of T-cell γ gene rearrangement studies using BIOMED-2–based polymerase chain reaction shows clonal peaks at the same location in both follicular T-cell lymphoma (A) and Lennert lymphoma components (B).

LeL is a rare variant of PTCL, NOS characterized by a prominent reactive infiltrate of epithelioid histiocytes that are distributed singly or, more typically, in small clusters. The tumor cells are usually small with slightly irregular nuclear contours.[4,5] Diagnosis of these tumors is usually based on pure morphology, and the differential diagnosis includes other epithelioid cell-rich lymphomas, especially AITL.[6] Some cases of AITL are considered to have histopathologic features that overlap with those of LeL. However, distinct diagnostic criteria for immunohistochemical properties or histopathologic features and definitive criteria for distinguishing between AITL and LeL have not yet been established.[6]

The TFH cell surface markers, PD-1, CXCL13, CD10, and BCL6, are frequently and characteristically expressed in AITL.[6] However, individual TFH cell markers can be expressed by other T-cell subsets,[3] and are detected in 20% to 41% of PTCL-NOS.[7] Recently, a significant number of LeL cases positive for these markers were described.[6] TFH marker–positive cases had a worse prognosis than marker-negative cases and showed a similar prognosis to AITL, although many clinicopathologic features differed significantly between TFH marker–positive LeL and AITL. TFH marker–positive LeL could be a subset of AITL because it exhibits some of the features of AITL, such as high expression of TFH markers, and a similar prognosis.[6]

In the present case, the LeL component was intimately admixed with the FTCL component, and the TFH markers CD10, PD1, and BCL6 were comparably positive for these two types of tumors. Taken together, these findings support the suggestion that LeL might be appropriately included under the category of TFH-derived lymphomas in addition to AITL and FTCL.

Conflicts of Interest

No potential conflict of interest relevant to this article was reported.

REFERENCES

1. Dogan A, Gaulard P, Jaffe ES, Muller-Hermelink HK, de Leval L. Angioimmunoblastic T-cell lymphoma and other nodal lymphomas of T follicular helper (TFH) cell origin. In: Swerdlow SH, Campo E, Harris NL, *et al*., eds. WHO classification of tumors of hematopoietic and lymphoid tissues. Revised 4th ed. Lyon: IARC Press, 2017; 407-12.
2. Huang Y, Moreau A, Dupuis J, *et al*. Peripheral T-cell lymphomas with a follicular growth pattern are derived from follicular helper T cells (TFH) and may show overlapping features with angioimmunoblastic T-cell lymphomas. Am J Surg Pathol 2009; 33: 682-90.
3. Hu S, Young KH, Konoplev SN, Medeiros LJ. Follicular T-cell lymphoma: a member of an emerging family of follicular helper T-cell derived T-cell lymphomas. Hum Pathol 2012; 43: 1789-98.
4. Jaffe E, Arber DA, Campo E, Harris NL, Quintanilla-Fend L. Hematopathology. 2nd ed. Philadelphia: Elsevier, 2017; 64405.
5. Hartmann S, Agostinelli C, Klapper W, *et al*. Revising the historical collection of epithelioid cell-rich lymphomas of the Kiel Lymph Node Registry: what is Lennert's lymphoma nowadays? Histopathology 2011; 59: 1173-82.
6. Kurita D, Miyoshi H, Yoshida N, *et al*. A clinicopathologic study of Lennert lymphoma and possible prognostic factors: the importance of follicular helper T-cell markers and the association with angioimmunoblastic T-cell lymphoma. Am J Surg Pathol 2016; 40: 1249-60.
7. Pileri SA, Weisenburger DD, Sng I, *et al*. Peripheral T-cell lymphoma, NOS. In: Swerdlow SH, Campo E, Harris NL, *et al*., eds. WHO classification of tumors of hematopoietic and lymphoid tissues. Revised 4th ed. Lyon: IARC Press, 2017; 403-6.


JPTM
Journal of Pathology and
Translational Medicine